A STUDY ON MODELING SOIL-STRUCTURE INTERACTION EFFECTS IN BUILDINGS

THE GRADUATE SCHOOL OF NATURAL AND APPLIED SCIENCES
OF
ATILIM UNIVERSITY

NAWAF HANI MUSLIM AL-DAYYENI

A MASTER OF SCIENCE
THESIS
IN
THE DEPARTMENT OF CIVIL ENGINEERING

APRIL 2019

A STUDY ON MODELING SOIL-STRUCTURE INTERACTION EFFECTS IN BUILDINGS

A THESIS SUBMITTED TO
THE GRADUATE SCHOOL OF NATURAL AND APPLIED SCIENCES
OF
ATILIM UNIVERSITY

BY

NAWAF HANI MUSLIM AL-DAYYENI

IN PARTIAL FULFILLMENT OF THE REQUIREMENTS
FOR
THE DEGREE OF MASTER OF SCIENCE
IN
THE DEPARTMENT OF CIVIL ENGINEERING

APRIL 2019

Approval of the Graduate School of Natural and Applied Sciences, Atılım University.

_____

Prof. Dr. Ali Kara
Director

I certify that this thesis satisfies all the requirements as a thesis for the degree of Master of Science in Civil Engineering, Atılım University.

_____

Asst. Prof. Dr. Gökhan Tunç
Head of Department

This is to certify that we have read the thesis "A Study on Modeling Soil-Structure Interaction Effects in Buildings" submitted by Nawaf Hani Muslim Al-dayyeni and that in our opinion it is fully adequate, in scope and quality, as a thesis for the degree of Master of Science.

_____

Asst. Prof. Dr. Ertan Sönmez
Supervisor

Examining Committee Members:

Asst. Prof. Dr. Gökhan Tunç
Civil Eng. Department, Atılım University _____

Asst. Prof. Dr. Ertan Sönmez
Civil Eng. Department, Atılım University _____

Asst. Prof. Dr. Onur Pekcan
Civil Eng. Dept., Middle East Technical University _____

Date: 26th of April, 2019

I hereby declare that all information in this document has been obtained and presented in accordance with academic rules and ethical conduct. I also declare that, as required by these rules and conduct, I have fully cited and referenced all material and results that are not original to this work.

Name, Last Name: Nawaf Hani Muslim Al-dayyeni

Signature:

ABSTRACT

A STUDY ON MODELING SOIL-STRUCTURE INTERACTION EFFECTS IN BUILDINGS

Nawaf Hani Muslim Al-dayyeni
M.S., Department of Civil Engineering
Supervisor: Asst. Prof. Dr. Ertan Sönmez

April 2019, 147 pages

Soil-structure interaction is usually not considered in the design of most buildings in civil engineering practice. Based on the assumption that these effects reduce the base shear (and the overall earthquake load) for most building structures and soil conditions due to period lengthening, omission of soil-structure effects is in general considered to be conservative and the buildings are designed as fixed base structures. This assumption does not hold for certain building structures and soil conditions (e.g., massive structures, tall buildings, and structures on soft soil).

In this thesis, soil-structure interaction effects in buildings are studied using relatively simple models prepared by a general-purpose structural analysis software (SAP2000). A symmetrical, 6-story, 6-bay reinforced concrete moment resisting frame is considered for both two-dimensional (2D) and three-dimensional (3D) building models. Seismic responses of three different building structures (with varying dynamic characteristics) on three different homogeneous, elastic soil mediums are computed and compared with the responses of the corresponding fixed base models. Soil-structure interaction effects are modeled by two approaches: (i) using soil springs representing the soil impedance functions (substructure method), and (ii) modeling the soil medium directly along with the structure and the foundation (direct analysis method). Two types of foundation are considered in the models: footing foundation

(i.e., isolated footings) and raft foundation. ASCE 7-10 acceleration response spectra are determined based on the soil properties and used to examine the seismic response of the models considered. A limited study is also performed by time-history analyses using an actual earthquake ground acceleration record (1940 El Centro).

Analyses of 2D and 3D models showed the well-known period lengthening effect of soil-structure interaction clearly. The results of this study indicate that spring models based on soil impedance functions that are widely used in practice lead to a lesser period lengthening effect compared to direct models. Similarly, by examining the base shear, story displacement, story drift, and foundation settlement results, it is observed that the soil-structure interaction effects were more significant in the direct models compared to the spring models.

Keywords: Soil-structure interaction, direct analysis, substructure analysis, seismic response of buildings

ÖZ

ZEMİN-YAPI ETKİLEŞİMİNİN BİNALAR ÜZERİNDEKİ ETKİLERİNİN MODELLENMESİ ÜZERİNE BİR ÇALIŞMA

Nawaf Hani Muslim Al-dayyeni
Yüksek Lisans, İnşaat Mühendisliği Bölümü
Tez Yöneticisi: Dr. Öğr. Üyesi Ertan Sönmez

Nisan 2019, 147 sayfa

Zemin-yapı etkileşimi, inşaat mühendisliği uygulamalarındaki çoğu binanın tasarımında genellikle göz önüne alınmaz. Zemin-yapı etkileşiminin bina doğal periyodunun uzamasına sebep olmasından dolayı taban kesme kuvvetinin (ve bina üzerindeki toplam deprem yükünün) azaldığı varsayılarak, çoğu bina yapıları ve zemin koşulları için bu etkileşimin ihmal edilmesi daha güvenli sayılır ve binalar zemine ankastre mesnetlenmiş olarak tasarlanır. Bu varsayım, bazı bina yapıları ve zemin koşulları (ağır yapılar, gökdelenler, ve yumuşak zemin gibi) için geçerli değildir.

Bu tezde binalardaki zemin-yapı etkileşimi, genel amaçlı bir yapısal analiz yazılımı (SAP2000) ile hazırlanmış görece basit modeller kullanılarak çalışılmıştır. İki boyutlu (2B) ve üç boyutlu (3B) bina modelleri için simetrik, 6 katlı, 6 açıklıklı moment dayanımlı betonarme bir çerçeve kullanılmıştır. Üç farklı homojen elastik zemin üzerinde üç farklı binanın (farklı dinamik karakteristiklere sahip) sismik tepkileri hesaplanmış ve zemine ankastre modellerin tepkileriyle karşılaştırılmıştır. Zemin-yapı etkileşimi iki farklı yaklaşımla modellenmiştir: (i) zemin empedans fonksiyonlarını temsil eden mesnet yayları kullanarak (altyapı yöntemi) ve (ii) zeminin üst yapı ve temel ile birlikte doğrudan modellenmesi (doğrudan analiz yöntemi) ile. Modellerde tekli temel ve radye temel olmak üzere iki tür temel dikkate alınmıştır. Modellerin

sismik tepkileri zemin özelliklerine göre belirlenen ASCE 7-10 ivme spektrumları kullanılarak hesaplanmıştır. Gerçek bir deprem yer ivmesi kaydı (1940 El Centro) kullanılarak zaman tanımlı analizler ile de sınırlı bir çalışma yapılmıştır.

2B ve 3B modellerin analiz sonuçları, zemin-yapı etkileşiminin binanın doğal periyodunu uzatma etkisini net bir şekilde göstermiştir. Bu çalışmada, uygulamada yaygın olarak kullanılan zemin empedans fonksiyonlarına dayalı, zeminin mesnet yayları ile temsil edildiği modellerde (yay modelleri) binanın doğal periyodunu uzatma etkisinin doğrudan analiz modellerine göre daha az olduğu gözlemlenmiştir. Benzer şekilde, taban kesme kuvveti, kat yer değiştirmesi, kat ötelemesi ve temel oturması sonuçları incelendiğinde, doğrudan analiz modellerinde zemin-yapı etkileşiminin, yay modellerine göre daha yüksek hesaplandığı görülmüştür.

Anahtar Kelimeler: Zemin-yapı etkileşimi, doğrudan analiz, altsistem analizi, binaların sismik tepkisi

DEDICATION

I would like to dedicate my thesis to Prof. Dr. Hani Al-dayyeni my father for being a source of developing and encouragement to me through my life. To my lovely mother Maha Al-dayyeni who words cannot describe her, a very special thanks to her for the myriad of ways in which, throughout my life, she has actively supported me in my determination to find and realize my potential and to make this contribution to our world. It is also dedicated to brother Fawaz Al-dayyeni and my sister Fatima Al-dayyeni who are also my friends and supporters in this life. I would also like to thank all my family and friends for helping me during my study journey. Finally, with your love and support, I was able to reach this goal.

ACKNOWLEDGMENTS

I would like to thank my supervisor Dr. Ertan Sönmez for his valuable guidance, encouragement and unselfish sharing of ideas and knowledge to improve this work. He is the initiator of this very interesting subject regarding the interaction between structural and geotechnical engineer. During the time working on my thesis, he guided me, was very critical and has given me a lot of feedback. This gave me a better understanding of the broad subject that this thesis project covered. Finally, I am very grateful to Dr. Ertan Sönmez for being my supervisor.

TABLE OF CONTENTS

LIST OF FIGURES

LIST OF TABLES

CHAPTER 1

INTRODUCTION

1.1 Statement of Problem

Buildings are generally designed as fixed base structures in civil engineering practice, ignoring the soil-structure interaction effects. This is based on the assumption that soil-structure interaction effects reduce the base shear (and the overall earthquake loads) for most building structures and soil conditions, and therefore their omission is usually considered to be conservative. However, this assumption does not hold for certain building structures and soil conditions. Therefore, it is important to have a good understanding of the soil-structure interaction effects and to know when these effects can be ignored and when they must be considered.

Depending on the location of the building, the supporting soil may have very different properties and two buildings identical to each other may have different structural behaviors under the same earthquake excitation if the soil beneath them have different characteristics. For example, if the structure is lightweight, flexible and built on a very stiff rock foundation, an adequate assumption is that the input motions at the base of the structure are the same as the free-field ground motions. Free-field motion, is a ground motion which is not influenced by the presence of the structure. Further, if the structure is very heavy and stiff, and the foundation is soft, then the motion at the base of the structure may be significantly different than the free-field motion. Soil-structure interaction (SSI) takes place due to the connection between the structure and the base. This process, in which the response of the soil influences the motion of the structure and the response of the structures influences the motion of the soil. The degree of influence of SSI on the response of structure depends on soil stiffness, dynamic characteristics of the structure itself (i.e., natural period and damping ratio), and stiffness and mass of the structure.

Foundation design of the structure depends on the collaboration of two civil engineers, who are: geotechnical and structural engineers. Geotechnical engineers perform tests and computations using soil samples from the field and provide the necessary data (i.e., soil stiffness, bearing capacity, etc.) to the structural engineers. Using the data presented in the soil report, structural engineers finalize the structural design of the foundation and the superstructure.

Modeling the interaction between structure and soil is not straightforward. The heterogeneous, anisotropic and nonlinear force-displacement characteristics of soil make its modeling difficult. To understand the SSI problem, it is necessary to have some information of the influence of local soil condition in changing the nature of free ground motion and have information of the earthquake wave propagation through the soil. When the seismic wave propagates through the soil as an input ground motion, its dynamic characteristics depend on the modification of the bedrock motion. The knowledge of the vibration characteristics of the soil medium is very useful in determining the soil impedance functions and fixing the boundaries for an infinite soil medium when the wave propagation analysis is implemented.

1.2 Literature Review

There has been a large number of studies on soil-structure interaction in the literature starting early last century. A brief summary of important contributions to this field is presented in this section.

In the 1920s, Okabe [1] and Mononobe et al. [2] studied the effect of the soil on the seismic response of a retaining wall by considering the retaining wall as a rigid body. This proposal was a simple extension to Coulomb's theory for the static case. Despite the many developments along the years, it is still commonly used in practice today (Roesset [3]). In about one decade later, Sezawa and Kanai (e.g. [4], [5], [6]) published their studies, using a model with thin cylindrical rod ended at the base by a hemispherical tip which is embedded in a homogenous half-space. In their work, the hemispherical base is subjected to plane, vertically propagating primary (P) waves,

which upon hitting the foundation, are partially dispersed in all directions and partially transferred into the rod, that in turn feeds back into the soil. They found that the response of the structure was limited due to the energy loss as some of the waves fed back into the soil, even for undamped superstructures; therefore, they concluded that the soil-structure interaction was beneficial for the structure. In 1940, Martel [7] introduced one of the earliest explanations on the seismic soil-structure effects in the United States, reporting observations which cite the results of studies on the Hollywood Storage Building during the 1933 Long Beach earthquake. In his observations, he inferred that the damage in buildings that rest on soft soils or high elevation could be more common than in buildings resting on rock or firm level. Later, Merritt and Housner [8] studied the effect of foundation compliance on seismic response of multi-story buildings using actual horizontal ground acceleration records. They found that the lateral compliance of the foundation does not have a significant effect on motions but the rocking could be more important. In their study, they used a simple system where the superstructure was idealized as a rigid block on a rotational spring whose stiffness was based on the moment of inertia of the base about the rocking axis together with the bearing capacity of the soil. They inferred that any beneficial effects of rocking in decreasing base shear depend on the earthquake characteristics and the height of the building. Three years later, Housner [9] revisited the subject by comparing the motions in the foundation in two directions (short dimension in the North-South direction and long dimension in the East-West direction), he noticed that waves in the ground which propagated over the long direction have been filtered, being the first researcher who demonstrated the kinematic interaction phenomenon, which happens because the stiff structure cannot conform to the ground deformations caused by waves shorter in wavelength than the foundation dimensions, and therefore the stiff structure filters them out.

During the 60s and 70s, the seismic soil-structure interaction has been paid more comprehensive attention by researchers due to the development and construction of nuclear power plants. Parmelee (e.g. [10], [11]) considered a simple rigid plate on an elastic half-space with three degrees of freedom, namely the translation of the top and the base, and rotation of the base, this model was included in Bigg [12]. The system was put on constant frequency independent springs (lateral and rocking springs) which

are based on Bycroft [13] stiffness functions to simulate the stiffness of the foundation. Parmelee [10] used just the static stiffness without any damping, thus, he obtained the harmonic response functions. But, in a later paper Parmelee [11], he took into consideration the frequency-dependence of the foundation impadences along limited frequency range that were available at that time and utilized artificial earthquakes with no greater than ten terms. Thereafter, Sarrazin [14] revisited Parmelee's model but the model was considered for the height of the center of mass of the foundation over the line of action of the soil spring. It is worthy to be noticed that both of them used frequency-dependent impedances and evaluated the impedance at the coupled soil-structure frequencies to be able to deal with frequency independent such as springs and dashpots. Moreover, they confirmed Housner's disagreement by saying that the main interaction effects are likely to be because of the base rotation rather than the changes in the translation and in most practical cases swaying is unimportant. In the following years, Maccalden and Matthiesen [15] extended Bycroft's work, which consists of an analytical model of a single rigid circular foundation over an elastic half-space and they improved a matrix formulation for the solution of the produced dynamic displacements of the foundations near a harmonically loaded foundations on an elastic half-space. Locu and Contesse [16] considered the two-dimensional anti-plane problem of the interaction between two or more shear walls put on rigid circular foundations and subjected to diagonally or vertically incident shear horizontal (SH) waves. They found a solution to the 2D wave diffraction problem by parametric studies and presented that very closely spaced groups of buildings might cause interaction effects near the fundamental frequencies of the buildings and at very low frequencies. Moreover, Triantafyllidis and Neidhart [17] used an analytical-numerical approach to analyze the dynamic cross-interaction of two rigid circular surface foundation on different surface types (such as linear elastic, homogenous, and isotropic half-space surface) that are subjected to Rayleigh waves impacting at random angle. They deduced that additional loads orthogonal to the propagation direction acted on the foundations due to scattered waves, with their intensity depended on the distance between the foundations and the excitation frequency.

As the soil-structure interaction field has matured, two types of interaction have been identified as kinematic interaction and inertial interaction. When the earthquake

ground motion in the free-field varies over the area corresponding to that of the rigid foundation, then it could be constrained and modified by the rigid foundation. This deviation from free field motion is called kinematic interaction between the soil and foundation. Further, inertial forces are generated by foundation motion during earthquakes, the inertial forces are distributed along the height of the structure cause a resultant base shear and an overturning moment at the foundation, which leads the compliant soil to deform which in turn increases translations and rotations at the base of the structure (Dutta and Rana [18]). Elsabee and Morray [19] studied these effects on for a soil stratum of finite depth over stiffer rock. Furthermore, Luco and Wong [20] studied the effects but for the viscoelastic half-space. Studies show that the kinematic interaction effect is very important for embedded foundations (e.g. [18], [19]). In reality, both effects occur together, so both of them should be taken into consideration when it comes to analysis and design (Scanlan [21]).

The above studies were based on the elastic half-space with shallow foundation on a homogenous soil layer, which allows engineers making simple and practicable analysis for the structure. Seed et al. [22] argued that these studies were not suitable for the dynamic interaction analysis of structures having deep foundations. Therefore, as the computers became more powerful, it became possible to model flexible foundations which were embedded in inhomogeneous media, irregular-shaped, and more complex effects such as the inelasticity of the soil. During that time, many sophisticated and efficient computing methods began being used in the modeling and analysis of the soil-structure interaction such as finite element method (FEM) is an efficient widely used method, which can discretize a continuum into a series of elements having limited sizes to calculate for the mechanics of the continuum. Moreover, the finite element method has the ability to deal with complex geometry and the non-linear behavior of the soil and the structure more efficiently than other methods. Gonzales [23], Roesset and Gonzales [24], and Solari et al. [25] used the finite element type formulation in conjunction with compatible boundaries to investigate the three-dimensional soil-structure interaction problem. Their model consists of two square rigid foundations resting on linear-elastic layer under vertically propagating S-waves (Lou et al. [26]). Later on, Rosset [27] concluded that the nonlinearity of soil controls the accuracy and rationality of the soil-structure

interaction analysis. Nevertheless, there has not been many studies considering the non-linear behavior of soil due to the complexity and time-consuming computation of the non-linear phenomena.

Another numerical method that has been used widespread in soil-structure interaction problems is the boundary element method (BEM). The FEM and BEM have both been developed in the 1950s; however, the BEM took much more time to become popular in the soil-structure interaction field. Dominguez [28] was one of the pioneers who found the first solutions for rectangular foundations employing the boundary element (boundary integral equation) method. Based on experimental verifications and the results obtained from the boundary element method (BEM), Gazetas [29] suggested expressions to compute the stiffness and damping coefficients for randomly shaped footings resting on homogeneous elastic half-space soil. Gazetas [29] established a benchmark literature in the field of dynamic soil-structure interaction. With the leaps that have been made by Kausel [30] and Luco and Luco and Apsel [31] in this field, using the publication of Green's functions for layered media, solutions became possible to be found for surface or embedded foundations of arbitrary shapes.

Two general methods have been developed to be used in the seismic soil-structure interaction analysis. The first one is the direct method in which the foundation and the structure are modeled together and analyzed in one step. Seed et al. [32] says the direct approach is "complete solution", it could be the best solution in a case where the non-linear time domain analysis is considered with three-dimensional models of the soil and the structure, permitting to take all types of waves into consideration. Nelson and Isenberg [33] proposed the soil island approach, which was developed for problems with significant nonlinear soil behavior. In this procedure, the analysis is performed in the time domain including the nonlinear soil behavior. The soil mass did not have to transmit or absorbing lateral boundaries; therefore, the procedure was not give an accurate solution for a linear elastic case or if the internal damping was very low. The second method is the substructure method. In this method, the problem is divided into three parts: determination of the foundation motion without any structure by using seismic waves, calculation of the dynamic stiffness for the foundation, and dynamic analysis of the structure with the foundation inserted and subjected to the motion

calculated in the first step. Kausel and Roesset [34] proposed the substructure method. Substructure method is more efficient than the direct method as most of the disadvantages of the direct method can be eliminated when the substructure method is carried out. It has the ability to break down the complicated soil-structure system into more manageable parts which can be more easily solved and checked. Veletsos [35] and Luco [36] provided more details regarding the substructure method. Lysmer et al. [37] developed a more accurate linear three-dimensional substructure solution in SASSI software.

Dutta and Rana [18] introduced procedures that take SSI in the seismic analysis of structures into account with a comprehensive review of the literature. A comprehensive discussion of the methods of dynamic soil-structure interaction analysis is presented in Wolf [38] and Wolf and Song [39].

1.3 Objectives and Scope of the Thesis

The aim of this thesis is to investigate soil-structure interaction effects in buildings, using relatively simple models prepared by the general-purpose structural analysis software SAP2000. For that purpose, seismic responses of different building structures with varying dynamic characteristics that are supported by different soil mediums are examined and compared with the responses of the corresponding fixed base models. Soil-structure interaction effects are modeled by two approaches: (i) defining soil springs representing the soil impedance functions (substructure method), and (ii) modeling the soil medium directly along with the structure and the foundation (direct analysis method). Two types of foundation are considered in the models: footing foundation (i.e., isolated footings) and raft foundation. ASCE 7-10 acceleration response spectra are determined based on the soil properties and used to examine the seismic response behavior of the models considered. A limited study is also performed by time-history analyses using an actual earthquake ground acceleration record (1940 El Centro).

The statement of the problem and the review of previous work are presented in the previous sections of this chapter. Chapter 2 provides detailed background information

about soil-structure interaction methods, modeling of soil medium, site response analysis, and various standard or recommended practice documents providing guidance on modeling of soil-structure interaction effects. The details regarding the soil models, acceleration response spectra and ground acceleration record used in this study are presented in Chapter 3. The descriptions of 2D & 3D models and their seismic response obtained by response spectrum analysis and time history analysis are given in Chapters 4 and 5. The final chapter summarizes the main points of this study and presents the concluding remarks.

CHAPTER 2

SOIL-STRUCTURE INTERACTION

This chapter presents background information about soil-structure interaction. In Section 2.1, analysis methods are discussed. In Section 2.2, the impedance functions are defined and the methods of obtaining impedance functions are summarized. In Sections 2.3 and 2.4, static and dynamic soil-structure interaction are described, respectively. In Section 2.5, several types of commonly used boundary conditions are explained. In Section 2.6, the site response analysis is described and the equivalent linear and nonlinear analysis are discussed. Finally, the guidance and requirements specified by various codes and recommended practice documents in regard to the soil-structure interaction are discussed.

2.1 Analysis Methods for Soil-Structure Interaction

2.1.1 Direct Analysis Method

The direct approach is one of many methods which is used to analyze the soil-structure interaction system. The direct approach is performed by utilizing the finite element method where the whole soil-structure interaction system is modeled and analyzed in one step. The equation of motion for the finite element model could be written as below:

$$M\ddot{u} + C\dot{u} + Ku = -M_{st}\, I\, \ddot{u}_g \tag{2.1}$$

where

M = Mass matrix for the entire structure, foundation, and soil

C = Damping matrix (material) of the structure and the soil

K = Stiffness matrix of the total system, which can be generated using standard assembling procedure

M_{st} = Mass matrix having non-zero masses for the structural degree of Freedom

I = Mass matrix having non-zero masses for the structural degree of freedom

u_{st} = Free field ground acceleration (can be calculated by doing one simple one-dimensional analysis of site model, prior to the soil-structure analysis)

u = the vector of relative displacement with respect to the base/foundation

The right side of the Eq. (2.1) shows the inertia force which attempts to deform the soil at the soil-structure interface when transferred to the foundation in the shape of shear force and moment. This deformation of soil which is resulted from the inertia forces at the interface propagates in a shape of radiation damping waves which affect the structure-foundation-soil response. If the radiation damping waves are not dissipated or reflected back from the boundary into the model, an error in the computation may occur. In order to overcome this error, some techniques have been made such as energy absorption boundaries of dampers. Figure 2.1 illustrates an overview of direct modeling method.

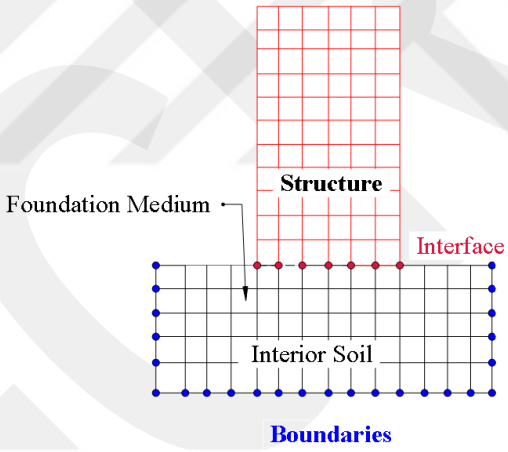

Figure 2.1 Direct method

In the case where the soil-structure interaction system is assumed as fully linear or equivalent linear, the analysis should be carried out in the frequency domain which is faster than time history analysis. On the other hand, if the system is treated as a nonlinear system, then the analysis can be carried out in the time domain.

2.1.2 Substructure Method

The substructure method consists of three steps. The first step of this method is calculation of the foundation input motion in the absence of the structure and foundation (model is assumed to have stiffness but no mass). This motion varies from the free field motion and includes translational and rotational components. The difference between the free-field motion and the foundation input motion represents the effects of kinematic interaction. This step needs that the earthquake input motion in the free-field being known at any point of the ground surface and the rock-outcrop. The second step is evaluation of the frequency dependent impedance functions. The stiffness and damping of the soil-foundation interaction can be represented by using a simple impedance function or a series of distributed dashpots and springs. This step shall account for the geometric and material properties of the foundation and soil using equivalent linear elastic properties for soil convenient for dynamic shear strains of the working site. The third step is computation of the response of the superstructure on frequency dependent foundation (soil springs) and exciting the system through the foundation by bumping the ends of the springs and dashpots employing the translational and rotational components of foundation input motion. Figure 2.2 illustrates the substructure method.

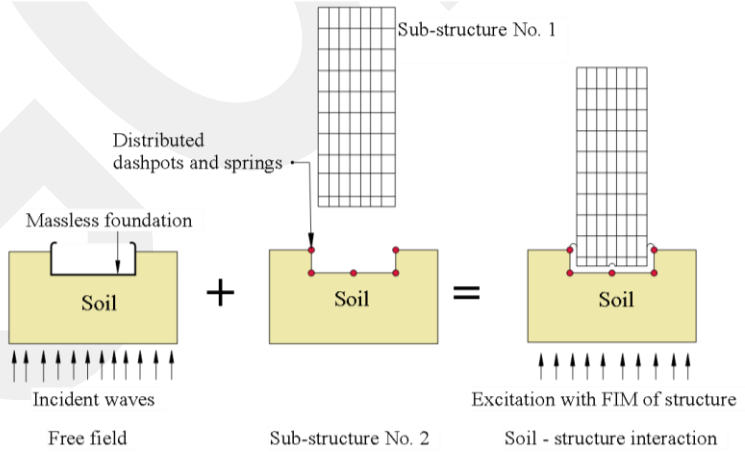

Figure 2.2 Substructure method

2.2 Impedance Functions

2.2.1 Definition of Impedances

The design and analysis of foundation under dynamic loads have grown considerably over the past decades. In order to perform such design and analysis, the determination of the dynamic response of the soil-foundation system is required. The relationship between forces and displacement is expressed by impedance functions. The dynamic soil impedance or stiffness is utilized to model the soil-foundation response to dynamic loads. The dynamic force-displacement relationship for the foundation can be written as follows:

$$p(w) = k(w) * U(w) \tag{2.2}$$

where

p = the dynamic load

k = the impedance or stiffness function

U = the displacement

w = the frequency

By definition, six dynamic degrees of freedom are required to formulate the dynamic equilibrium of a foundation when the 3D system is considered. The degrees of freedom are three translational and three rotational. So, Eq. (2.2) can be written in form of matrices as below:

$$\begin{Bmatrix} P_x \\ P_y \\ P_z \\ M_x \\ M_y \\ M_z \end{Bmatrix} = \begin{bmatrix} K_{xx}(\omega) & 0 & 0 & 0 & K_{x,my}(\omega) & 0 \\ 0 & K_{yy}(\omega) & 0 & K_{y,mx}(\omega) & 0 & 0 \\ 0 & 0 & K_{zz}(\omega) & 0 & 0 & 0 \\ 0 & K_{mx,y}(\omega) & 0 & K_{mx}(\omega) & 0 & 0 \\ K_{my,x}(\omega) & 0 & 0 & 0 & K_{my}(\omega) & 0 \\ 0 & 0 & 0 & 0 & 0 & K_{mz}(\omega) \end{bmatrix} * \begin{bmatrix} U_x \\ U_y \\ U_z \\ U_{rx} \\ U_{ry} \\ U_{rz} \end{bmatrix}$$

where

P_x = the lateral excitation force

P_y = the lateral excitation force

P_z = the vertical excitation force

M_x = the interaction overturning moment about x-axis

M_y = the interaction overturning moment about y-axis

M_z = the torsional moment z-axis

U_x = the horizontal translation

U_y = the horizontal translation

U_z = vertical translation.

U_{rx} = the rocking rotations about x-axis

U_{ry} = the rocking rotations about y-axis

U_{rz} = torsional rotation about z-axis

Çelebi et al. [40] stated that the foundation stiffness and damping depended on the frequency of excitation. The relation between impedance, applied load and displacement can be written as follows:

$$K(\omega) = \frac{P(\omega)}{U(\omega)} \tag{2.3}$$

Procedures that have been developed to calculate the frequency dependent dynamic impedances of different types of soil supported foundation are discussed in the following section.

2.2.2 Methods to Obtain Impedance Functions

2.2.2.1 Finite Element Method

Finite element method is one of the methods that can be used in the seismic soil-structure interaction analysis. The structure which has finite dimension interacts dynamically through the structure-soil interface with the soil of infinite dimensions, which is called the unbounded medium. The unbounded medium can be modeled with finite elements by using special treatment (Wolf and Song [41]).

In the substructure method, the dynamic properties of the unbounded medium are demonstrated by the interaction force-motion equation which is defined on the structure-medium interface.

$$R(t) = \int_0^t M^{\Theta}(t-T) * \{\ddot{u}(T)\} dT \tag{2.4}$$

where

$M^{\Theta}(t)$ = the unit-impulse response matrix of the medium relating the accelerations $\ddot{u}(T)$ to the interface forces $R(t)$

In the direct method, the adjacent medium to the structure-medium interface is modeled by employing finite elements to the artificial boundaries, that act as transmitting boundaries. Many methods such as damping-solvent extraction method and doubly-asymptotic multi-directional transmitting boundary method used artificial boundaries in modeling unbounded soil medium (Wolf and Song [41]). As an alternative, the similarity-based formulation is proposed by Wolf and Song [41], using the finite element method and standard matrix operations could be exercised to calculate $M^{\Theta}(t)$ in Eq. (2.4).

A two-dimensional half-space with a discretized structure-medium interface is shown in Figure 2.3 to demonstrate the concept. A similar imaginary interface is created by selecting the similarity center C. The two similar interfaces are defined via their characteristic lengths r_i and r_o. A relationship between the unit-impulse response matrices at the two interfaces of the unbounded medium is derived by utilizing the dimensional analysis. The area between the two interfaces is discretized with finite elements. Standard finite element formulation provides another relationship between the two unit-impulse response matrices (Wolf and Song [41]). So, the $M^{\Theta}(t)$ value can be calculated using these two relationships.

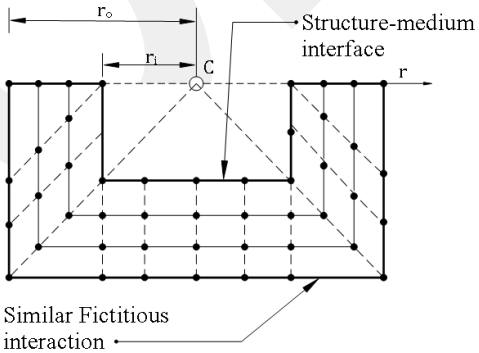

Figure 2.3 Finite element domain for the unbounded soil medium

In the damping-solvent extraction method which is proposed by Wolf and Song and Wolf (e.g. [41], [42]) the dynamic stiffness matrix $[S^{\Theta}(\omega)]$ that utilized in a frequency-domain analysis based on the substructure method could efficiently be calculated. In this method, damping is assumed to be a solvent for calculating the dynamic stiffness matrix in the frequency domain of the undamped unbounded medium. There are three

steps are involved in this procedure. The first step is modeling a finite region of the unbounded medium close to the structure and a bounded medium by using finite elements. Hence, damping is introduced artificially as a solvent in the actual medium. The damping effects are reducing the amplitudes of the outgoing waves (ω) which propagate from the structure-medium interface to the outer boundaries and diminishing the amplitudes of the reflected waves (R). These effects result in negligible amplitudes when waves reach the structure-medium interface. Thus, the structure-medium interface's motion depends only on the outgoing waves (ω). The second step is assuming that the dynamic stiffness matrix of the artificially damped bounded medium which is calculated in the first step to be equal to the dynamic-stiffness matrix of the unbounded medium has the same artificial damping. The third step is extracting the influence of the artificial damping on the dynamic-stiffness matrix. This elimination of the damping solvent should be independently performed for each element of the matrix for every frequency, employing the following equation:

$$S^{\Theta}(w) = \frac{1}{1+2i\xi}\left([S_{\xi}(w)] + \left(\sqrt{1+2i\xi}-1\right)w\frac{d[S_{\xi}(w)]}{dw}\right) \tag{2.5}$$

2.2.2.2 Boundary Element Method

The boundary element method is a numerical method that is used for a wide class of problems in applied mechanics. This method has two advantages (Beskos [43]): (i) reducing the dimensionality of the problem by one and (ii) having a high accuracy for a wide class of problems in linear elastodynamics, particularly when the medium is infinite or semi-infinite.

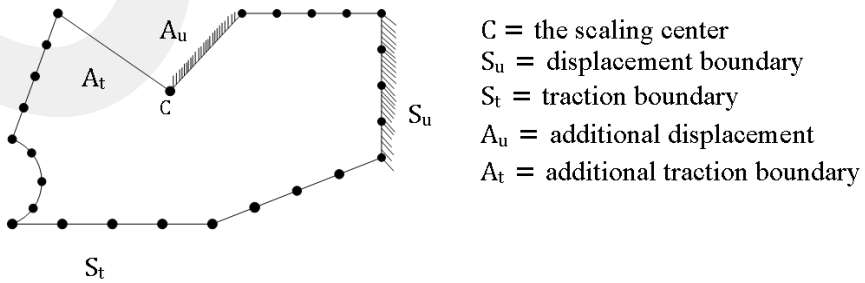

Figure 2.4 Illustration of the boundary element method

Beskos [43] stated that the analytic solution of the boundary integral equations was only possible for very simple geometries and time variations functions in the elastic dynamic solutions. Moreover, Beskos demonstrated that the elasto-dynamic numerical solution should be performed for the general case of arbitrary geometries and time variation functions. In the elasto-dynamic numerical solution, the time domain approach has two steps. The first step is discretization of the real-time axes into a series of equally spaced time values having a constant variation of displacements and tractions over every time interval. The second step is discretization of the boundary S of the region into a number of flat triangular or quadrilateral elements over each of which constant distribution of displacements and tractions. For the frequency domain approach, the same procedure is used for spatial discretization. The direct BEM is used in both time domain and frequency domain.

2.2.2.3 Perfectly Matched Layer Technique (PML)

The perfectly matched layer is a numerical technique that is utilized as absorbing and transmitting boundaries. In other words, the perfectly matched layer (PML) absorbs and attenuates all the waves inside the layer. The PML is placed adjacent to a truncated bounded or unbounded domain. Then, the continuum PML is mathematically formulated through applying a complex-valued coordinate stretching to the elastic wave equation, so all waves with all angles of incidence are absorbed without any reflecting from the interface. Therefore, the PLM is called "perfectly matched" to the truncated domain. The attenuated waves are reflected towards the truncated domain from the outer boundaries of the PML which might be fixed boundaries. The coordinate stretching values can be explained as follows: Given a plane wave propagating in a lossless domain expressed by e^{ikx}, a coordinate stretching is a change of variable by letting x equals to $x'(\alpha' + i\alpha')$. Then, e^{ikx} becomes $e^{ikx-k\alpha' x'}$. It can be said that a wave becomes attenuative in the stretched x' coordinate when the stretching variable is complex. Figure 2.5 illustrates the PML technique.

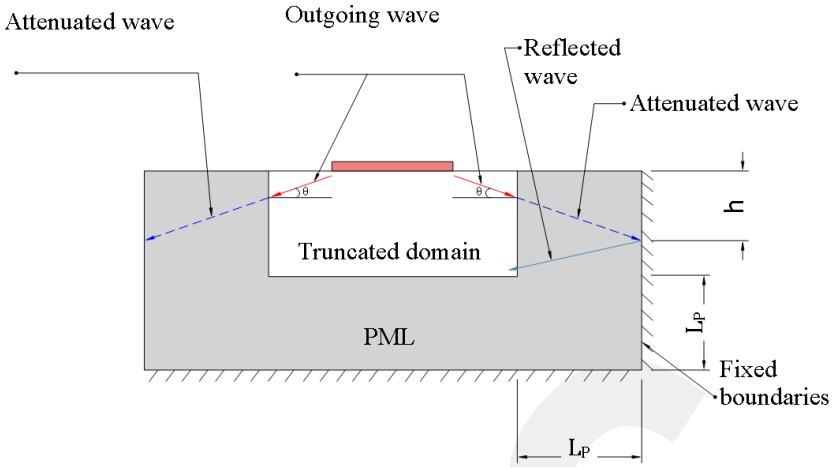

Figure 2.5 Perfectly matched layer (PML) technique

2.2.2.4 Thin Layer Method (TLM)

The thin-layer method is a semi-discrete numerical procedure which is used for the dynamic analysis. Basically, this method consists of a partial discretization of the wave equation in the direction of layering. Therefore, the finite element solution is utilized for the layering coordinate direction and closed-form solutions or other numerical approaches are utilized for the remaining coordinate directions. In order to solve the wave equation, the physical domain is divided into layers which are thin in the finite element sense. The number of layers depends on the interpolation order m which used for the thin-layer formulation. The thin layers are labeled from top to the bottom as shown in Figure 2.6. Tractions are applied to preserve the equilibrium of the exposed surfaces. The following equation represents a partial discretization of the displacement field in the direction of layering:

$$u = N * U \tag{2.6}$$

where

$N = N(z) =$ is the matrix containing the interpolation polynomials

$U = U(x, y, t) =$ the column vector composed of the interface displacement vectors.

$$U = [U_i^T \quad U_{i+1}^T \quad \dots \quad U_{i+m}^T]^T \tag{2.7}$$

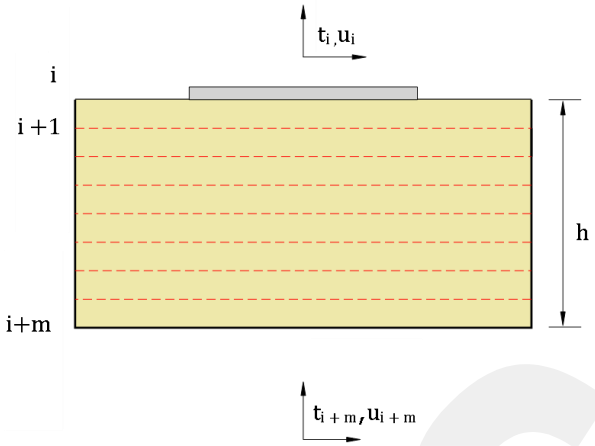

Figure 2.6 Discrete thin layer as free domain

Finally, the equation below can represent the complete system of layers. The interface tractions $P = P(x, y, t)$ where applied at the layer interfaces with the displacements $U = U(x, y, t)$. This system which is accurately banded has a total of $3N$ degrees of freedom, where N is the number of active interfaces which depends on the number of layers.

$$P = M\ddot{u} - A_{xx}\frac{\delta^2 U}{\delta x^2} - A_{xy}\frac{\delta^2 U}{\delta x\,\delta y} - A_{yy}\frac{\delta^2 U}{\delta y^2} - B_x\frac{\delta U}{\delta x} - B_y\frac{\delta U}{\delta y} + GU \quad (2.8)$$

where

$$M = \left\{\int_0^h N^T N_P\, dz\right\}$$

$$A_{xx} = \left\{\int_0^h N^T D_{\propto\propto} N\, dz\right\}, \propto = x, y$$

$$A_{yy} = \left\{\int_0^h N^T \left(D_{xy} + D_{yx}\right) N\, dx\right\}$$

$$B_{\propto} = \left\{\int_0^h N^T D_{\propto z} N'\, dz\right\} - \left\{\int_0^h N'^T D_{z\propto} N\, dz\right\}, \propto = x, y$$

$$G = \left\{\int_0^h N'^T D_{zz} N'\, dz\right\}$$

All the coefficients listed above are matrices which are given in Kausel [44].

2.2.2.5 Simple Physical Models

Foundations on deformable soils can be represented by simple physical models to be used for soil-structure interaction analysis. (Wolf [45]). These simple physical models

can be used to obtain the interaction force-displacement relationship (dynamic stiffness). Moreover, the simple physical models can be utilized for everyday practical foundation vibration analysis, having a small number of degrees of freedom and some springs, dashpots, and masses which have frequency-independent coefficients. Two types of simple physical models are considered: the truncated cones and the spring-dashpots mass models.

To represent many practical dynamic cases, some assumptions are proposed such as disk on surface half-space, cylinder embedded in half-space, disk on the surface of the layer, cylinder embedded in the layer, hammer foundation with a partial uplift anvil, and soil pressure on a vertical wall for seismic excitation in Wolf [45].

The disk on the surface half-space assumption is divided into three models. The first model is the truncated cone model, which is represented in Figure 2.7 for translational (vertical) and rotational (rocking) components of motion. In this model, a rigid massless foundation with area A_o and moment of inertia I_o are put on the surface of homogeneous half-space with mass density ρ, shear wave velocity C_S, Poisson's ratio ν, and dilatational (primary) wave velocity C_P. The truncated cone model has an equivalent radius r_o and a height z_o. Shear (secondary) wave velocity C_S and dilatational wave velocity C_P are obtained from the following equations:

$$C_S = \sqrt{\frac{G}{\rho}} \tag{2.9}$$

$$C_P = \sqrt{\frac{E_c}{\rho}} \tag{2.10}$$

where

G = the shear modulus

E_c = the constrained modulus which is calculated by using the equation below:

$$E_c = \frac{2G(1-\nu)}{(1-2\nu)} \tag{2.11}$$

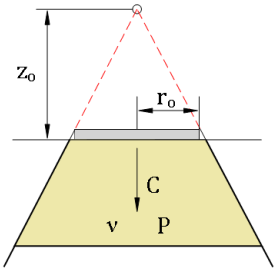

Figure 2.7 Truncated cone model

For the practical application purposes, the translational and rotational cones can be constructed by using springs and dashpots which denoted as a discrete-element model, shown in Figure 2.8. Table 2.1 shows the properties of the cones and coefficient of the springs and dashpots models.

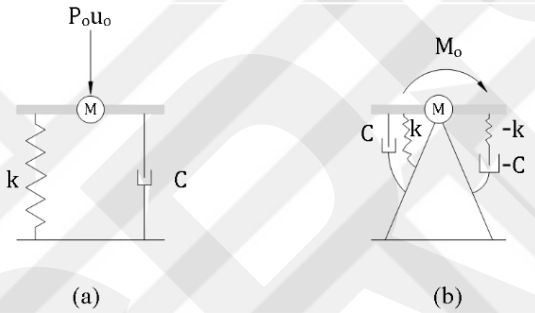

Figure 2.8 Equivalent spring-dashpot models: (a) discrete-element model for translational cone; (b) discrete-element model for rotational cone

Table 2.1 Geometry and wave velocity of cone model and coefficients of a spring-dashpot-mass model for the disk on half-space

Motion	Horizontal	Vertical		Rocking		Torsional
Equivalent radius r_o	$\sqrt{\frac{A_o}{\pi}}$	$\sqrt{\frac{A_o}{\pi}}$		$\sqrt[4]{\frac{4I_o}{\pi}}$		$\sqrt[4]{\frac{2I_o}{\pi}}$
Aspect ratio z_o/r_o	$\frac{\pi}{8}(2-\nu)$	$\frac{\pi}{4}(1-\nu)(\frac{C}{C_S})^2$		$\frac{9\pi}{32}(1-\nu)(\frac{C}{C_S})^2$		$\frac{9\pi}{32}$
Poisson's ratio ν	All ν	$\nu \le \frac{1}{3}$	$\frac{1}{3} < \nu < \frac{1}{2}$	$\nu \le \frac{1}{3}$	$\frac{1}{3} < \nu \le \frac{1}{2}$	All ν
Wave velocity C	C_S	C_P	$2C_S$	C_P	$2C_S$	C_S
Trapped mass ΔM, $\Delta M\Theta$	0	0	$2.4\left(\nu-\frac{1}{3}\right)PA_o r_o$	0	$1.2\left(\nu-\frac{1}{3}\right)PA_o r_o$	0
Discrete-element model	$K = P_C^2 \frac{A_O}{z_O}$ $C = P_C A_O$			$K_\Theta = 3P_C^2 \frac{I_O}{z_O}$ $C_S = P_C I_O$ $M_O = P z_O I_O$		

The second model is a spring-dashpot-mass model without an internal degree of freedom which is shown in Figure 2.8. The static stiffnesses and dimensionless coefficients are presented in Table 2.2. To calculate the dashpot's damping coefficient and mass moment of inertia for rotation, the following equations should be used:

$$C = \frac{r_o}{C_S}\gamma\, k \tag{2.12}$$

$$M = \frac{r_o}{C_S}\mu\, k \tag{2.12}$$

where

$r_o =$ the equivalent radius

$C_S =$ the shear wave velocity

$k =$ the stiffness of spring

$\gamma =$ the dimensionless coefficient of dashpot

$\mu =$ the dimensionless coefficient of mass

Table 2.2 Static-stiffness and dimensionless coefficients of a spring-dashpot-mass model for the disk on half-space

Motion	Static stiffness k	The dimensionless coefficient of dashpot γ	The dimensionless coefficient of mass μ
Horizontal	$\frac{8Gr_o}{2-v}$	0.58	0.095
Vertical	$\frac{4Gr_o}{2-v}$	0.85	0.27
Rocking	$\frac{8Gr_o^3}{3(1-v)}$	$\frac{0.3}{1+\frac{3(1-v)m}{8r_o^5 p}}$	0.24
Torsional	$\frac{16Gr_o^3}{3}$	$\frac{0.433}{1+\frac{2\,m}{p\,r_o^5}}\sqrt{\frac{m}{p\,r_o^5}}$	0.045

The third model is the spring-dashpot-mass with an internal degree of freedom (u_0) which is shown in Figure 2.9. The static stiffnesses and dimensionless coefficients are listed in Table 2.3. The model has a spring with a static stiffness coefficient, k and a dashpot having a damping coefficient of C_o. The dashpot connects the disk with its mass M_O (mass moment of inertia for rotation) to a rigid support and, an internal degree of freedom u_1 at its own mass M_1 (mass moment of inertia for rotation) is introduced. The M_1 is connected by a dashpot $C_1$to the disk. To calculate the dashpot

damping values C_O and C_1 and mass moment of inertia for rotation M_O and M_1, the following equations should be used:

$$C_o = \frac{r_o}{C_S}\,\gamma_o\,k \tag{2.13}$$

$$C_1 = \frac{r_o}{C_S}\gamma_1 k \tag{2.15}$$

$$M_o = \frac{r_o^2}{C_S^2}\mu_o\,k \tag{2.16}$$

$$M_1 = \frac{r_o^2}{C_S^2}\mu_1\,k \tag{2.17}$$

where

$r_o =$ the equivalent radius

$C_S =$ the shear wave velocity

$k =$ the stiffness of spring

$\gamma_o, \gamma_1 =$ dimensionless coefficients of dashpots

$\mu_O, \mu_1 =$ dimensionless coefficients of masses

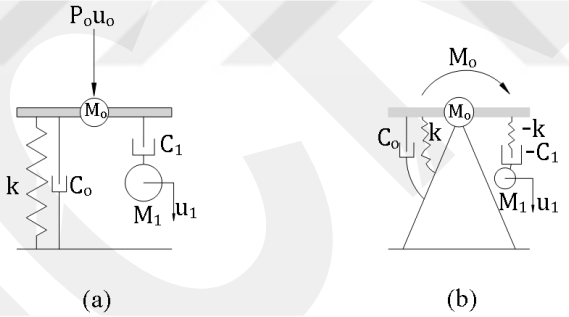

Figure 2.9 Equivalent spring-dashpot models with an internal degree of freedom: (a) discrete-element model for translational cone; (b) discrete-element model for rotational cone

Table 2.3 Static-stiffness and dimensionless coefficients of a spring-dashpot-mass model for the disk on half-space

Motion	Static stiffness K	Dimensionless coefficients of			
		Dashpots		Masses	
		γ_0	γ_1	μ_o	μ_1
Horizontal	$\frac{8Gr_o}{2-\nu}$	$0.78-0.4\nu$	-	-	-
Vertical	$\frac{4Gr_o}{2-\nu}$	0.8	$0.34-4.3\nu^4$	$\nu < \frac{1}{3}$: 0 $\nu > \frac{1}{3}$: $0.9\left(\nu-\frac{1}{3}\right)$	$0.4-4\nu^4$
Rocking	$\frac{8Gr_o^3}{3(1-\nu)}$	-	$0.42-0.3\,\nu^2$	$\nu < \frac{1}{3}$: 0 $\nu > \frac{1}{3}$: $0.61\left(\nu-\frac{1}{3}\right)$	$0.34-0.2\nu^4$
Torsional	$\frac{16Gr_o^3}{3}$	0.017	0.291	-	0.171

2.3 Static Soil-Structure Interaction

The modulus of the subgrade reaction is a fundamental soil property. It is a function of soil elastic properties which are the initial response and the long-term response due to the soil unification from the permanent loading, loading intensity which influences the long-term unification settlement, the amount of surface area loaded and load shape over which the load is applied, and the stiffness of the slab which influences the distribution of the soil bearing pressure. The following equation represents this relationship between the modulus of the subgrade reaction and the settlement and pressure:

$$P = K * \Delta \tag{2.18}$$

where

$P =$ the reaction pressure

$\Delta =$ the deflection (settlement)

$K =$ the modulus of subgrade reaction

In order to obtain the modulus of subgrade reaction, the plate load test is performed. In this test, the soil layer is subjected to the compressive stress applied through a number of rigid plates of increasing sizes. Next, the deflections are measured for various stress values. After this procedure, a graph is plotted as the average settlement in mm on the x-axis and the load in kN/mm^2 on the y-axis. The pressure p

corresponding to a settlement of 1.25 mm is calculated from the graph. The modulus of subgrade reaction K is calculated from Eq. (2.18).

Walker and Holland [46] stated that using the subgrade reaction (Winkler foundations) had other analytical limitations such as the displacement at one location did not affect the settlement at other points. In their opinion, the Winkler foundations are not correct. Winkler foundations are shown in Figure 2.10.

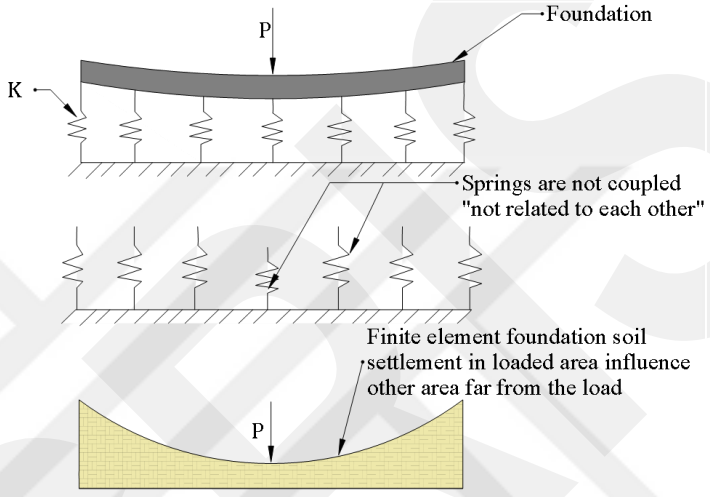

Figure 2.10 Uncoupled and coupled analytical systems

In this case, the Winkler foundations are considered as an uncoupled foundation because the springs do not interact simultaneously. By contrast, the soil settlement can be considered as coupled by using the solid finite element foundation model. Determination of the convenient subgrade reaction values for wide area sustained loading is more complex compared to short-term loadings. Terzaghi [47] concluded that the soil settlements utilized to modify the plate load subgrade reaction were settlements over the nearly uniform soil pressure elevation, as illustrated in Figure 2.11, which is used to determine the subgrade reaction.

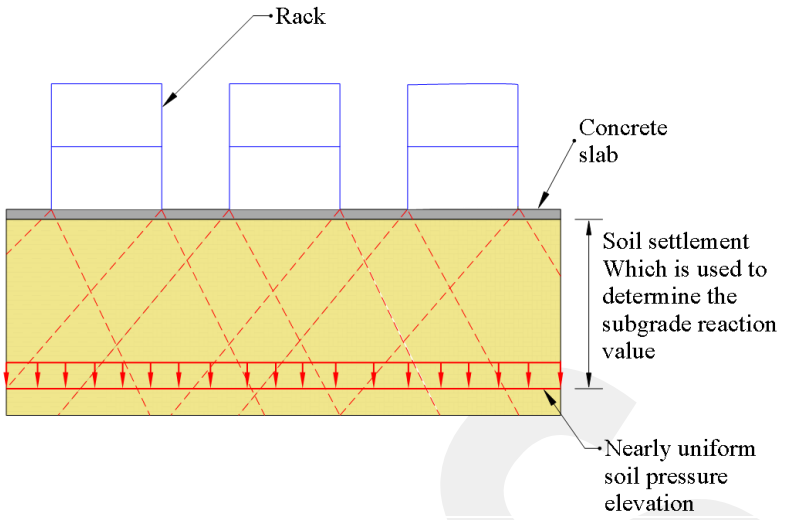

Figure 2.11 Soil settlements used for evaluating subgrade reaction for wide area long-term loads

2.4 Dynamic Soil-Structure Interaction

Seismic waves are generated when a fault ruptures, and they propagate in all directions from their source. Wave propagation of seismic waves through the soil medium, the foundation and the structure are illustrated in Figure 2.12. Incoming seismic waves (indicated as E_0) through the soil medium transform into two types when they hit to the bottom of the foundation. The first type is transmission waves (indicated as E_1), which enter in the structure. The second type is reflecting waves (indicated as F_0), which are reflected back the soil. When the transmission waves enter the structure, they travel in the upward direction which induces the structure to vibrate. After that, waves reflect at the top and travel back down to the foundation of the building (indicated as F_1). At this stage, soil-structure interaction phenomenon happens. Soil structure interaction (SSI) is the process which the response of the soil influences the motion of the structure and the motion of the structure influences the response of the soil. Again, a part of the wave is transmitted into the ground, however, the rest is reflected and starts moving in the upward direction through the structure (indicated as F_2). The waves which are transmitted to the ground are radiation waves (indicated as R_1). When the radiation waves are of small magnitude, the seismic waves transmitted into the structure continue to be trapped in it, then the structure starts to vibrate continuously for a long time, similar to lightly damped structures. Radiation waves produce a damping which is known as radiation damping of the soil. Radiation damping

increases the total damping of the soil-structure system in comparison to the building itself.

Basically, two essential interactions are involved in the phenomenon of the dynamic soil-structure interaction which defined in the following subsections.

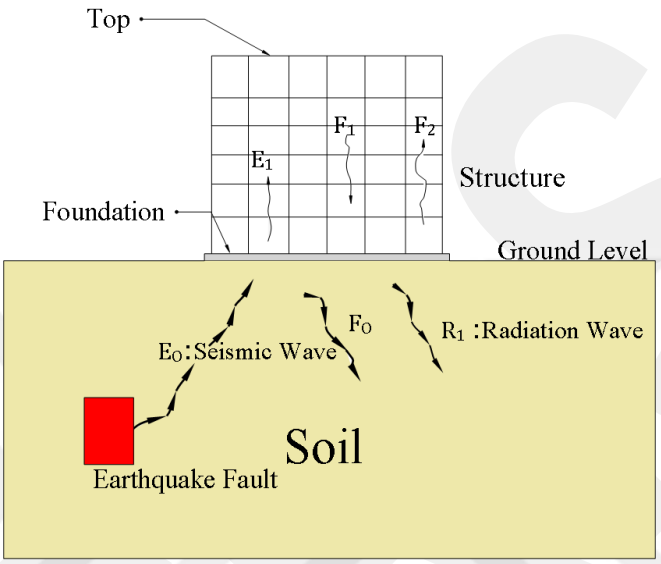

Figure 2.12 Wave propagation during soil-structure interaction

2.4.1 Inertial Interaction

Inertial forces are generated by foundation motion during earthquakes. They are distributed along the height of the structure, causing a resultant base shear and an overturning moment at the foundation, which leads the compliant soil to deform which in turn increases translations and rotations at the base of the structure. As a result, structures become more flexible when the vibration periods increase. Foundations which are subjected to earthquake excitation act as a finite source of vibration that transmits waves propagating through the soil towards infinity. There are six degrees of freedom of the foundation motion that allows the deformation to propagate away from the structure. The compliance of soil could be modeled by using springs and dashpots. The effect of soil-structure interaction can be estimated by comparing the system without and with springs and dashpots.

The inertial interaction could be analyzed as illustrated in Figure 2.13 (a) using a single degree of freedom structure of mass m and lateral stiffness K, and height h on a fixed foundation. The system is excited by static force F which cases deflection Δ. The following equation represents the relationship between the force and the deflection:

$$\Delta = \frac{F}{K} \tag{2.19}$$

The undamped natural vibration frequency ω and the period T of the structure are defined as:

$$\omega = \sqrt{\frac{k}{m}} \tag{2.20}$$

$$T = \frac{2\pi}{\omega} = 2\pi\sqrt{\frac{m}{k}} \tag{2.21}$$

After substituting Eq. (2.19) into Eq. (2.20) and Eq. (2.21), square of the period is obtained as:

$$T^2 = (2\pi)^2 \frac{m\,\Delta}{F} \tag{2.22}$$

In Figure 2.13 (b), the same structure is considered with vertical, horizontal and rotational springs at its foundation. These springs represent the effects of soil flexibility against a rigid foundation. The vertical spring stiffness in the z-axis is K_z, while the horizontal spring stiffness in the x-axis is K_x, and the rotational spring in the $x-z$ plane is K_{yy}. When the mass is subjected to a force F in the x-direction, the structure deflects. The base shear deflects the horizontal spring by u_f, while the base moment deflects the rotational spring by θ. The base moment can be obtained by multiplying the applied force by the height of the structure. The total deflection Δ' with respect to the free-field at the top of the structure can be obtained from Eq. (2.23) or Eq. (2.24).

$$\Delta' = \frac{F}{K} + u_f + \theta.h \tag{2.23}$$

$$\Delta' = \frac{F}{K} + \frac{K}{K_x} + \left(F.\frac{h}{K_{yy}}\right) h \tag{2.24}$$

The flexible base period T' is obtained after substituting Eq. (2.24) into Eq. (2.22):

$$T' = (2\pi)^2 \frac{m\Delta'}{F} = (2\pi)^2 m \left(\frac{1}{K} + \frac{1}{K_x} + \frac{h^2}{K_{yy}}\right) \tag{2.25}$$

By combining Eq. (2.21) and Eq. (2.24), the following equations are obtained:

$$\left(\frac{T'}{T}\right)^2 = K\left(\frac{1}{K} + \frac{1}{K_x} + \frac{h^2}{K_{yy}}\right)$$

$$\frac{T'}{T} = \sqrt{\left(1 + \frac{K}{K_x} + \frac{Kh^2}{K_{yy}}\right)} \tag{2.26}$$

Eq. (2.26) can be employed for the multi-degree of freedom (MDOF) structures by using the height h, as the height of the center of the mass. This height is called the effective model height which is approximately used as 0.7 or two-thirds of structure height in ASCE codes.

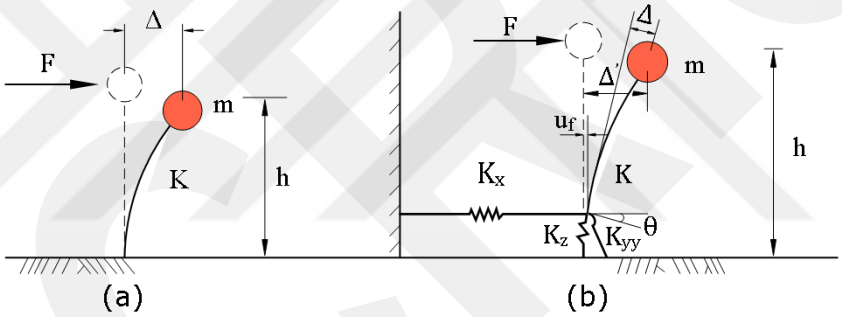

Figure 2.13 A simplified model for analysis of inertial interaction: (a) fixed-base model; (b) model with vertical, horizontal, and rotational flexibility at its base

2.4.2 Kinematic interaction

When the earthquake ground motion in the free-field varies over the area corresponding to that of the rigid foundation, then it could be constrained and modified by the rigid foundation. This deviation from free field motion is termed as kinematic interaction between the soil and foundation. In other words, the kinematic interaction resulted from the presence of a stiff foundation on or in the soil medium. The deviation occurs because of embedment effects as well. The kinematic interaction deals with wave propagations. Wave propagation affects the structure foundation considering the geometry and stiffness properties of the structural foundation and soil. The seismic wave propagation happens by deformation in the soil medium. The foundation cannot deform by the same amount as the soil because of the foundation is assumed to be very

rigid in comparison to the soil deposits. The effects which result from the wave propagation is known as kinematic interaction effects (Gazetas [29]). The analysis output from the kinematic interaction is an effective input motion, which is called as foundation input motion (FIM). The mathematical transformation from the free field motions to the foundation input motions can be performed by a frequency dependent transfer function which is a site-specific curve (Ghalimath et al. [48]).

Kinematic interaction is explained by tau (τ) effect in Clough and Penzien [49]. This kinematic interaction is due to translational excitation along the rigid slab. In Figure 2.14, the shear wave moves in the y-direction producing ground motion in the x-direction that various with y-direction. Tau (τ) is defined as the ratio of the amplitude component of translational motion to the amplitude of a harmonic component of free field motion which is formed in the following equation:

$$\tau = \frac{1}{\alpha'} \sqrt{2(1 - cos\alpha')} \tag{2.27}$$

$$\alpha' = \frac{w\, D}{V_a} = \frac{2\pi\, D}{\lambda(w)} \tag{2.28}$$

where

$V_a =$ apparent wave velocity

$D =$ the dimension of the base in the y-direction

$\lambda(w) =$ the wavelength which can be obtained from the following equation:

$$\lambda(w) = \frac{2\pi\, V_a}{w} \tag{2.29}$$

In the case where the foundation dimension is very small compared with the wavelength of the ground motion, the values of τ decreases. Therefore, the tau effect can be negligible. In contrast, when the foundation dimension is large enough compared to the wavelength of the ground motion, the tau effect should be taken into consideration. In this case, the foundation motion could be less than the free-field ground motion. The kinematic interaction produces rocking and torsion modes of vibration in the structure. These two modes do not exist in the case of free field motion.

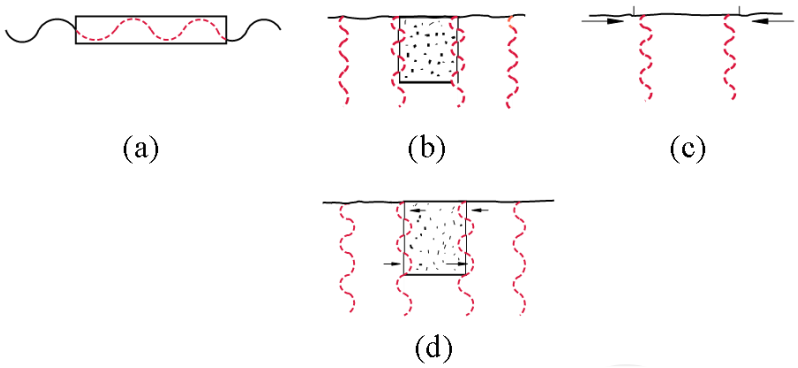

Figure 2.14 Kinematic interaction: (a) vertical motion modified, (b) horizontal motion modified, (c) incoherent ground motion prevented, and (d) rocking motion

Kramer [50] proposed a computation procedure to calculate the deformation caused by the kinematic interaction assuming that the structure and foundation with stiffness don't have masses. Eq. (2.30) represents this assumption.

$$[M_{soil}]\,\{\ddot{u}_{KI}\} + [K]\{u_{KI}\} = -[M_{soil}]\,\ddot{u}_b(t) \qquad (2.30)$$

where

$[M_{soil}]$ = the mass matrix assuming that the structure and foundation are massless

$[u_{KI}]$ = the foundation input motion

K = the stiffness matrix

$\ddot{u}_b$ = the acceleration at the boundary

2.4.2.1 Free field ground motion (FFM)

The free field ground motion (FFM) refers to the ground motion that is located far enough from any foundation and is not affected by the presence of any foundation. In other words, the free field ground motion is the ground motion which is not affected by the motion of any nearby structures.

2.4.2.2 Foundation input motion (FIM)

When the ground start to vibrate due to seismic waves, the motion of the foundation and the free ground become different from each other, with the foundation motion becomes smaller. This foundation motion is termed as a foundation input motion (FIM) which is used in the analysis of the structure. Kinematic soil-structure interaction is a result of the inability of a rigid foundation to adapt to the deformation pattern of the soil at the foundation-soil interface. Therefore, the foundation cannot

follow the FFM. The motion of the foundation, neglecting inertial interaction, is known as the foundation input motion. The differences between the FFM and the FIM are referred as the kinematic interaction effects.

2.4.3 Radiation Damping

In addition to period lengthening, the dynamic response of the structure is also affected by the damping resulting from soil-foundation interaction (referred as foundation damping). This damping consists of two parts: (i) contributions from soil hysteresis (hysteretic damping), and (ii) radiation of energy away, in the form of stress waves, from the foundation (radiation damping). It should be noted that the radiation damping depends on the properties of the structure, the geometry of the foundation soil contact area, and properties of the underlying soil medium. Radiation damping occurs when the fundamental period of the soil is greater than the effective fundamental period of the structure. Radiation damping causes increasing the total damping of the soil-structure system in comparison to the building itself. Eq. (2.31) represents the fundamental period of the soil.

$$T_{soil} = \frac{4\,H_s}{V_s} \tag{2.31}$$

where

$H_s =$ the depth of the soil layer

$V_s =$ the shear wave velocity of the underlying soil

Çelebi [51] concluded that radiation damping could be substantial and beneficial for the buildings. He referred that it should be incorporated into the design and analysis procedures.

2.5 Boundary Conditions

In order to model the semi-infinite soil medium, artificial boundaries with finite degrees of freedoms should be used. This approach leads to a manageable model size. Five types of boundary conditions that are commonly used in the literature are described in the following subsections.

2.5.1 Free Boundaries

In the free boundary condition, the points at the side of the soil model are free to move individually without any constraints.

2.5.2 Tied Boundaries

In this boundary condition, the two opposite points which are located at the two sides of the soil model are tied to each other. Therefore, their horizontal and vertical displacements are the same during the seismic excitation. This boundary condition is based on an assumption that neglects the effect of the structure on the soil vibration far away from the structure. Figure 2.15 illustrates the tied boundary condition.

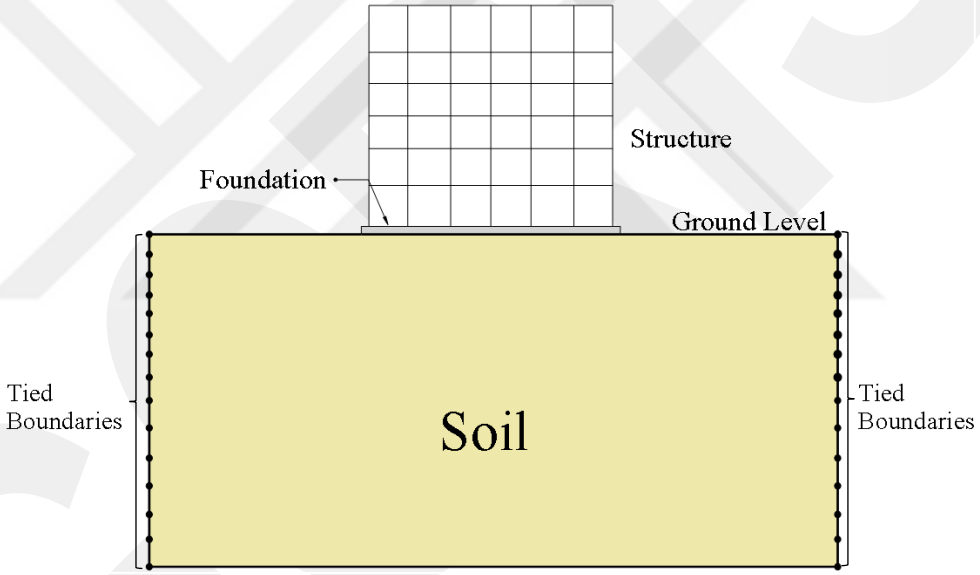

Figure 2.15 Tied boundary condition

Moradi [52] carried out a series of test runs on a finite element model which has only the soil layer to generate motions that fed back to the bottom of the soil layer in SAP2000 model. Then, he compared the generated motions with the initial free field spectrum. Among three types of lateral boundary conditions free, tied, and transmitting condition, the tied boundary condition shows a good agreement with the original record for the horizontal component of the considered earthquake. Therefore, the tied boundary condition is used at the sides and pined boundaries at the bottom of direct model in this study.

2.5.3 Transmitting Boundaries

In this boundary condition, the viscous dampers are used as transmitting boundaries to represent the truncated soil. The transmitting boundaries are also referred to as absorbing boundaries or viscous dampers. These boundaries have the ability to absorb body waves which propagate toward the boundaries. Lysmer and Kuhlemeyer [53] introduced the damping coefficients of the horizontal and vertical dampers as below:

$$C_h = -\rho\, V_p\, A \tag{2.32}$$

$$C_v = -\rho\, V_s\, A \tag{2.33}$$

$$V_p = \sqrt{\frac{K}{\rho}} \tag{2.34}$$

$$V_s = \sqrt{\frac{G}{\rho}} \tag{2.35}$$

$$G = \frac{E}{2(1+v)} \tag{2.36}$$

$$K = \sqrt{\frac{E(1-v)}{\rho(1+v)(1-2v)}} \tag{2.37}$$

where

C_h = the coefficient of the horizontal viscous damper

C_v = the coefficient of the vertical viscous damper

V_p = the compressive velocity in the soil

V_s = the shear wave velocity in the soil

A = the effective nodal area for the node which is attached to the damper or the total area of each element around the considered node on the boundary.

E = the elastic modulus of the soil material

G = the dynamic shear modulus of the soil material

K = the bulk modulus of the soil material

v = the poisons ratio of the soil material

2.5.4 Free-field Boundaries

The boundary conditions that previously mentioned are designed to absorb outgoing waves. Hence, they can be utilized when the source of excitation is within the model.

While, the free-field boundary condition should be considered when the excitation is originated from outside the model. This outer excitation is defined as an incoming seismic wave. The incoming wave field is specified as a group of independent perpendicular acceleration time histories. These time histories are changed into time-varying tractions and they are applied to the base of the model where they become vertically propagating S- and P-waves, S is secondary wave and P is primary wave. The free-field boundary is represented by two columns at the two sides of the model which are called free-field soil columns (Zienkiewicz et al. and Wolf (e.g. [54], [55])). This technique consists of two columns that are placed in parallel next to the main model and is used to analyze the response of horizontally layered soil/rock systems which is subjected to vertically propagated waves S- and P- waves. As shown in Figure 2.16, the lateral boundaries of the main model are connected to the free-filed boundary conditions by using viscose dashpots. The free-field motions of the columns are converted to the boundary tractions which are applied to the main model. This technique assumes that the information moves from the free field to the main model, not the other way. Therefore, the free field response is not affected by the soil-structure interaction within the main model when the columns are put at some distance from the central region of the main model. In other words, these boundaries should be placed at appropriate distance to reduce wave reflections and obtain free-field conditions. The unbalanced forces that come from the free-field columns are applied to the main model. Both conditions that applied to the left boundary are formed in the following equations:

$$F_x = -\left[\rho\, C_p\left(v_x^m - v_x^{ff}\right) - \sigma_{xx}^{ff}\right]\Delta S_y \tag{2.38}$$

$$F_y = -\left[\rho\, C_s\left(v_y^m - v_y^{ff}\right) - \sigma_{xy}^{ff}\right]\Delta S_y \tag{2.39}$$

where

F_x = the unbalanced force from the free-field conditions to the main model boundary in the x-direction

F_y = the unbalanced force from the free-field conditions to the main model boundary in y-directions

ρ = density of material along the vertical model boundary

C_s = the s wave speed at the left boundary

C_p = the p wave speed at the left boundary

S_y = the mean vertical zone size at the boundary point

v_x^m = the x-velocity of the point in the main model at the left boundary

v_y^m = the y-velocity of the point in the main model at left boundary

v_x^{ff} = the x-velocity of the point in the free field

v_y^{ff} = the y-velocity of the point in the free field

σ_{xx}^{ff} = the mean horizontal free-field stress

σ_{xy}^{ff} = the mean free-filed shear stress

Same equations might be written for the right boundary condition. In this way, plane waves propagate upward without suffering any modifications at the boundary because the free-field boundary provides conditions which are identical to those in infinite models. In the case where the main model differs from that of the free-field because of the surface structure which radiates secondary waves, the dashpots act to absorb energy in a way similar to the action of quite boundaries.

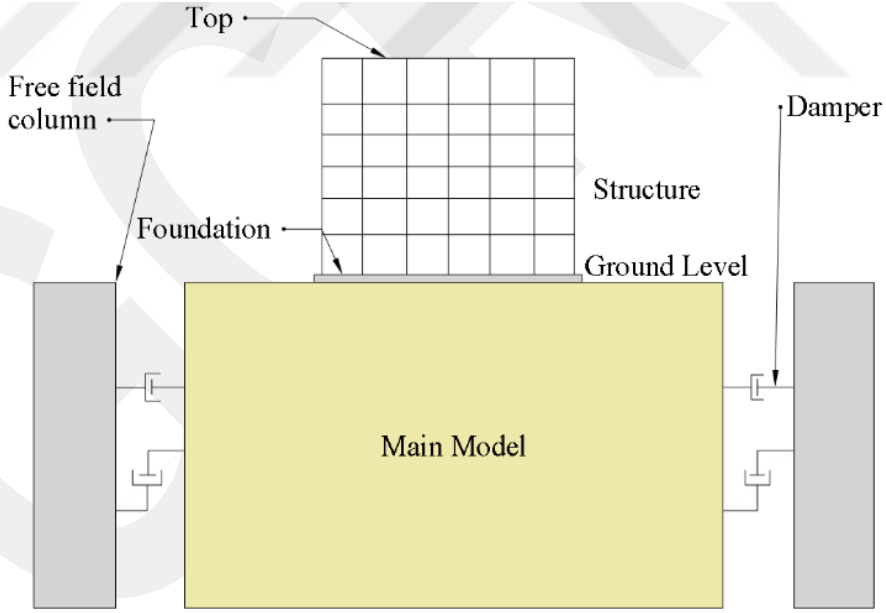

Figure 2.16 Free-field boundary

2.5.5 Rigid Boundary

The rigid boundary is used to model bedrock for dynamic soil-structure interaction. This type of boundary transmits the seismic excitation directly to the soil model

without any modifications. Therefore, it is considered the most appropriate and realistic condition for modeling the bedrock (Kocak and Mengi [56]).

2.6 Site Response Analysis

After a seismic fault ruptures, the waves travel through the earth and refract as they pass through different types of soil until they reach the ground surface and transform into surface waves. The process of the waves traveling upwards through the soil and being modified and amplified is referred to as site response. Some methods of analyzing the response are discussed in the following subsections.

2.6.1 Equivalent Linear Analysis

The linear systems are the most basic systems which adopted to the analysis. The ground motions probably developed near the surface of the soil deposit. These ground motions might be referred primarily to the upward propagation of the shear waves from the underlying rock. If the rock surface, the ground surface, and the boundaries between different soil layers are inclined, the finite element method can be used for the analyses of the response of the soil deposit. While, if the rock surface, the ground surface, and the boundaries between different soil layers are horizontal, the lateral extent of the deposit has no effects on the response and the deposit might be considered as a series of semi-infinite layers. In such cases, the induced ground motions at the base due to seismic excitation are the result of the shear deformations in the soil deposit. In order to represent the soil stress-strain response, the equivalent linear model is used which is based on a Kelvin-Voigt model. Figure 2.17 shows the equivalent linear model.

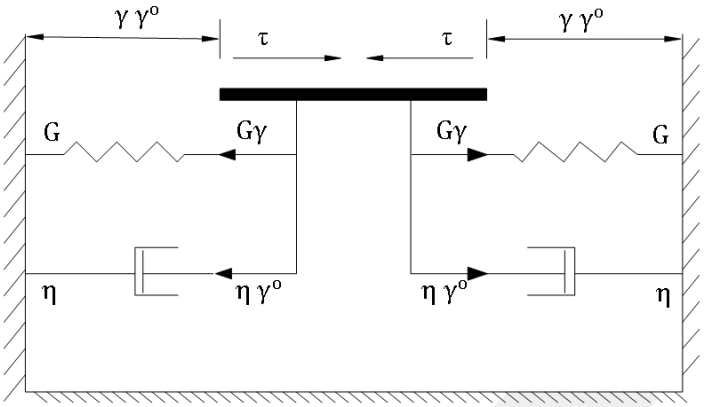

Figure 2.17 Schematic representation of the stress-strain model used in the equivalent-linear model

The relationship between the shear stress τ and the shear strain γ can be written as follows (Bardet et al. [57]):

$$\tau = G\gamma + \eta\dot{y} \tag{2.40}$$

where

$\tau =$ the shear stress

$\gamma =$ the shear strain

$\dot{y} =$ the shear strain's rate

$G =$ the shear modulus

$\eta =$ the velocity

In the one-dimensional shear beam column, the shear strain and its rate are defined from the horizontal displacement $u(z,t)$ at depth z and time t as below:

$$\gamma = \frac{\partial u(z,t)}{\partial z} \tag{2.41}$$

$$\dot{y} = \frac{\partial \gamma(z,t)}{\partial t} = \frac{\partial^2 u(z,t)}{\partial z\, \partial t} \tag{2.42}$$

In the case where harmonic motion exists, the displacement, strain, and strain rate are formed as follows:

$$u(z,t) = U(z)e^{i\omega t} \tag{2.43}$$

$$\gamma(z,t) = \frac{dU}{dz}\, e^{i\omega t} = \Gamma(z)e^{i\omega t} \tag{2.44}$$

$$\dot{y}(z,t) = iw\gamma(z,t) \tag{2.45}$$

where

$U(z)$ = the amplitude of displacement

$\Gamma(z)$ = the amplitude of shear strain

By using Eq. (2.43), Eq. (2.44), and Eq. (2.45), the stress-strain relation (Eq. (2.40)) becomes as follows when the loadings are harmonic:

$$\tau(z,t) = \sum(z)e^{i\omega t} = (G + iw\eta)\frac{dU}{dz}e^{i\omega t} = G^*\frac{dU}{dz}e^{i\omega t} = G^*\gamma(z,t) \quad (2.46)$$

where

G^* = the complex shear modulus

$\sum(z)$ = the amplitude of shear stress

After introducing the critical damping ratio ξ,

$$\xi = \frac{\omega\eta}{2G} \quad (2.47)$$

the complex shear modulus becomes:

$$G^* = G + i\omega\eta = G(1 + 2i\xi) \quad (2.48)$$

During a complete loading cycle, the energy dissipated (W_d) can be written as:

$$W_d = \int_{\tau_c}^{o} \tau \, d\gamma \quad (2.49)$$

The maximum strain energy stored in the system is:

$$W_s = \frac{1}{2}\tau_c\gamma_c = \frac{1}{2}G\gamma_c^2 \quad (2.50)$$

Moreover, the critical damping ratio ξ is expressed in terms of W_d and W_s as:

$$\xi = \frac{W_d}{4\pi W_s} \quad (2.50)$$

2.6.1.1 1D Equivalent Linear Analysis

One-dimensional site response analysis considers only waves propagating in one direction, which is vertical. These waves do not have the ability to handle refraction, therefore, layer boundaries should be perpendicular to the wave propagation direction. Among several programs, SHAKE [58] is the first and one of the most commonly used site response analysis program which performs one-dimensional linear analysis. The one-dimensional motion for vertically propagating shear waves can be written as:

$$P\frac{\partial^2 u}{\partial t^2} = \frac{\partial \tau}{\partial z} \tag{2.52}$$

where

$P =$ the unit mass in any layer

2.6.1.2 2D/3D Equivalent Linear Analysis

In this case, waves propagate in two and three dimensions. QUAD4 and FLUSH (e.g. [59], [60]) are among the programs that can perform two- and three-dimensional site response analysis, respectively.

2.6.2 Nonlinear Analysis

Nonlinear behavior of the soils during the seismic excitation plays a main role in the site response analysis. The nonlinearity occurs in the model when material stress-strain relationship depends on load history which is a plasticity problem, load duration which is a creep problem, and temperature. Moreover, it can occur when the applied load causes large strain, large displacement or rotation. Iwan and Mroz ([e.g. [61], [62]) proposed a model to represent the nonlinear stress-strain curves by utilizing a series of n mechanical elements with different stiffnesses K_i and sliding resistance R_i. Their model is known as the IM model. Figure 2.18 shows the IM model. The model's sliders have increasing resistance (i.e., $R_1 < R_1 < \cdots < R_n$). All the sliders have residual stresses equal to zero at the beginning. Slider i yields when the shear stress τ becomes equal to R_i during the monotonic loading. After that, the slider i saves a positive residual stress equal to R_i. The stress-strain curve is generated by using IM model for two sliders, whereas the tangential modulus H and the corresponding slope changes in steps. The tangential modulus is denoted as relationship between the stress increasement $d\tau$ and strain increasement $d\gamma$, which is formed in the following equation:

$$H = \frac{d\tau}{d\gamma} \tag{2.53}$$

where the tangential modulus H is:

$$H = \begin{cases} H_1 = K_1 & if\ 0 \le \tau < R_1 \\ H_2 = (K_1^{-1} + K_2^{-1})^{-1} & if\ R_1 \le \tau < R_2 \\ H_{n-1} = (K_1^{-1} + K_2^{-1} + \cdots + K_{n-1}^{-1})^{-1} & if\ R_{n-2} \le \tau < R_{n-1} \\ H_n = (K_1^{-1} + K_2^{-1} + \cdots + K_{n-1}^{-1} + K_n^{-1})^{-1} & if\ R_{n-1} \le \tau < R_n \\ 0 & if\ \tau = R_n \end{cases}$$

The stress-strain curve is considered as a backbone curve during the loading process. In the case where the load changes its direction (unloading), the residual stress in slider i decreases. Hence, the slider i yields when its residual becomes equal to -R_i. To calculate the stress-strain curves an algorithm developed by Bardet and Tobita [63] is used. This algorithm calculates the exact value of stress τ independently of the strain increment amplitude $\Delta\gamma$.

In addition, the nonlinear backbone curve can be described in terms of shear modulus G and shear strain γ as below:

$$H_i = \frac{G_{i+1}\gamma_{i+1} - G_i\gamma_i}{\gamma_{i+1} - \gamma_i} \tag{2.54}$$

Assuming that the back-stress α_i is equal to zero at the beginning, R_i is:

$$R_i = G_i\gamma_i \tag{2.55}$$

From Eq. (2.54) and Eq. (2.55), it can be concluded that the maximum shear resistance is:

$$R_n = G_n\gamma_n \tag{2.56}$$

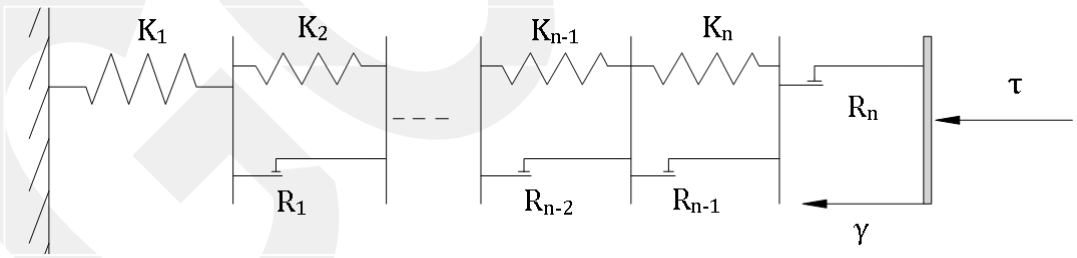

Figure 2.18 Nonlinear site response analysis model used by Iwan [61] and Mroz [62]

2.6.2.1 1D Nonlinear Analysis

There are three analysis programs that can be used for the one-dimensional nonlinear site response analysis. They are DESRA, DMOD, and OpenSees (e.g. [64], [65], [66]).

2.6.2.2 2D/3D Nonlinear Analysis

For two- and three-dimensional nonlinear site response analysis, the available programs are TARA, FLAC, and PLAXIS (e.g. [67], [68], [69]).

2.7 Guidelines for Soil-Structure Interaction in Codes and Standards

Guidelines suggest recommendations for the soil-structure interaction buildings. These recommendations are described in the following sections according to their guidelines.

2.7.1 ASCE 7-10

In the case where the effects of soil-structure interaction are considered, the requirements of this code should be applied in the calculation of the design earthquake forces and corresponding displacements of the structure. It should be noted that if the structure has a flexible-base foundation, the requirements of this guideline should not be used in the structural response model.

The following requirements should be taken into considerations:

1. The base shear, V, should be reduced by ΔV as defined below:

$$V' = V - \Delta V \tag{2.57}$$

$$\Delta V = [C_S - C_S' \left(\frac{0.05}{\beta'}\right)^{0.4} W' \leq 0.3V \tag{2.58}$$

where

$C_S =$ the seismic design coefficient computed by using the fundamental natural period of the fixed-base structure (T)

$C_S' =$ the value of C_S computed by using the fundamental natural period of the flexibly supported structure (T')

$\beta' =$ the effective damping factor for the structure-foundation system.

$W' =$ the effective seismic weight of the structure, that should be used as $0.7W$, except that for structures where the gravity load is concentrated at a single level, the effective seismic weight should be taken equal to W

2. An effective building period T' should be calculated as below:

$$T' = T\sqrt{1 + \frac{K'}{K_y}\left(1 + \frac{K_y(h')^2}{K_\theta}\right)} \tag{2.59}$$

where

$T =$ the fundamental period of the structure

h' = the effective height of the structure which is equal $0.7h$, except that for structures where the gravity load is effectively concentrated at a single level, the effective height should be used as the height to that level

K_y = the lateral stiffness of the foundation

K_θ = the rocking stiffness of the foundation

g = the acceleration gravity

K' = the stiffness of the structure where fixed base at the base, which can be calculated as below:

$$K' = 4\pi^2 \left(\frac{W'}{gT^2} \right) \tag{2.60}$$

3. The effective damping factor β' for the structure-foundation system should be calculated as below:

$$\beta' = \beta_o \frac{0.05}{\left(\frac{T'}{T} \right)^3} \tag{2.61}$$

where

β_o = the foundation damping factor, which is determined by linear interpolation in (ASCE 7-10 Figure 19.2-1)

4. There are many other effects should be determined such as the modified story shears, torsional effects, and overturning moments for the structures without interaction by utilizing the reduced lateral forces.

5. The modified deflection δ_x' should be determined as below:

$$\delta_x' = \frac{V'}{V} \left[\frac{M_o h_x}{K_\theta} + \delta_x \right] \tag{2.62}$$

where

M_o = the overturning moment at the base calculated by using the unmodified seismic forces and not including the reduction allowed in the design of the foundation

h_x = the height above the base to the considered level

δ_x = the deflection of the fixed-base structure calculated by using the unmodified seismic forces

6. The P-delta effects and the modified story drifts should be calculated by using the modified story shears and deflections.

2.7.2 ATC-40

In this guideline, the basic steps to determine the stiffness properties of bearing geotechnical components are explained. These properties represent the stiffness and strength behavior of geotechnical components to be used in models of foundation elements. The bearing stiffness calculation steps are summarized below:

1. Determination the uncoupled total surface stiffness K_i, of the foundation element through assuming that the foundation is a rigid plate bearing at the surface of semi-infinite elastic half-space. Stiffness equations are listed in ATC-40 Table 10.2.

2. After determination the uncoupled total surface stiffnesses, modifications are applied to them by multiplying the stiffnesses by embedment factors for generating the uncoupled total embedment stiffnesses K_i. Embedment factors are listed in ATC-40 Table 2.3.

3. Calculation of the individual distributed stiffness intensities, K_i, by dividing the uncoupled total embedment stiffness K_i, by the corresponding area of contact or moment of inertia as follows:

$$K_z = \frac{K_z}{LB} \tag{2.63}$$

$$K_y = \frac{K_y}{Ld} \tag{2.64}$$

$$K_x = \frac{K_x}{Bd} \tag{2.65}$$

$$K_{\theta x} = \frac{K_{\theta x}}{I_x} \tag{2.66}$$

$$K_{\theta y} = \frac{K_{\theta y}}{I_y} \tag{2.67}$$

where

$L =$ the length of footing

$B =$ the width of the footing

d = the thickness of footing

I_x = the moment of inertia in the x-direction

I_y = the moment of inertia in the y-direction

4. Making a comparison of the vertical stiffness intensities K_z, $K_{\theta x}$, and $K_{\theta y}$. Generally, the stiffness intensities are not equal. In the case where two-dimensional analysis exists, one of the rotational intensities is not used. If the difference between the vertical translational stiffness intensity, K_z, and the vertical rotational stiffness intensity, K_θ, is small, a representative average, might be used in the sixth step. Whereas, if the difference is large, one of them may be used in sixth step when the footing acts primarily in vertical translation or rotation. While, if the difference is large and the actions are highly coupled, the approximate procedure in fifth step is used for refining the component stiffnesses.

5. Creating end zones of the rectangular footings. The end zone length is one-sixth of the footing width, as shown in Figure 2.19. The vertical intensity in the middle zone is equal to the vertical translational of an infinitely long strip footing which is $\frac{L}{B} = \infty$. Whereas, the vertical stiffness intensity in the end zones on the vertical translational stiffness is $\frac{B*B}{6}$ of the isolated plate.

where

K = the appropriate stiffness per unit length for the end or middle zones

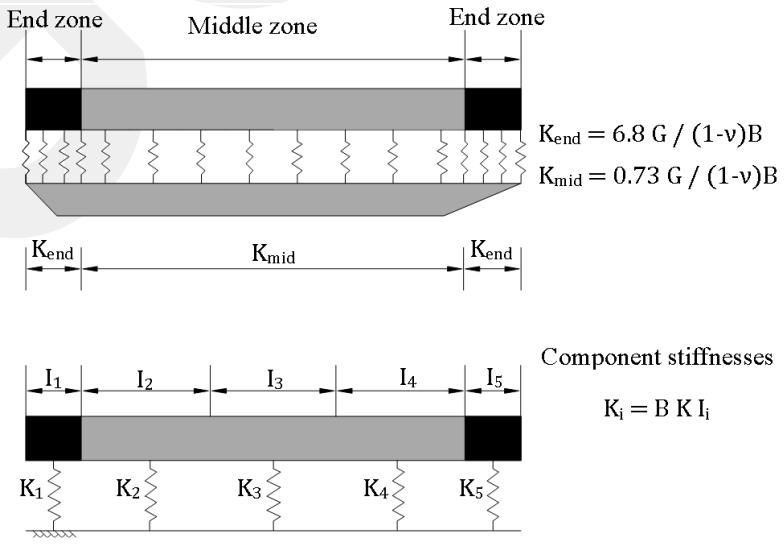

Figure 2.19 Winkler component model of rectangular spread footing

6. Calculation of the individual geotechnical component stiffnesses by multiplying the appropriate stiffness intensity by the spacing of the components in every direction.

In this guideline, the shear modulus, G, can be calculated as follows:

$$G = \frac{E}{2(1+\upsilon)} \tag{2.68}$$

where

E = the modulus of elasticity

υ = Poisson's ratio can be obtained from Table 10.4 in ATC-40 for typical soils

The initial shear modulus, G_0, represents the relationship between the shear wave velocity at low strain, V_s, and the mass density of the soil, P, as below:

$$G_o = P * V_s^2 \tag{2.69}$$

In the case where mass density is converted into unit weight, γ, then the initial shear modulus is calculated as follows:

$$G_o = \frac{\gamma}{g} V_s^2 \tag{2.70}$$

where

g = the acceleration due to gravity

2.7.3 FEMA 356

According to FEMA 356, soil-structure interaction should be considered for the buildings if the increase in the fundamental period due to SSI results in an increase in spectral acceleration. The effects of damping can be neglected in the calculation of soil-structure interaction when the SSI effects are required to be calculated. The soil-structure interaction might modify the seismic demand on the structure. The effects of soil-structure interaction on structures should be evaluated for the near-field and soft soil sites in which the increase in period because the SSI increases the spectral accelerations. Two procedures are adopted by this guideline the simplified and the explicit modeling procedure. When the simplified procedure is used to calculate the SSI effects, the calculation should conform to the procedure in ASCE 7-10 using effective fundamental damping ratio and the effective fundamental period of the

foundation-structure system. In the case where the simplified procedure is used, the reduction in seismic demands on components and elements should not exceed 25% of the demands obtained without the soil-structure interaction effects. In order to calculate the SSI effects, the explicit modeling shall be used to model the stiffness and damping of individual foundation elements explicitly. The foundation stiffness parameters should conform with the requirements of Section 4.4.2 of FEMA 356. Instead of using explicit modeling damping, the effective damping ratio β of the structure-foundation system should be calculated using the simplified procedure. The damping ratio which is used for individual foundation elements should not be more than the value that is used for the elastic superstructure. The effective damping ratio of the foundation-structure system should be utilized to account the spectral demands for the nonlinear static procedure (NSP). In the case where the simplified procedure is employed to calculate the effective damping ratio, the reduction in seismic demands should not be more than 25% of the demands that is calculated without the soil-structure interaction effects.

2.7.4 FEMA 450

This guideline has been based on the ASCE code. Hence, this guideline recommends the same requirements as ASCE 7-10 to be applied in the case of soil-structure interaction.

CHAPTER 3

SOIL MODEL AND SEISMIC EXCITATION

In this chapter, the modeling of the soil medium and the seismic excitation considered in this study are described.

3.1 Modeling of Soil Medium

3.1.1 Soil Profiles

Soil medium is often considered either as homogeneous isotropic linear elastic half-space (uniform soil profile) or as layered linear elastic half-space (layered soil profile) in most studies in the soil-structure interaction literature. In the following subsections, these two soil models are briefly described. In this study, only homogeneous isotropic linear elastic half-space is considered.

3.1.1.1 Homogeneous Isotropic Linear Elastic Half-Space (Uniform Soil Profile)

The homogeneous isotropic elastic half-space models are used for soil idealization. There are two parameters which are used in these models, modulus of elasticity $\boldsymbol{E}$ and poisson's ratio υ. The modulus of elasticity associates the deformation in the soil and the stresses applied to soil in the case where these are in the same direction. The horizontal deformation in the medium is related to the stress applied to the medium in the vertical direction and vice versa. This relationship is expressed by Poisson's ratio. In order to represent the soil as a medium having homogeneous isotropic properties, a half-space model is created as a continuum elastic body with infinite depth and infinite horizontal dimensions. In this study, three cases are considered which are soft, medium, and hard soil model.

3.1.1.2 Layered Linear Elastic Half-Space (Layered Soil Profile)

A half-space is the geometry of structure with one side infinite or semi-infinite. The layered half-space is a structure having multi-layers within the half-space. To model the layered elastic half-space, four-node for two dimensional or eight-node for three dimensional solid elements are used. Elements are based on fully integrated formulation having three degrees of freedom per node. In this study, two cases are considered. The first case is a soft layer placed on a hard layer, as shown in Figure 3.1 (a). The second case is a soft layer placed on a hard layer then a hard layer placed on the soft layer, as shown in Figure 3.1 (b). Every layer has its own characteristics as listed in Table 3.1.

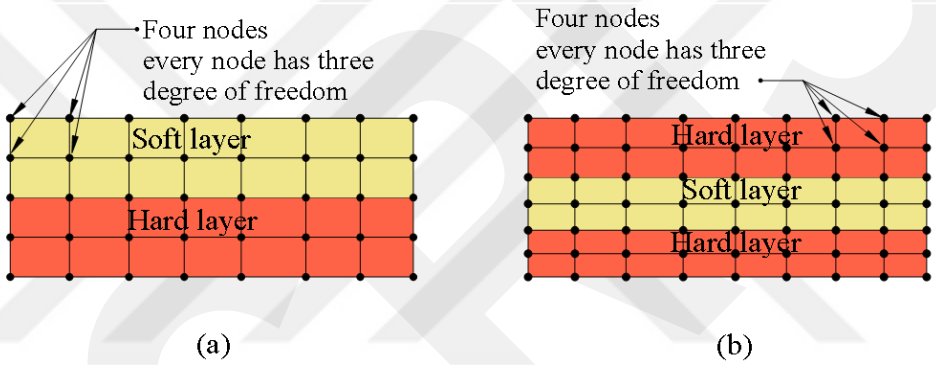

Figure 3.1 Layered linear elastic half-space soil cases (2D Model): (a) soft on hard; (b) hard on soft on hard

3.1.2 Elastic Continuum Model

In continuum mechanics, the continuum is defined as a continuously distributed matter through space. Hook's law describes the simplest elastic continuum with the constitutive relation of linear elastic isotropic behavior (Irgens [70]). The elastic medium has infinite compression and tension capacity without failure criteria. There are many constitutive relations with different failure criteria in compression and tension that appropriately capture soil behavior such as Mohr-Coulomb constitutive relation. Reissner [71] developed a solution for a simplified continuum having finite height. The following equation for an elastic medium presenting soil:

$$q(x,y) - \frac{G_s\, H^2}{12\, E_s}\nabla^2 q(x,y) = \frac{E_s}{H} w(x,y) - \frac{G_s\, H}{3}\nabla^2 w(x,y) \qquad (3.1)$$

where

H = the height

E_s = the elasticity modulus

G_s = the shear modulus

q = the distributed load

w = the vertical surface displacement at any point

The elastic medium is assumed as weightless in the Reissner equation (Horvath and Colasanti [72]). Shear and horizontal normal stresses are zero also the horizontal displacements at the top and the bottom of the medium. Therefore, Reissner differential equation shall be applied near the surface only and it is not efficient for studying stresses inside the medium (Teoduro [73]). A continuum model can be analyzed with numerical methods such as FEM and BEM method for soil-structure analysis.

3.1.2.1 Soil Elements

The soil can be defined as a continuum material and continuity of the soil-structure corresponds to the transverse shear stress that is not taken into consideration in Winkler models due to the presence of independent springs. The subgrade is modeled by using the solid plane strain elements with a linear elastic isotropic material.

3.1.2.2 Interface Elements

The interface elements have been formulated to idealize interfacial behavior between the underlying soil and foundation beam element supporting the plane framed superstructure. The presence of the interface elements is important to get the practical and real nature behavior of structures applied to the lateral load (Shoaei et al. [74]). Many types of joint elements have been proposed and formulated for different applications in the case where the interfacial behavior has been concerned. Generally, the interface elements have been categorized into two main types, known as nodal interfaces, zero-thickness and continuum elements (thin layer elements) (Wang and Wang [75]).

In order to model the gap elements, two parameters should be specified the spring constant or stiffness, K, and the gap separation, d. The interface elements are illustrated in Figure 3.2.

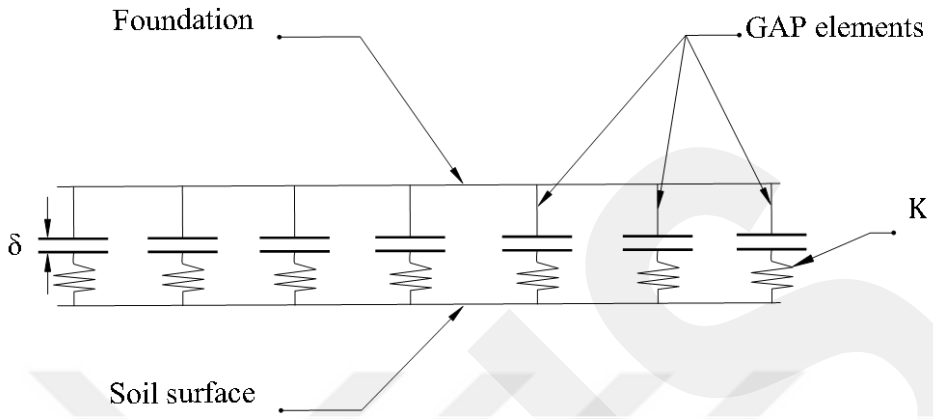

Figure 3.2 Interface gap elements

The force deformation relation for gap element is given as below:

$$f = \begin{cases} K(d+\delta) & if\ d+\delta < 0 \\ 0 & otherwise \end{cases}$$

where

δ = the initial gap separation ($\delta \geq 0$)

K = contact stiffness

3.1.2.3 Lateral Boundary Conditions

The artificial absorbing boundaries have been often used to represent the free-field response. One of the widely used boundaries is the viscous boundary of Lysmer and Kuhlemeyer [53]. This boundary is described by two series of dashpots oriented normal and tangential to the boundary of the mesh. In this approach, the viscous boundaries are suitable for harmonic and non-harmonic wave due to their frequency independence (Kontoe et al. [76]).

3.1.2.4 Bedrock Boundary Condition

In the bottom surface of the subgrade, a rigid condition is assumed. To represent the rigid bedrock condition, the bottom surface of the subgrade is restricted in the tangential and vertical direction.

3.1.3 Winkler Model using Foundation Impedances

In the soil structure interaction problem, the first step is an evaluation of the foundation impedance corresponding to each mode of vibration. In the case where the foundation is rigid and soil is much softer than the foundation, there are six modes of vibration which are three translational (dynamic displacements over the x, y, and z-axis) and three rotational (dynamic rotations around the same axes). For each mode, the soil can be substituted by a dynamic spring of stiffness K and by a dashpot of modulus C for the dynamic analysis (Mylonakis et al. [77]). To find the dynamic stiffness functions, approximate formulas are proposed for describing the variation with frequency of the dynamic stiffnesses of foundations. Hence, Mylonakis, et al. [77] prepared formulas to calculate the dynamic impedances for different shapes of the foundation by fitting mathematical expressions to accurate numerical solutions. Pais and Kausel (1988) [78] proposed impedance calculation formulas as well.

3.1.3.1 Static Stiffness of Rigid Footings

The proposed static stiffnesses of rigid footings by Pais and Kausel [78] are presented in Table 3.2.

Table 3.1 Static spring stiffnesses for arbitrarily shaped foundations on surface of homogeneous half-space

Stiffness DOF	Pais and Kausel (1988)
$K_{z,sur} =$	$\frac{GB}{1-\upsilon}\left[3.1\left(\frac{L}{B}\right)^{0.75}+1.6\right]$
$K_{y,sur} =$	$\frac{GB}{2-\upsilon}\left[6.8\left(\frac{L}{B}\right)^{0.65}+0.8\left(\frac{L}{B}\right)+1.6\right]$
$K_{x,sur} =$	$\frac{GB}{2-\upsilon}\left[6.8\left(\frac{L}{}\right)^{0.65}+2.4\right]$
$K_{zz,sur} =$	$GB^3\left[4.25\left(\frac{L}{B}\right)^{2.45}+4.06\right]$
$K_{yy,sur} =$	$\frac{GB^3}{1-\upsilon}\left[3.73\left(\frac{L}{B}\right)^{2.4}+0.27\right]$
$K_{xx,sur} =$	$\frac{GB^3}{1-\upsilon}\left[3.2\left(\frac{L}{B}\right)+0.8\right]$

Table 3.1 (continued)

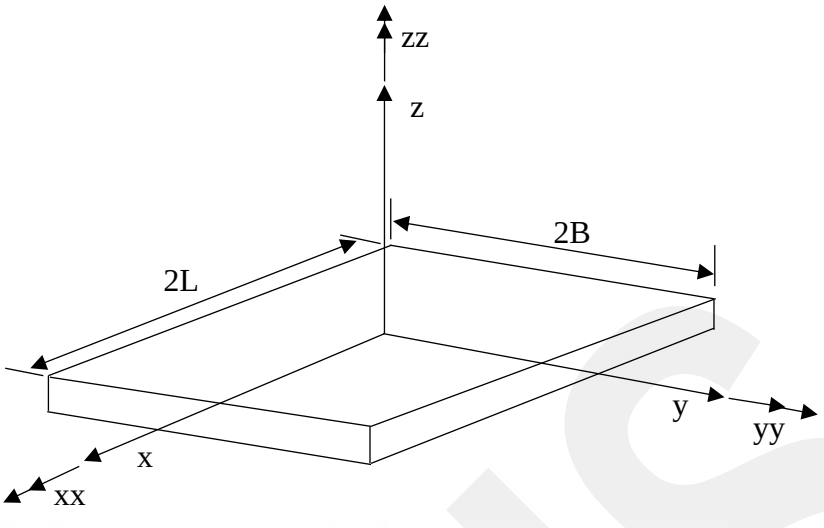

where

$K_{z,sur}$ = Translation along z-axis

$K_{y,sur}$ = Translation along y-axis

$K_{x,sur}$ = Translation along x-axis

$K_{zz,sur}$ = Torsion about z-axis

$K_{yy,sur}$ = Rocking about y-axis

$K_{xx,sur}$ = Rocking about x-axis

$x = \frac{Ab}{4L^2}$

Ab = Area of the foundation considered

B and L= Half-width and half-length of a rectangular foundation, respectively

$J_t = I_x + I_y$ polar moment of inertia of the soil-foundation contact surface

I_i= area moment of inertia of soil-foundation contact, i refers to the axis

G = Shear modulus

In the case where the foundation is embedded in the soil medium, correction factors should be used for embedment case. For each degree of freedom $K_{emb} = \eta K_{sur}$ In the following Table embedment factors are shown according to Pais and Kausel [78].

Table 3.2 Embedment correction factors for static spring stiffness of rigid footings

Stiffness DOF	Pais and Kausel (1988)
$\eta_z =$	$\left[1.0 + \left(0.25 + \frac{0.25}{\frac{L}{B}}\right)\left(\frac{D}{B}\right)^{0.8}\right]$
$\eta_y =$	$\left[1.0 + \left(0.33 + \frac{1.34}{1 + \frac{L}{B}}\right)\left(\frac{D}{B}\right)^{0.8}\right]$
$\eta_x =$	η_y
$\eta_{zz} =$	$\left[1.0 + \left(1.3 + \frac{1.32}{\frac{L}{B}}\right)\left(\frac{D}{B}\right)^{0.9}\right]$
$\eta_{yy} =$	$\left[1.0 + \frac{D}{B} + \left(\frac{1.6}{0.35 + \left(\frac{L}{B}\right)^4}\right)\left(\frac{D}{B}\right)^2\right]$
$\eta_{xx} =$	$\left[1.0 + \frac{D}{B} + \frac{1.6}{0.35 + \frac{L}{B}}\left(\frac{D}{B}\right)^2\right]$

where

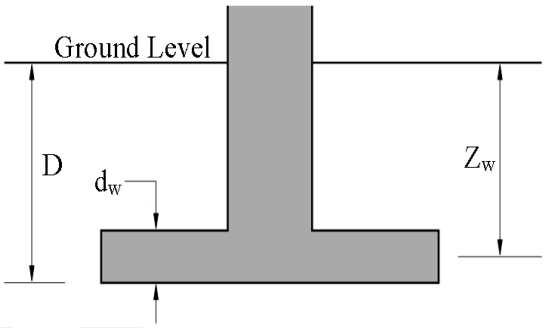

η_z = Translation along z-axis

η_y = Translation along y-axis

η_x = Translation along x-axis

η_{zz} = Torsion about z-axis

η_{yy} = Rocking about y-axis

η_{xx} = Rocking about x-axis

D = the depth of foundation

d_w = the height of effective side wall contact (may be less than total foundation height)

z_w = the depth to the centroid of effective sidewall contact

A_w = the sidewall-solid contact area, for constant effective contact height, d_w along perimeter

3.1.3.2 Dynamic Stiffness and Radiation Damping Ratios of Rigid Footing

The proposed dynamic stiffness modifiers and radiation damping coefficients of rigid footings by Pais and Kausel [78] are presented in Table 3.3.

Table 3.3 Dynamic stiffness modifiers and radiation damping ratios for rigid footings (adapted from Pais and Kausel, 1988)

DOF	Surface Stiffness Modifiers	Radiation Damping
$\alpha_z =$	$1.0 - \left[\dfrac{\left(0.4 + \dfrac{0.2}{\frac{L}{B}}\right)a_o^2}{\left(\dfrac{10}{1 + 3\left(\frac{L}{B} - 1\right) + a_o^2}\right)}\right]$	$\beta_z = \left[\dfrac{4\psi\left(\frac{L}{B}\right)}{\frac{K_{z,sur}}{GB}}\right]\left[\dfrac{a_o}{2\alpha_z}\right]$
$\alpha_y =$	1.0	$\beta_y = \left[\dfrac{4\left(\frac{L}{B}\right)}{\frac{K_{y,sur}}{GB}}\right]\left[\dfrac{a_o}{2\alpha_y}\right]$
$\alpha_x =$	1.0	$\beta_x = \left[\dfrac{4\left(\frac{L}{B}\right)}{\frac{K_{x,sur}}{GB}}\right]\left[\dfrac{a_o}{2\alpha_x}\right]$
$\alpha_{zz} =$	$1.0 - \left[\dfrac{\left(0.33 - 0.03\sqrt{\frac{L}{B} - 1}\right)a_0^2}{\left(\dfrac{0.8}{1 + 0.33\left(\frac{L}{B} - 1\right) + a_o^2}\right)}\right]$	$\beta_{zz} = \left[\dfrac{\frac{4}{3}\left[\left(\frac{L}{B}\right)^3 + \left(\frac{L}{B}\right)\right]a_o^2}{\left(\frac{K_{zz,sur}}{GB^3}\right)\left[\left(\dfrac{1.4}{1 + 3\left(\frac{L}{B} - 1\right)^{0.7}}\right) + a_o^2\right]}\right]\left[\dfrac{a_o}{2\alpha_{zz}}\right]$
$\alpha_{yy} =$	$1.0 - \left[\dfrac{0.55\,a_o^2}{\left(0.6 + \dfrac{1.4}{\left(\frac{L}{B}\right)^3}\right) + a_o^2}\right]$	$\beta_{yy} = \left[\dfrac{\left(\frac{4\psi}{3}\right)\left(\frac{L}{B}\right)^3 a_o^2}{\left(\frac{K_{yy,sur}}{GB^3}\right)\left[\left(\dfrac{1.8}{1 + 1.75\left(\frac{L}{B} - 1\right)}\right) + a_o^2\right]}\right]\left[\dfrac{a_o}{2\alpha_{yy}}\right]$
$\alpha_{xx} =$	$1.0 - \left[\dfrac{\left(0.55 + 0.01\sqrt{\frac{L}{B} - 1}\right)a_0^2}{\left(2.4 - \dfrac{0.4}{\left(\frac{L}{B}\right)^3}\right) + a_o^2}\right]$	$\beta_{xx} = \left[\dfrac{\left(\frac{4\psi}{3}\right)\left(\frac{L}{B}\right)a_o^2}{\left(\frac{K_{xx,sur}}{GB^3}\right)\left[\left(2.2 - \dfrac{0.4}{\left(\frac{L}{B}\right)^3}\right) + a_o^2\right]}\right]\left[\dfrac{a_o}{2\alpha_{yy}}\right]$

where

$\alpha_z =$ Translation along z-axis

$\alpha_y =$ Translation along y-axis

$\alpha_y =$ Translation along x-axis

$\alpha_{zz} =$ Torsion about z-axis

$\alpha_{yy} =$ Rocking about y-axis

$\alpha_{xx} =$ Rocking about x-axis

$\alpha_o = \omega B / V_S$

$$\psi = \sqrt{\frac{2(1-v)}{(1-2v)}} \qquad \psi \leq 2.5$$

In the case where the foundation is embedded in the soil medium, correction factors should be used for embedment case. The embedment factors according to Pais and Kausel [78] are shown in Table 3.5.

Table 3.4 Dynamic stiffness modifiers and radiation damping ratios for embedded footings (adapted from Pais and Kausel, 1988)

DOF	Radiation Damping
$\beta_z =$	$\left[\frac{4\left[\psi\left(\frac{L}{B}\right)+\left(\frac{D}{B}\right)\left(1+\frac{L}{B}\right)\right]}{\frac{K_{z,emb}}{GB}}\right]\left[\frac{a_o}{2\alpha_z}\right]$
$\beta_y =$	$\left[\frac{4\left[\left(\frac{L}{B}\right)+\left(\frac{D}{B}\right)\left(1+\frac{\psi L}{B}\right)\right]}{\frac{K_{y,emb}}{GB}}\right]\left[\frac{a_o}{2\alpha_y}\right]$
$\beta_x =$	$\left[\frac{4\left[\left(\frac{L}{B}\right)+\left(\frac{D}{B}\right)\left(\psi+\frac{L}{B}\right)\right]}{\frac{K_{x,emb}}{GB}}\right]\left[\frac{a_o}{2\alpha_x}\right]$
$\beta_{zz} =$	$\left[\frac{\frac{4}{3}\left[3\left(\frac{L}{B}\right)\left(\frac{D}{B}\right)+\psi\left(\frac{L}{B}\right)^3\left(\frac{D}{B}\right)+3\left(\frac{L}{B}\right)^2\left(\frac{D}{B}\right)+\psi\left(\frac{D}{B}\right)+\left(\frac{L}{B}\right)^3\left(\frac{L}{B}\right)\right]a_o^2}{\left(\frac{K_{zz,emb}}{GB^3}\right)\left[\left(\frac{1.4}{1+3\left(\frac{L}{B}-1\right)^{0.7}}\right)+a_o^2\right]}\right]\left[\frac{a_o}{2\alpha_{zz}}\right]$
$\beta_{yy} =$	$\left[\frac{\frac{4}{3}\left[\left(\frac{L}{B}\right)^3\left(\frac{D}{B}\right)+\psi\left(\frac{D}{B}\right)^3\left(\frac{L}{B}\right)+\left(\frac{D}{B}\right)^3+3\left(\frac{L}{B}\right)^2\left(\frac{D}{B}\right)+\psi\left(\frac{L}{B}\right)^3\right]a_o^2}{\left(\frac{K_{yy,emb}}{GB^3}\right)\left[\left(\frac{1.8}{1+1.75\left(\frac{L}{B}-1\right)}\right)+a_o^2\right]}+\frac{\left(\frac{4}{3}\right)\left(\frac{L}{B}+\psi\right)\left(\frac{D}{B}\right)^3}{\left(\frac{K_{yy,emb}}{GB^3}\right)}\right]\left[\frac{a_o}{2\alpha_{yy}}\right]$
$\beta_{xx} =$	$\left[\frac{\frac{4}{3}\left[\left(\frac{D}{B}\right)+\left(\frac{D}{B}\right)^3+\psi\left(\frac{L}{B}\right)\left(\frac{D}{B}\right)^3+3\left(\frac{D}{B}\right)\left(\frac{L}{B}\right)^2+\psi\left(\frac{L}{B}\right)^3\right]a_o^2}{\left(\frac{K_{xx,emb}}{GB^3}\right)\left[\left(\frac{1.8}{1+1.75\left(\frac{L}{B}-1\right)}\right)+a_o^2\right]}+\frac{\left(\frac{4}{3}\right)\left(\psi\frac{L}{B}+1\right)\left(\frac{D}{B}\right)^3}{\left(\frac{K_{xx,emb}}{GB^3}\right)}\right]\left[\frac{a_o}{2\alpha_{xx}}\right]$

where

β_z = Translation along z-axis

β_y = Translation along y-axis

β_x = Translation along x-axis

β_{zz} = Torsion about z-axis

β_{yy} = Rocking about y-axis

β_{xx} = Rocking about x-axis

$\alpha_o = \omega B / V_S$

$\psi = \sqrt{\frac{2(1-\nu)}{(1-2\nu)}} \qquad \psi \leq 2.5$

3.2 Design Response Spectra for Response Spectrum Analysis

3.2.1 Design Acceleration Spectra and SSI provisions in ASCE 7-10

In American Society of Civil Engineering (ASCE 7-10), soils are classified to site classes which are based on soil properties such as shear wave velocity, standard penetration resistance, undrained shear strength, and soil profile description. Hence, there are A, B, C, D, E, F site classes which refer to the type of soil such as hard rock, rock, very dense soil, and soft rock, stiff soil, soft clay soil, and needs site response analysis (ASCE 7-10, Chapter 21), respectively. In order to choose a site class, there are many parameters should be known as indicators to site class type as shown in Table 3.8.

Table 3.5 Site classification according to ASCE 7-10 (reproduced from ASCE 7-10 Table 20.3-1)

Site Class	V_s	N or N_{ch}	S_u
A. Hard rock	>5,000 ft/s	NA	NA
B. Rock	2,500 to 5,000 ft/s	NA	NA
C. Very dense soil and soft rock	1,200 to 2,500 ft/s	>50	>2,000 psf
D. Stiff soil	600 to 1,200 ft/s	15 to 50	1,000 to 2,000 psf
E. Soft clay soil	<600 ft/s Any profile with more than 10 ft of soil having the following characteristics: -Plasticity index PI > 20, -Moisture content $w \geq 40\%$, -Undrained shear strength < 500 psf	<15	<1,000 psf
F. Soils requiring site response analysis in accordance with Section 21.1 in ASCE 7-10	See Section 20.3.1 in ASCE 7-10		

The main two parameters which refer to Mapped Acceleration are S_s and S_1. S_s is Mapped Maximum Considered Earthquake (MCE), 5% damped, spectral response acceleration parameter at short periods (at site class B). S_1 is Mapped Maximum Considered Earthquake (MCE), 5% damped, spectral response acceleration parameter at the period of 1.0 Sec (at site class B). These two parameters should be obtained from the 0.2 and 1.0 sec spectral response accelerations given in Figures 22-1, 22-3, 22-5, of the code for S_s, and Figures 22-4, 22-5, 22-6 for S_1.

The parameters S_{Ms} for short periods and S_{M1} at 1.0 sec period should be calculated in accordance to equations given below:

$$S_{Ms} = F_a S_s \quad (3.4)$$

$$S_{M1} = F_v S_1 \quad (3.5$$

where

F_a and F_v are defined in Tables 3.8 and 3.9, respectively.

F_a = short-period site coefficient (at 0.2 s-period)

F_v = long-period site coefficient (at 1.0 s-period)

Table 3.6 Site coefficient, F_a

Site Class	$S_s \leq 0.25$	$S_s = 0.5$	$S_s = 0.75$	$S_s = 1.0$	$S_s \geq 1.25$
A	0.8	0.8	0.8	0.8	0.8
B	1.0	1.0	1.0	1.0	1.0
C	1.2	1.2	1.1	1.0	1.0
D	1.6	1.4	1.2	1.1	1.0
E	2.5	1.7	1.2	0.9	0.9
F	See section 14.7 in ASCE 7-10				

Table 3.7 Site coefficient, F_v

Site Class	$S_1 \leq 0.1$	$S_1 = 0.2$	$S_1 = 0.3$	$S_1 = 0.4$	$S_1 \geq 0.5$
A	0.8	0.8	0.8	0.8	0.8
B	1.0	1.0	1.0	1.0	1.0
C	1.7	1.6	1.5	1.4	1.3
D	2.4	2.0	1.8	1.6	1.5
E	3.5	3.2	2.8	2.4	2.4
F	See section 14.7 in ASCE 7-10				

Design earthquake spectral response acceleration parameters, S_{Ds} for short period, and S_{D1} at 1.0 sec period should be obtained from Equations 3.6 and 3.7, respectively:

$$S_{Ds} = \frac{2}{3} S_{Ms} \quad (3.6)$$

$$S_{D1} = \frac{2}{3} S_{M1} \quad (3.7)$$

where

S_{Ds} = design, 5% damped, spectral response acceleration parameter at short periods

S_{D1} = design, 5 % damped, spectral response acceleration parameter at a period of 1.0 sec

The design response spectrum is required by ASCE 7-10 but, site-specific ground motion procedures are not. Hence, the ASCE 7-10 suggests a response spectrum curve which should be developed by depending on the following points:

1. In the case where periods (T) are $T < T_o$ then, the design spectral response acceleration, S_a, should be taken as given in equation (3.8):

$$S_a = S_{Ds}\left(0.4 + 0.6\left(\frac{T}{T_o}\right)\right) \quad (3.8)$$

2. In the case where periods (T) are $T_o \leq T \leq T_s$then, the design spectral response acceleration, S_a, should be taken as below:

$$S_a = S_{Ds} \quad (3.9)$$

3. In the case where periods (T) are $T_s \leq T \leq T_L$then, the design spectral response acceleration, S_a, should be taken as given in equation (3.10):

$$S_a = \frac{S_{D1}}{T} \quad (3.10)$$

4. In the case where Periods (T) are $T > T_L$ then, the design spectral response acceleration, S_a, should be taken as given in equation (3.11):

$$S_a = \frac{S_{D1} T_L}{T^2} \quad (3.11)$$

where

T = the fundamental period of the building

$$T_o = \frac{0.2 S_{D1}}{S_{Ds}}$$

$$T_s = \frac{S_{D1}}{S_{Ds}}$$

T_L = Long-period transition period (sec) is obtained from Figures 22-12 through 22-16 in ASCE 7-10.

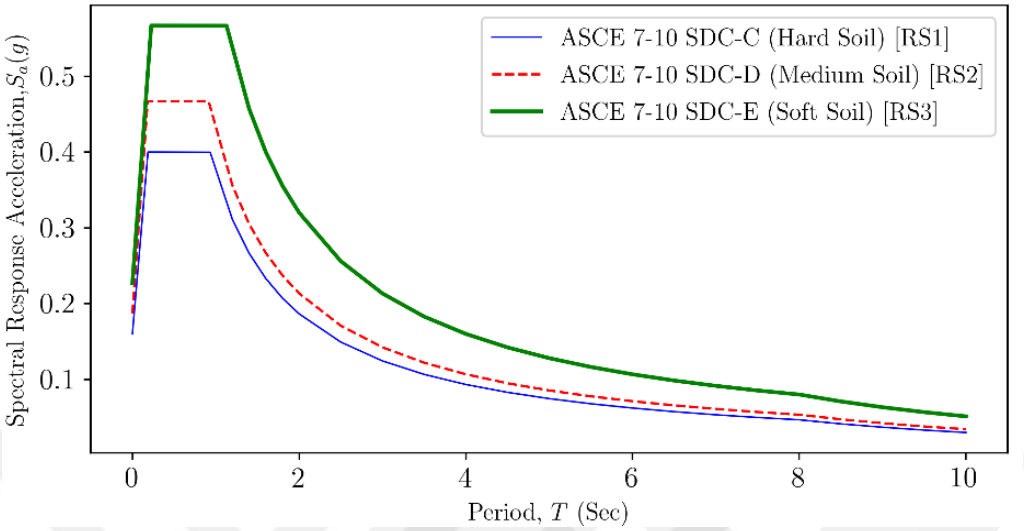

Figure 3.3 Design response spectrum

Importance factor, I_c, is assigned to each structure by obtaining it from Table 3.10

Table 3.8 Importance factor, I_c

Risk Category from table 1.5-1 in ASCE 7-10	Seismic Importance Factor, I_c
I	1.0
II	1.0
III	1.25
IV	1.50

Each structure should be assigned to a seismic design category based on its risk category and the design spectral response acceleration parameters S_{Ds} and S_{D1}. The following tables are used for that purpose.

Table 3.9 Seismic design category based on short period response acceleration parameter

Risk Category		
Value of S_{Ds}	I or II or III	IV
$S_{Ds} < 0.167$	A	A
$0.167 \leq S_{Ds} < 0.33$	B	C
$0.33 \leq S_{Ds} < 0.50$	C	D
$0.50 \leq S_{Ds}$	D	D

Table 3.10 Seismic design category based on 1 sec period response acceleration parameter

Risk Category		
Value of S_{D1}	I or II or III	IV
$S_{D1} < 0.067$	A	A
$0.067 \leq S_{D1} < 0.133$	B	C
$0.133 \leq S_{D1} < 0.20$	C	D
$0.20 \leq S_{D1}$	D	D

In the case where Risk Category I, II, or III structures have mapped spectral response acceleration parameter at 1.0 sec period, S_1, is more than or equal to 0.75 then, structures should be assigned to seismic design category E. Meanwhile, risk category IV structures have mapped spectral response acceleration parameter at 1.0 sec period, S_1, is more than or equal to 0.75 should be assigned to seismic design category F. In the case where S_1 < 0.75, the seismic design category is allowed to be obtained from Table 3.9, alone where all of the following apply:

1. In each of the two perpendicular directions, an approximate fundamental period of the structure is determined as below:

T_a< 0.8 T_s, where T_a and T_s are determined according to below equations:

$$T_a = C_1(h_n)^x \tag{3.12}$$

$$T_s = \frac{S_{D1}}{S_{Ds}} \tag{3.13}$$

where

C_1 and x from Table 2.5 in ASCE 7-10.

$h_n =$ the structural height (The vertical distance from the base to the highest level of the seismic force- resisting system of the structure)

2. In each of two perpendicular directions, the fundamental period of the structure, T, which is utilized to calculate the story drift is not more than T_s.

3. In order to determine the seismic response coefficient C_s, equation 12.8.2 in ASCE 10-7 is used.

4. Diaphragms are rigid or for flexible diaphragms, the vertical distance between vertical elements of the seismic-force-resisting system does not pass 40 ft.

3.3 Earthquake Ground Motion Records for Time History Analysis

The seismic motion can be represented in terms of appropriate ground acceleration time histories and related quantities like displacement and velocity. Selecting and scaling the records define the seismic input for structural analysis. There are two main things that define the seismic input for structural analysis which predicts the structure response: selecting and scaling the records (Nevine et al. [79]). In the case where the appropriate ground motion time histories satisfying duration and amplitude requirements of seismic design codes are not available to carry out time history analysis, the ground motion records should be scaled to make them consistent with the code-specific hazards levels. In order to fit the ground motion to response spectra, a process that consists of scaling ground motion in the time domain, matching spectra in the frequency domain, matching spectral by wavelets, and generating artificial record compatible with spectrum, should be performed.

3.3.1 Earthquake Ground Motion Record

1940 El Centro earthquake ground acceleration record is used for time history analyses in this study. The ground acceleration record for this earthquake is plotted in Figure 3.4. No scaling is performed in this study.

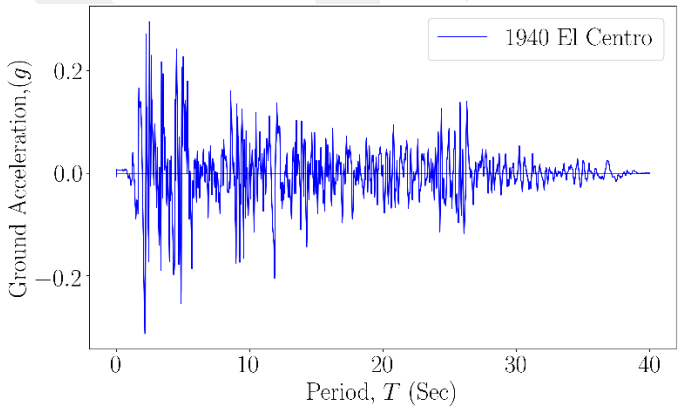

Figure 3.4 Ground acceleration record for 1940 El Centro earthquake

CHAPTER 4

SOIL-STRUCTURE INTERACTION EFFECTS IN 2D MODEL

This chapter presents the description of the two-dimensional analysis models used to examine soil-structure interactions effects and discussion of the results obtained from those models.

4.1 Description of Soil-Structure Models

This study considers the soil-structure interaction effects on buildings and investigates the effects of some significant analytical modeling parameters on the static and dynamic responses of the buildings under seismic excitations. There are many parameters that affect the soil-structure interaction; therefore, this study concentrates on the effects of structure type, foundation type, soil type and mass, the dimensions of soil model and the boundary conditions.

The analysis models used in this study are prepared by using SAP2000's Application Programming Interface (API) for python programming language. For this purpose, python scripts were written to prepare and run the SAP2000 models automatically. The results of the analyses are also extracted and post-processed to prepare the figures presented in this chapter.

A reinforced concrete building frame of 6 bay and 6 story, with three different levels of total mass is considered in this chapter. Joint masses are applied uniformly throughout the building frame to adjust the fundamental period of the fixed building model to 0.5 s, 1.0 s, and 2.0 s, which are referred as stiff building, medium building, and soft building, respectively.

The reinforced columns and beams were modelled by using elastic frame elements assuming cross-section properties. Geometric and material properties of the building are shown in Table 4.1. Non-modeled parts of the building are considered indirectly as part of the dead loads. The floor and roof dead loads are assumed to be 3 kN/m. Building walls are indirectly modeled as a uniformly distributed load of 10.5 kN/m.

In addition to the fixed base model, a spring-supported building model and a direct model of building frame along with the underlying soil are also considered. Similar to the modelling of superstructure, three types of homogeneous, elastic half-space soil are considered for the spring and direct models. The soil properties are selected such that the fundamental period of soil model alone is 0.5 s, 1.0 s, and 2.0 s, which are referred as hard soil, medium soil, and soft soil, respectively. The soil properties are shown in Table 4.2.

ASCE 7-10 code is used to determine the design acceleration spectrum corresponding to each type of soil. Using the selected soil properties, shear wave velocity is calculated and then the site class is determined from Table 3.8, which is reproduced from ASCE 7-10 Table 20.3-1. To calculate the shear wave velocities Eq. (4.1) is used.

$$V_s = \sqrt{\frac{E}{2 * P\ (1 + v)}} \tag{4.1}$$

where

E = the elastic modulus

P = the mass density

v = the Poisson ratio

The building damping ratio is taken as 5 %, which is a typical value for reinforced concrete structures. All models were subjected to three types of response spectrum according to the type of soil hard (C site class), medium (D site class), and soft (E site class), having S_s equal to 0.5 g, S_1 equal to 0.4 g, and T_L equal to 8. These response spectra are selected in accordance with Section 3.2.1 of ASCE 7-10.

Table 4.1 Geometric and materials properties of the building frame

Component	Description	Data
Frame Dimensions	Number of stories	6
	Number of bays	6
	Story height	3 m
	Bay width	5 m
	Size of beam	0.8 m × 0.4 m
	Size of column	0.6 m × 0.6 m
	The thickness of the slab	0.15 m
Structural Frame Material	The elastic modulus of concrete (E)	33000000 kN/m^2
	Poisson ratio (v)	0.2
	Concrete compressive strength (fc)	30 MPa
	The unit weight (γ)	24.99 kN/m^3

Table 4.2 Soil properties

Soil Properties	Hard	Modulus of elasticity (E)	2240000 kN/m^2
		Poisson ratio (v)	0.28
		The unit weight (γ)	21 kN/m^3
		Site class	C
	Medium	Modulus of elasticity (E)	467000 kN/m^2
		Poisson ratio (v)	0.35
		The unit weight (γ)	18 kN/m^3
		Site class	D
	Soft	Modulus of elasticity (E)	102000 kN/m^2
		Poisson ratio (v)	0.4
		The unit weight (γ)	14 kN/m^3
		Site class	E

A parametric investigation was performed assuming three models of building fixity to the ground. The first model is the fixed base model. The second model is the flexible base model which is supported by springs based on the impedance functions. The third one is the direct model that rests on viscoelastic-half space soil medium. The three models are described in detail below.

4.1.1 Fixed Base Model

The properties explained above are assigned to the fixed base model. The fixed base model is shown in Figure 4.1.

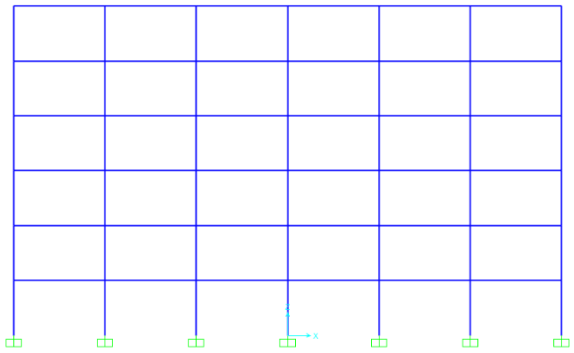

Figure 4.1 Fixed base model (2D)

4.1.2 Spring Model

The soil-structure interaction effects are represented by using equivalent Winkler springs with three degrees-of-freedom (DOF). The stiffnesses along these 3 degrees of freedoms were calculated as per Pais and Kuasel (1988) [76], Table 3.2 in chapter 3. Two types of foundation footing and raft foundation are considered in this research to study the soil-structure interaction effects on buildings.

4.1.2.1 Footing Foundation

Footing foundation of size 2 m × 2 m with 0.8 m thickness is considered for the footing case. The spring model for the footing foundation is presented in Figure 4.2. The shear modulus, G, is calculated for each type of soil by using Eq. (4.2).

$$G = \frac{E}{2(1+v)} \tag{4.2}$$

where

E = Soil modulus of elasticity

v = Poisson ratio.

The values of static and dynamic stiffness for the hard, medium and soft soil are calculated in presented as follows.

Table 4.3 Static spring stiffness values for footing foundation

Soil type	G (kN/m^2)	K_x (kN/m)	K_z (kN/m)	K_{yy} (kN.m/rad)
Hard	875000.000	4680230	5711810	4.81×10^6
Medium	172962.965	964399	1250655	1.06×10^6
Soft	36428.571	209464	285357	2.42×10^5

Table 4.4 Dynamic spring stiffness values for footing foundation

Soil type	G (kN/m^2)	K_x (kN/m)	K_z (kN/m)	K_{yy} (kN.m/rad)
Hard	875000.000	4680230	5711672	4.86×10^{6}
Medium	172962.965	964399	1250534	1.06×10^{6}
Soft	36428.571	209464	2852640	2.42×10^{5}

Table 4.5 Radiation damping ratios for footing foundation

Soil type	G(kN/m^2)	β_x	β_z	β_{yy}
Hard	875000.000	7.36×10^{-3}	1.09×10^{-2}	9.21×10^{-7}
Medium	172962.965	1.43×10^{-2}	2.30×10^{-2}	8.05×10^{-6}
Soft	36428.571	2.56×10^{-2}	4.61×10^{-2}	5.43×10^{-5}

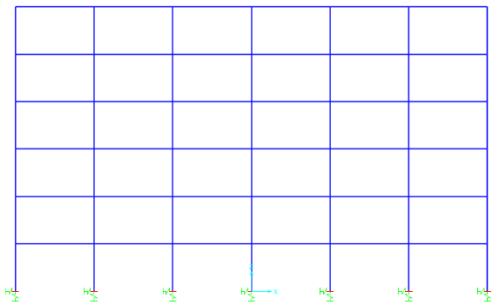

Figure 4.2 Spring model with footing foundation (2D)

4.1.2.2 Raft Foundation

For the second case of the spring model, a raft foundation of size 32 m × 32 m with thickness 0.8 m is considered. The raft foundation is assumed to have modulus of elasticity, E, equal to 39000 N/mm, Poisson ratio, v, equal to 0.2, the concrete compressive strength, F_c, equal to 60 MPa, and unit mass equal to 24.99 kN/m^2. The model for the raft foundation with spring supports is shown in Figure 4.3. To determine the stiffnesses along 3 DOF, a special calculation should be made, using Pais and Kuasel (1988) [76] formulas for raft foundation. For the side springs, the horizontal K_x and the vertical K_z should be divided by the tributary area of the spring, however, for the rocking K_{yy} is used same as the footing foundation case because the model is a 2D model. At the side of the raft, the horizontal K_x and the vertical K_z involved in the SSI representation. Whereas, at the center of the raft, three components involved the horizontal K_x, the vertical K_z, and the rocking K_{yy} stiffness. The raft foundation stiffnesses along 3 degrees of freedoms are shown in Table 4.6 through 4.8.

Table 4.6 Static Spring stiffness values for raft foundation

Soil type	Spring Location	K_x(kN/m)	K_z(kN/m)	K_{yy}(kN.m/rad)
Hard	End Springs	1170058.1	1427951.4	-
	Between End and Center Springs	2340116.3	2855902.8	-
	Center Spring	2340116.3	2855902.8	1.991×10^{10}
Medium	End Springs	241099.8	312663.8	-
	Between End and Center Springs	482199.7	625327.6	-
	Center Spring	482199.7	625327.6	4.359×10^{9}
Soft	End Springs	52366.0	71339.2	-
	Between End and Center Springs	104732.1	142678.5	-
	Center Spring	104732.1	142678.5	9.947×10^{8}

Table 4.7 Dynamic Spring stiffness values for raft foundation

Soil type	Spring Location	K_x(kN/m)	K_z(kN/m)	K_{yy}(kN.m/rad)
Hard	End Springs	1170058.1	1420249.4	-
	Between End and Center Springs	2340116.3	2840498.8	-
	Center Spring	2340116.3	2840498.8	1.943×10^{10}
Medium	End Springs	241099.8	306011.4	-
	Between End and Center Springs	482199.7	612022.8	-
	Center Spring	482199.7	612022.8	3.987×10^{9}
Soft	End Springs	52366.0	66847.8	-
	Between End and Center Springs	104732.1	133695.5	-
	Center Spring	104732.1	133695.5	7.925×10^{8}

Table 4.8 Radiation damping ratios for raft foundation

Soil type	Spring Location	β_x	β_z	β_{yy}
Hard	End Springs	6.87×10^{-6}	2.59×10^{-3}	-
	Between End and Center Springs	1.37×10^{-5}	5.19×10^{-3}	-
	Center Spring	1.37×10^{-5}	5.18×10^{-3}	3.06×10^{-3}
Medium	End Springs	1.32×10^{-5}	5.33×10^{-3}	-
	Between End and Center Springs	2.65×10^{-5}	1.06×10^{-2}	-
	Center Spring	2.65×10^{-5}	1.07×10^{-2}	2.12×10^{-2}
Soft	End Springs	2.29×10^{-5}	9.91×10^{-3}	-
	Between End and Center Springs	4.59×10^{-5}	1.98×10^{-2}	-
	Center Spring	4.59×10^{-5}	1.98×10^{-2}	8.33×10^{-2}

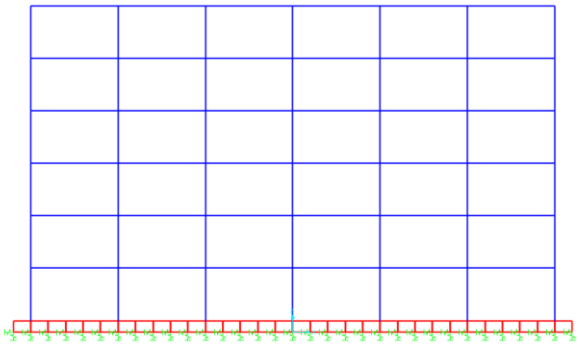

Figure 4.3 Spring model with a raft foundation (2D)

4.1.3 Direct Model

The direct model is used to investigate the soil-structure response when subjected to seismic excitation. The soil is assumed to be 180 m length by 80 m deep, having multilayers. The soil in the direct model is assumed to be massless. The soil depth is taken as more than 2.5 times the foundation length of the structure. As explained in Section 2.5.2, tied boundary conditions are used at the sides and pinned boundaries are assumed at the bottom of the model. Gap link elements are used between the frame and the soil. These gap elements consist of elastic springs with integrated opening that does not allow the transmission of the tensile forces between the frame and the soil. The behavior of gap elements is linear elastic under compressive forces. The stiffnesses of the gap elements are calculated so that the compressive forces are transferred with neglected relative displacements between the frame foundation and the soil. Therefore, the gap elements located every one meter along the foundation length, having sufficiently spring stiffness value equal to 10^6 kN/m. Moreover, linear spring elements were used to resist the lateral forces, having 10^4 kN/m lateral spring stiffness. The space between the bottom of the foundation and soil was assumed to be 0.01m. For all corresponding nodes between the foundation and soil, an equal horizontal displacement constraint was imposed. In this research, two types of the foundation were assumed footing and raft foundation to be investigated for the soil-structure interaction effects on buildings.

4.1.3.1 Footing Foundation

The abovementioned frame properties were assigned to the structure. The frame foundation was considered as a footing with 2 m × 2 m × 0.8 m length, width, and depth,

respectively. The footing properties were assumed as modulus of elasticity, E, equal to 39000 N/mm, Poisson ratio, v, equal to 0.2, the concrete compressive strength, Fc, equal to 60 MPa, and unit mass equal to 24.99 kN/m^2. The soil element sizes increase as we move far away from the structure to get the closest representation of reality, starting from 1 m, 2 m, and 5 m. The soil medium was modelled using plan-strain elements having thickness 2 m. The direct model with footing foundation is illustrated in Figure 4.4.

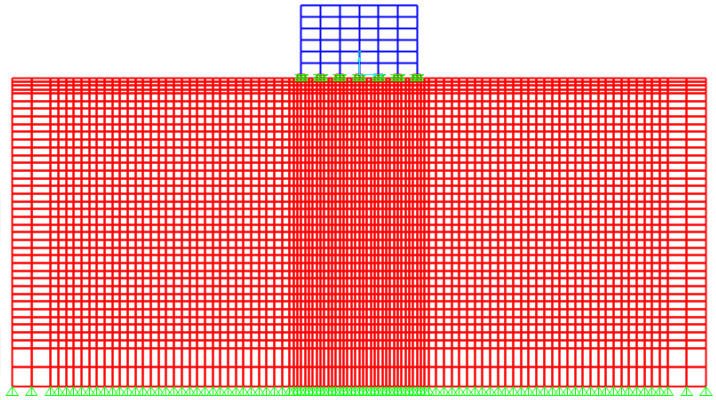

Figure 4.4 Direct model with footing foundation (2D)

For all soil layers a damping ratio of 5 % is assumed. Gap link elements are shown in Figure 4.5.

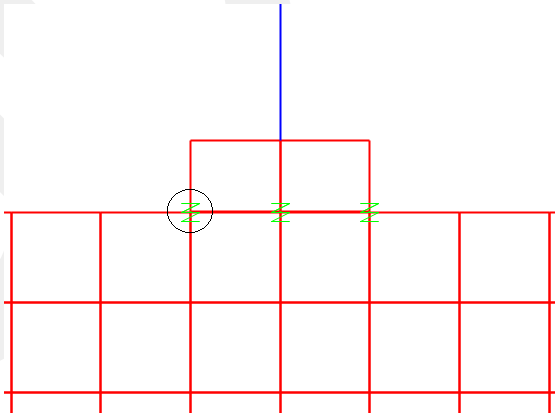

Figure 4.5 Gap link elements in direct model (2D)

4.1.3.2 Raft Foundation

For the raft foundation direct model, a raft foundation is placed under the frame with the same properties as the raft foundation in spring raft foundation model. The gap link

elements are put every one meter between the frame and the soil medium. The direct raft foundation model is shown in Figure 4.6.

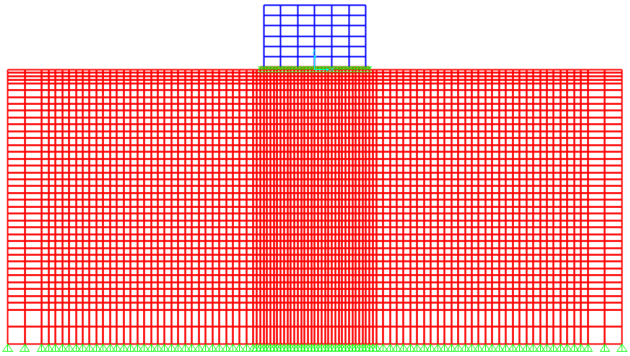

Figure 4.6 Direct model with raft foundation (2D)

4.2 Results and Discussions

The results of the two-dimensional analysis models (i.e., natural periods and mode shapes, base shear, story displacements, story drifts and foundation settlement) of fixed, spring, and direct model are presented and discussed below.

4.2.1 Natural periods and Mode Shapes

4.2.1.1 Natural periods and Mode Shapes from Static Analysis

The fundamental periods (first mode natural periods) of the fixed base, spring and direct models, having three types of soils (i.e., hard, medium and soft) are shown in Table 4.9. For medium building only, the first mode shapes of the fixed base, spring, and direct models are shown in Figures 4.7 through 4.12. From Table 4.9, it is observed that the fundamental periods of the spring models (using static spring stiffnesses given by Pais [78]) are lower than the fundamental periods of the corresponding direct models for both the footing foundation and the raft foundation. In direct models, footing foundation leads to higher fundamental periods (i.e., softer system) for all soil types and structure types, whereas in spring models this is only the case for soft soils. For structures on hard and medium soil, spring models with footing foundation are stiffer than the ones with raft foundation.

Table 4.9 Fundamental periods of the 2D static models

Structure Type	Fixed Model Fundamental Period (s)	Soil Type	Spring Model Fundamental Period (s)		Direct Model Fundamental Period (s)	
			Footing	Raft	Footing	Raft
Stiff	0.497	Hard	0.503	0.522	0.634	0.535
		Medium	0.524	0.535	0.711	0.619
		Soft	0.595	0.581	0.981	0.927
Medium	1.000	Hard	1.013	1.050	1.275	1.076
		Medium	1.054	1.077	1.426	1.237
		Soft	1.197	1.169	1.961	1.804
Soft	2.001	Hard	2.026	2.100	2.549	2.151
		Medium	2.109	2.153	2.851	2.469
		Soft	2.395	2.338	3.915	3.578

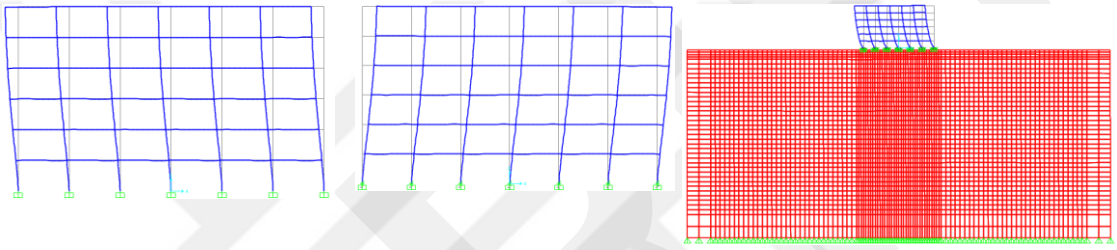

Figure 4.7 First natural mode shapes for medium building with footing foundation on hard soil: fixed (T_1= 1 sec), spring (T_1= 1.03 sec), and direct (T_1= 1.276 sec) models

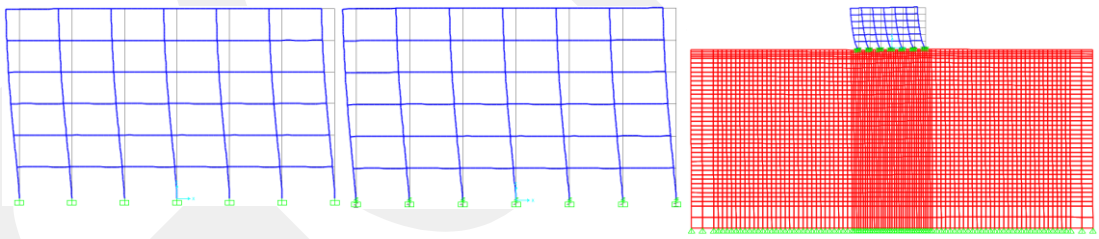

Figure 4.8 First natural mode shapes for medium building with footing foundation on medium soil: fixed (T_1= 1 sec), spring (T_1= 1.05 sec), and direct (T_1= 1.432 sec) models

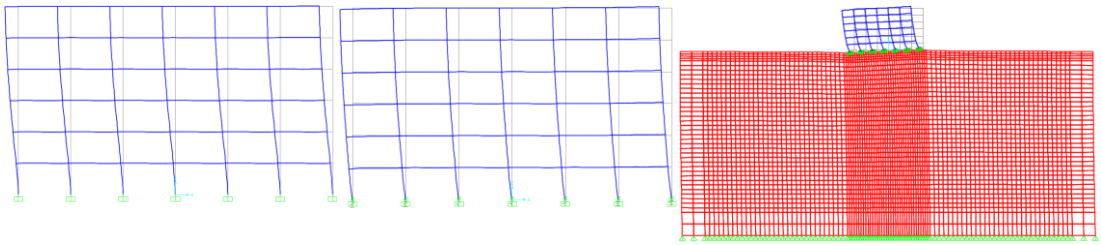

Figure 4.9 First natural mode shapes for medium building with footing foundation on soft soil: fixed (T_1= 1 sec), spring (T_1= 1.19 sec), and direct (T_1= 1.98 sec) models

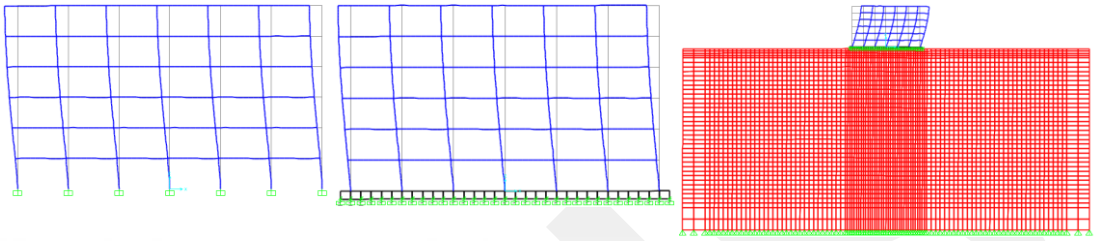

Figure 4.10 First natural mode shapes for medium building with raft foundation on hard soil: fixed (T_1= 1 sec), spring (T_1= 1.05 sec), and direct (T_1= 1.09 sec) models

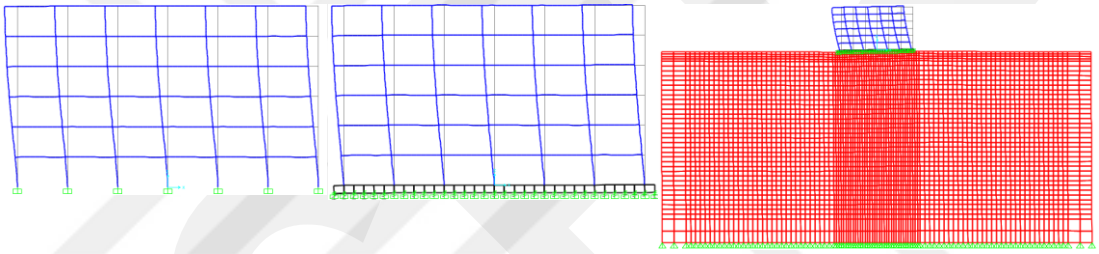

Figure 4.11 First natural mode shapes for medium building with raft foundation on medium soil: fixed (T_1= 1 sec), spring (T_1= 1.07 sec), and direct (T_1= 1.26 sec) models

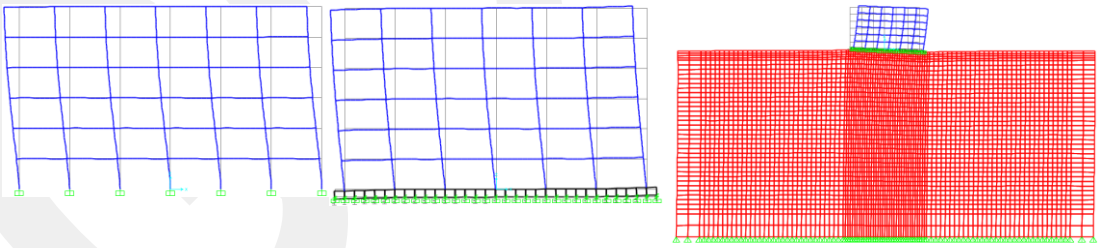

Figure 4.12 First natural mode shapes for medium building with raft foundation on soft soil: fixed (T_1= 1 sec), spring (T_1= 1.17 sec), and direct (T_1= 1.83 sec) models

4.2.1.2 Natural Periods and Mode Shapes from Dynamic Analysis

The fundamental periods of the fixed base and spring models subjected to 1940 El Centro earthquake, having three types of soils (hard, medium and soft) are shown in Table 4.10. For medium building only, the first mode shapes of the fixed base, spring, and direct models are shown in Figures 4.13 through 4.18. For both footing foundation

and raft foundation, the fundamental periods of spring models (using dynamic spring stiffnesses given by Pais [78]) are almost identical to the values presented in Table 4.9 (based on static spring stiffnesses given by Pais [78]).

Table 4.10 Fundamental periods of the 2D dynamic models

Structure Type	Fixed Model Fundamental Period (s)	Soil Type	Spring Model Fundamental Period (s)	
			Footing	Raft
Stiff	0.497	Hard	0.503	0.522
		Medium	0.524	0.535
		Soft	0.595	0.584
Medium	1.000	Hard	1.013	1.050
		Medium	1.054	1.077
		Soft	1.197	1.170
Soft	2.001	Hard	2.026	2.100
		Medium	2.109	2.153
		Soft	2.395	2.338

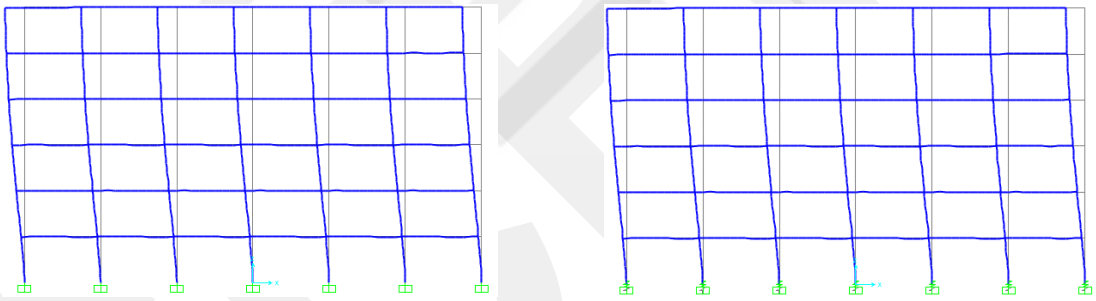

Figure 4.13 First natural mode shapes for medium building with footing foundation on hard soil: fixed (T_1= 1 sec) and spring (T_1= 1.01 sec) models

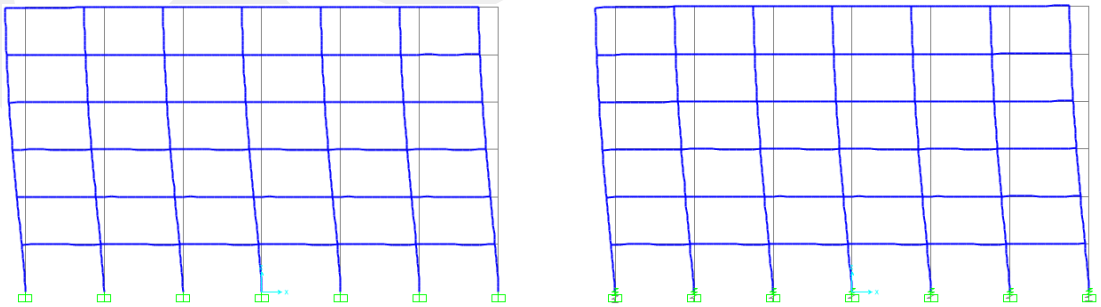

Figure 4.14 First natural mode shapes for medium building with footing foundation on medium soil: fixed (T_1= 1 sec) and spring (T_1= 1.05 sec) models

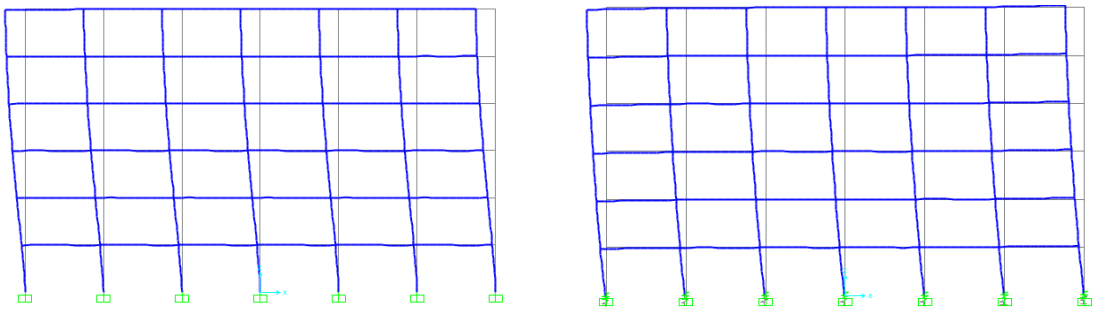

Figure 4.15 First natural mode shapes for medium building with footing foundation on soft soil: fixed (T_1= 1 sec) and spring (T_1= 1.19 sec) models

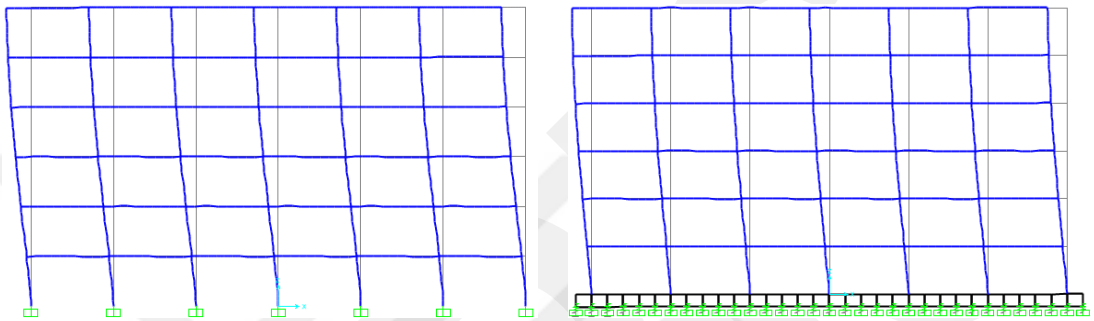

Figure 4.16 First natural mode shapes for medium building with raft foundation on hard soil: fixed (T_1= 1 sec) and spring (T_1= 1.05 sec) models

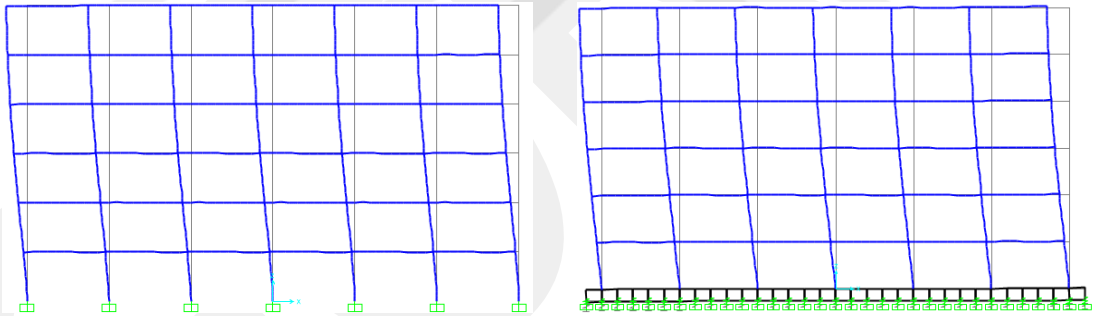

Figure 4.17 First natural mode shapes for medium building with raft foundation on medium soil: fixed (T_1= 1 sec) and spring (T_1= 1.07 sec) models

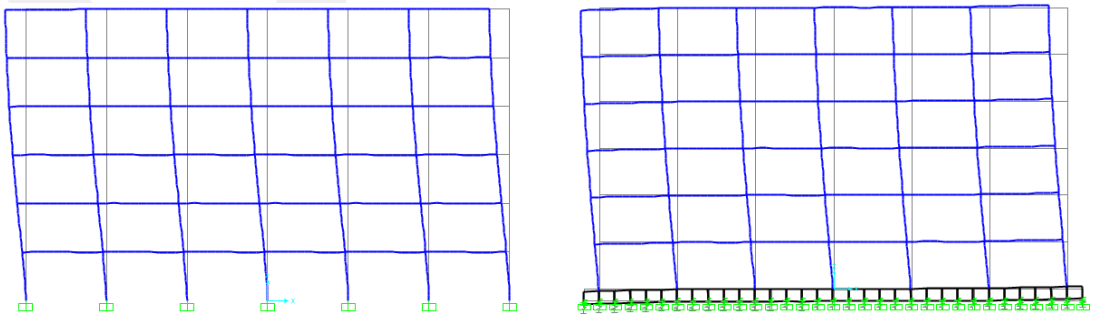

Figure 4.18 First natural mode shapes for medium building with raft foundation on soft soil: fixed (T_1= 1 sec) and spring (T_1= 1.17 sec) models

4.2.2 Response Spectrum Analysis Results

4.2.2.1 Base Shear and Story Shears

Story shear results of buildings with footing and raft foundations on different type soils are plotted in Figures 4.19 and 4.20, respectively. Base shear values are also tabulated in Table 4.11. From the figures and table below, it is observed that fixed based models have lower (unconservative) base and story shears for the stiff structure on all three types of soil (i.e., hard, medium, soft). As the structure and underlying soil become softer, the fixed based models start to have higher (conservative) base and story shears. This effect is more pronounced for direct models of medium and soft buildings on all soil types whereas it becomes significant in spring models only for soft building on soft soil.

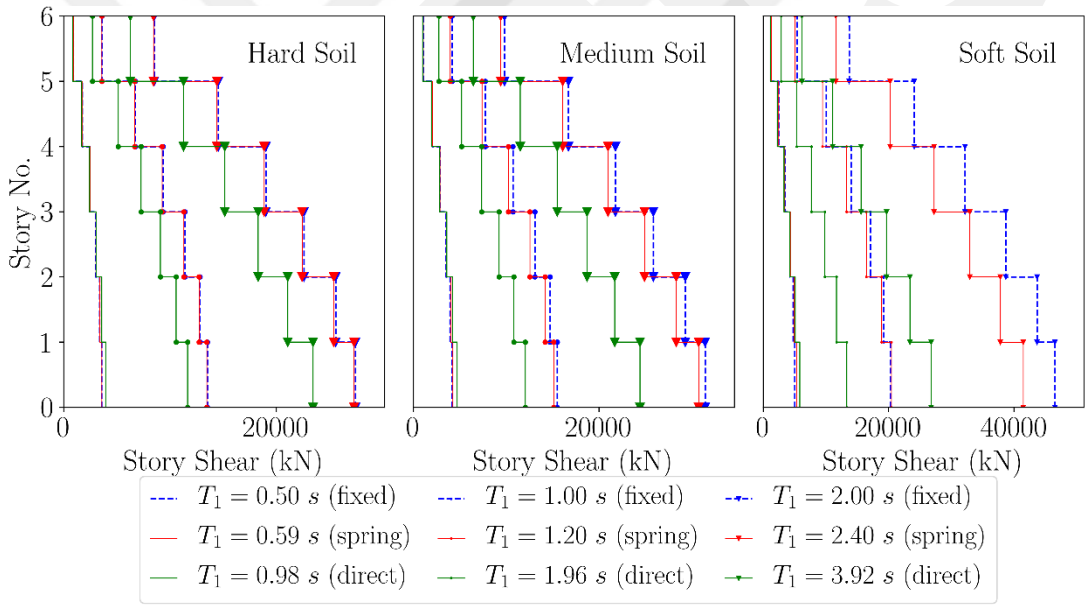

Figure 4.19 Story shears of buildings with footing foundation on hard, medium, and soft soil

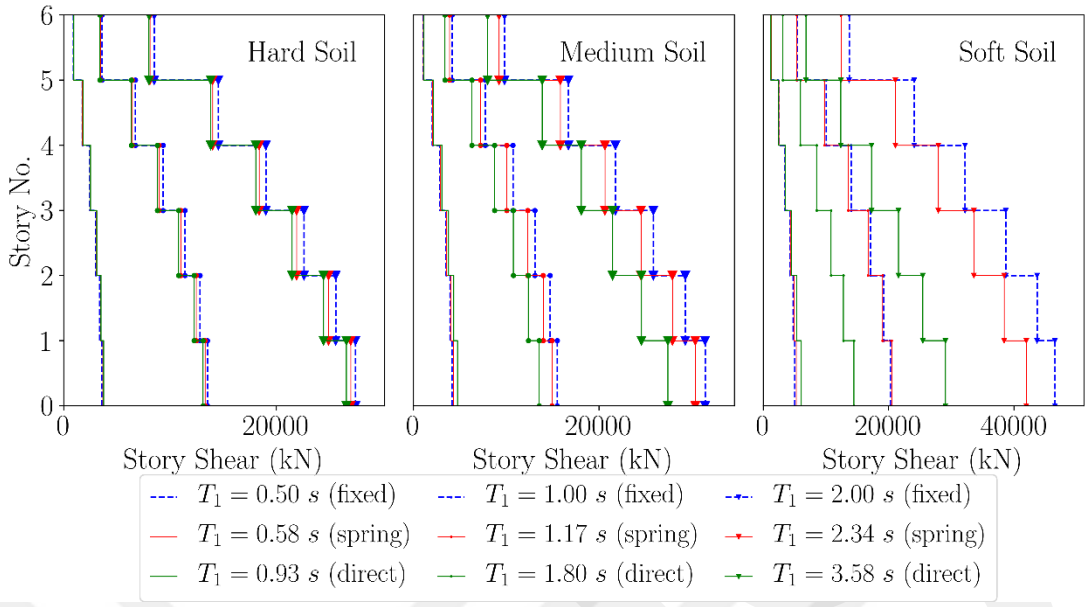

Figure 4.20 Story shears of buildings with raft foundation on hard, medium, and soft soil

Table 4.11 Base shears of buildings on hard, medium, and soft soil

Structure Type	Soil Type	Fixed Model Base Shear (kN)	Spring Model Base Shear (kN)		Direct Model Base Shear (kN)	
			Footing	Raft	Footing	Raft
Stiff	Hard	3548	3570	3655	3943	3752
	Medium	4144	4244	4291	4700	4742
	Soft	5023	5339	5273	5814	6058
Medium	Hard	13502	13434	13284	11656	13098
	Medium	15518	15114	14933	12066	13564
	Soft	20250	20422	20468	13339	14457
Soft	Hard	27449	27326	27004	23464	26605
	Medium	31472	30758	30404	24429	27438
	Soft	46526	41480	41976	26780	29060

4.2.2.2 Story Displacements and Drifts

Story displacements and drifts of the fixed base, spring and direct models are plotted in Figures 4.21 through 4.24 for footing and raft foundation cases. The values of story displacements and drifts are also tabulated in Tables 4.12 through 4.17.

For both footing and raft foundations, as building and soil become softer, story displacements increase as expected due to two reasons, which are: (i) higher flexibility of building and soil, and (ii) higher design spectral acceleration for softer soil.

For a given structure with footing or raft foundation, as soil becomes softer, the differences between the fixed model and SSI models (spring and direct) become more pronounced. For any given soil, the difference between fixed model and SSI models increases as the structure becomes stiffer. This effect is more visible in direct models (compared to the spring models) and in spring models on soft soil.

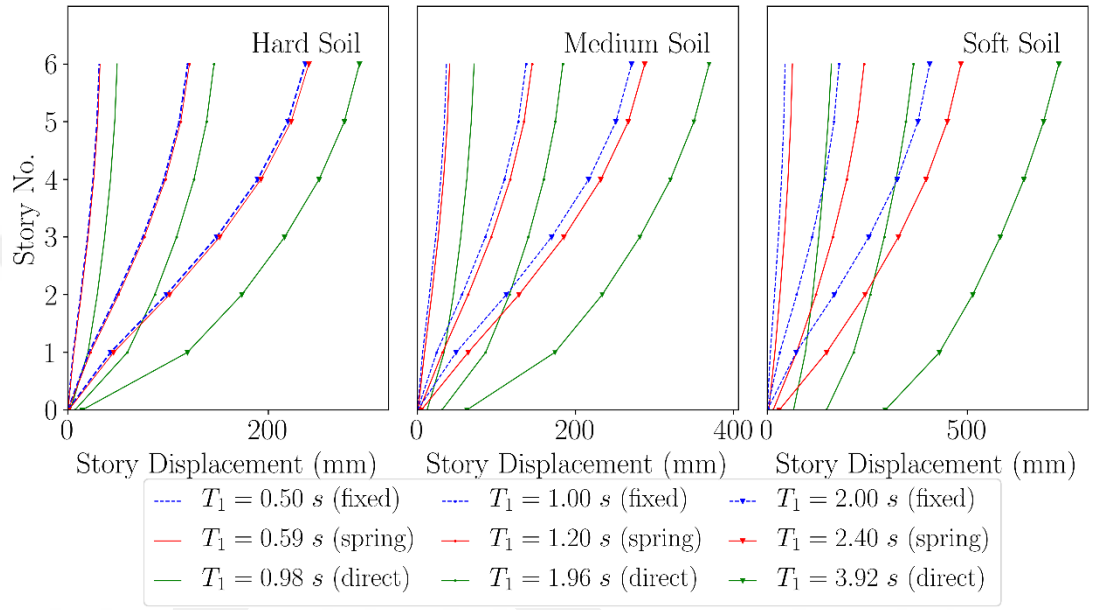

Figure 4.21 Story displacements of buildings with footing foundation on hard, medium, and soft soil

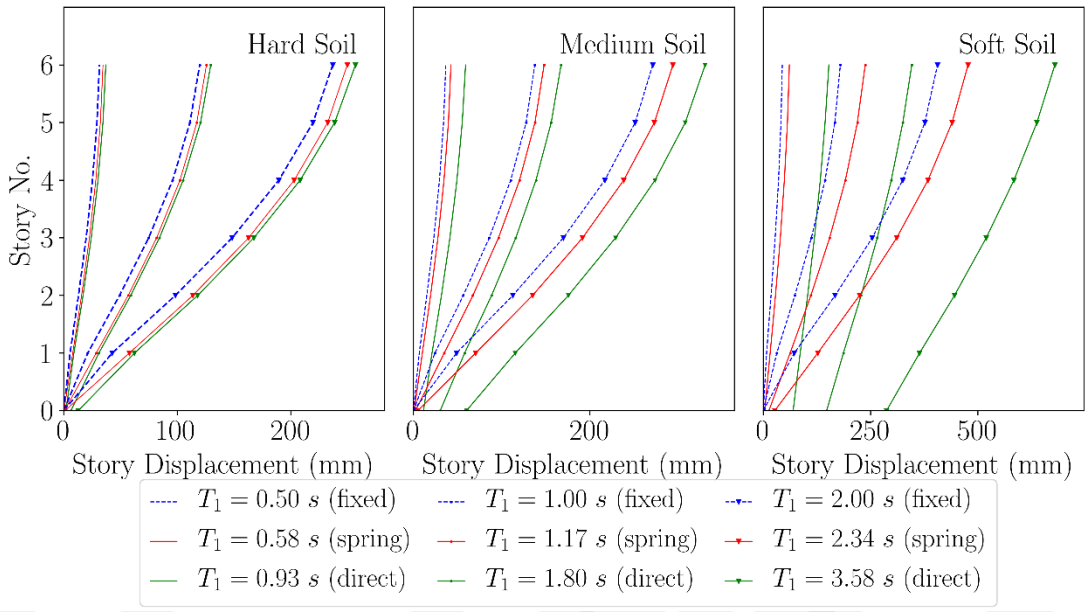

Figure 4.22 Story displacements of buildings with raft foundation on hard, medium, and soft soil

Tables 4.12 through 4.17 present the story drifts both in mm and as percentage of the story height. Similar to the story displacements, the story drift values increase as the structure and the soil get softer. For fixed base models, the largest story drift occurs in the second story columns, whereas the largest story drift occurs in the first story columns for direct models with footing or raft foundation. Spring models on hard and medium soil have the largest drift in the second story columns similar to the fixed models, but as the soil becomes softer, the largest drift occurs in the first story columns of the spring models.

For a given structure as the soil gets softer, the drifts of the SSI models (spring and direct) increases with respect to fixed based model drifts for both footing and raft foundations. This effect is higher in direct models. For a given soil, as the structure gets softer, the drifts of the SSI models decrease with respect to fixed base model drifts for both footing and raft foundations.

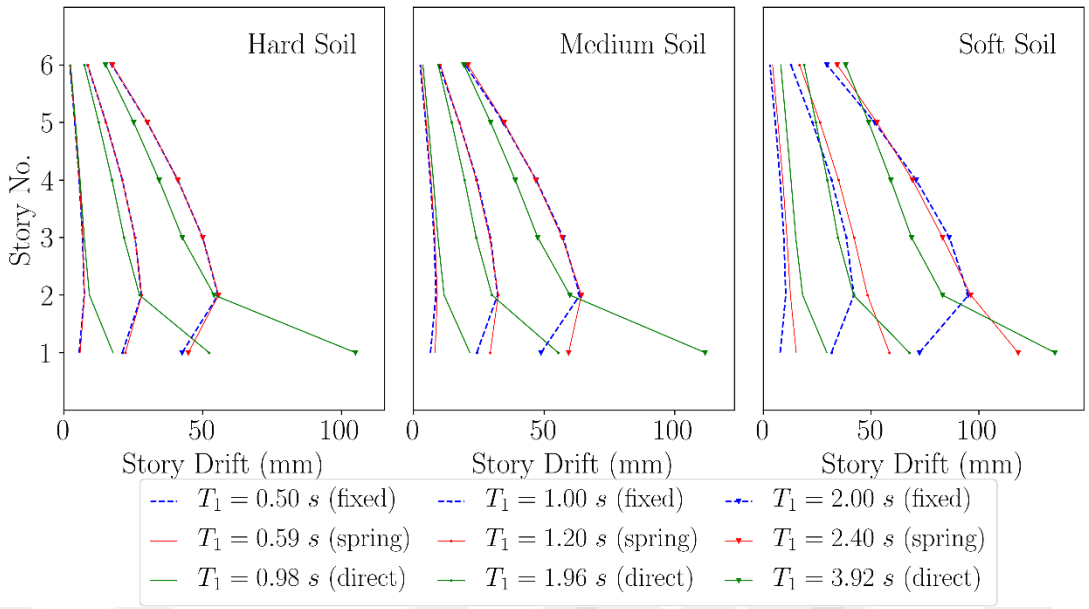

Figure 4.23 Story drifts of buildings with footing foundation on hard, medium, and soft soil

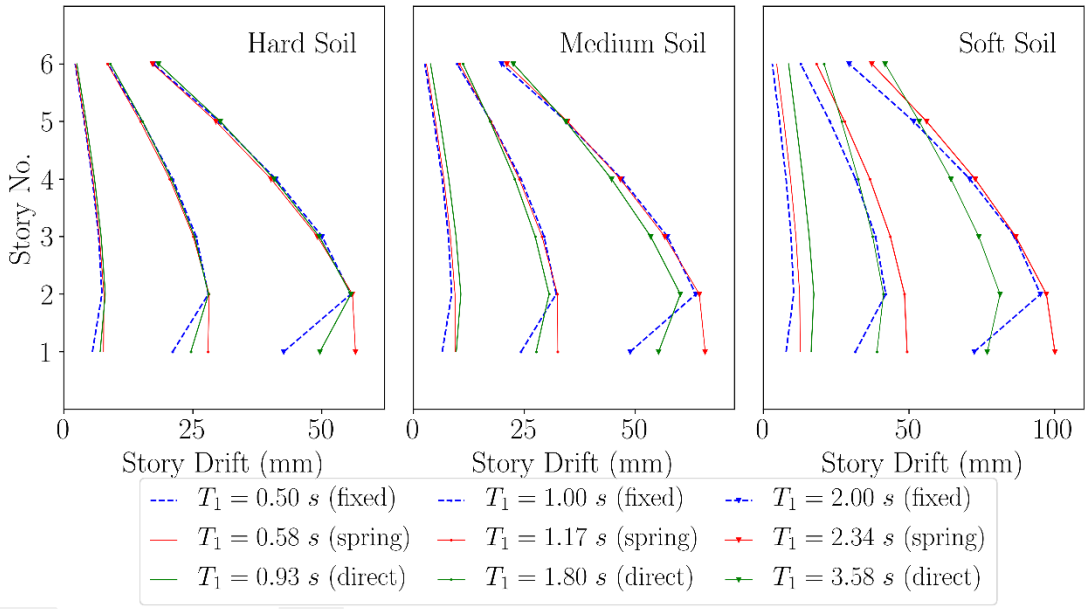

Figure 4.24 Story drifts of buildings with raft foundation on hard, medium, and soft soil

Table 4.12 Story displacements and drifts of stiff building with footing foundation on hard, medium, and soft soil

Soil	Story	Fixed			Spring			Direct		
		Disp. (mm)	Drift (mm)	Drift %	Disp. (mm)	Drift (mm)	Drift %	Disp. (mm)	Drift (mm)	Drift %
Hard Soil	6	31.36	2.19	0.07	32.15	2.25	0.08	49.19	2.44	0.08
	5	29.17	3.97	0.13	29.90	4.01	0.13	46.75	4.19	0.14
	4	25.20	5.53	0.18	25.89	5.59	0.19	42.56	5.86	0.19
	3	19.67	6.75	0.23	20.30	6.81	0.23	36.70	7.34	0.25
	2	12.92	7.38	0.25	13.49	7.48	0.25	29.36	9.23	0.31
	1	5.54	5.54	0.19	6.01	5.89	0.19	20.13	17.72	0.59
Medium Soil	6	36.62	2.56	0.09	40.66	2.81	0.09	71.62	3.61	0.12
	5	34.06	4.63	0.15	37.85	4.88	0.16	68.01	5.64	0.19
	4	29.43	6.46	0.22	32.97	6.73	0.22	62.37	7.58	0.25
	3	22.97	7.89	0.26	26.24	8.20	0.27	54.79	9.36	0.31
	2	15.00	8.60	0.29	18.04	9.12	0.30	45.43	11.70	0.39
	1	6.48	6.48	0.22	8.92	8.25	0.28	33.73	21.57	0.72
Soft Soil	6	44.45	3.11	0.10	63.04	4.32	0.14	160.3	8.17	0.27
	5	41.34	5.62	0.19	58.72	6.80	0.23	152.2	10.56	0.35
	4	35.72	7.85	0.26	51.92	9.10	0.30	141.6	12.89	0.43
	3	27.87	9.57	0.32	42.82	10.99	0.37	128.7	15.10	0.50
	2	18.30	10.45	0.35	31.83	12.63	0.42	113.6	18.27	0.61
	1	7.85	7.85	0.26	19.20	15.30	0.51	95.35	29.51	0.98

Table 4.13 Story displacements and drifts of medium building with footing foundation on hard, medium, and soft soil

Soil	Story	Fixed			Spring			Direct		
		Disp. (mm)	Drift (mm)	Drift %	Disp. (mm)	Drift (mm)	Drift %	Disp. (mm)	Drift (mm)	Drift %
Hard Soil	6	119.6	8.56	0.29	121.3	8.65	0.29	145.7	7.40	0.25
	5	111.1	15.22	0.51	112.6	15.23	0.51	138.3	12.54	0.42
	4	95.84	21.10	0.70	97.38	21.07	0.70	125.8	17.37	0.58
	3	74.74	25.65	0.86	76.31	25.61	0.85	108.4	21.68	0.72
	2	49.09	28.00	0.93	50.70	28.08	0.94	86.75	27.28	0.91
	1	21.09	21.09	0.70	22.62	22.18	0.74	59.47	52.35	1.75
Medium Soil	6	137.4	9.83	0.33	145.1	10.25	0.34	183.9	9.44	0.32
	5	127.6	17.49	0.58	134.9	17.51	0.58	174.5	14.64	0.49
	4	110.1	24.24	0.81	117.3	24.01	0.80	159.9	19.54	0.65
	3	85.88	29.46	0.98	93.33	29.16	0.97	140.3	24.00	0.80
	2	56.42	32.18	1.07	64.17	32.43	1.08	116.3	30.01	1.00
	1	24.24	24.24	0.81	31.74	29.36	0.98	86.32	55.36	1.85
Soft Soil	6	179.6	12.84	0.43	242.0	16.88	0.56	365.5	18.98	0.63
	5	166.8	22.86	0.76	225.1	26.32	0.88	346.5	24.43	0.81
	4	143.9	31.71	1.06	198.8	34.94	1.17	322.1	29.71	0.99
	3	112.2	38.54	1.29	163.9	42.10	1.40	292.3	34.67	1.16
	2	73.69	42.05	1.40	121.8	48.33	1.61	257.7	41.89	1.39
	1	31.64	31.64	1.06	73.45	58.53	1.95	215.8	67.73	2.26

Table 4.14 Story displacements and drifts of soft building with footing foundation on hard, medium, and soft soil

Soil	Story	Fixed			Spring			Direct		
		Disp. (mm)	Drift (mm)	Drift %	Disp. (mm)	Drift (mm)	Drift %	Disp. (mm)	Drift (mm)	Drift %
Hard Soil	6	236.7	17.36	0.58	240.3	17.56	0.59	290.8	15.07	0.50
	5	219.4	30.07	1.00	222.7	30.14	1.00	275.7	25.16	0.84
	4	189.3	41.07	1.37	192.6	41.05	1.37	250.6	34.33	1.14
	3	148.3	50.06	1.67	151.5	50.01	1.67	216.2	42.69	1.42
	2	98.22	55.60	1.85	101.5	55.77	1.86	173.5	54.17	1.81
	1	42.62	42.62	1.42	45.74	44.86	1.49	119.4	105.1	3.50
Medium Soil	6	271.1	19.90	0.66	287.8	20.83	0.69	369.2	19.33	0.64
	5	251.2	34.42	1.15	266.9	34.73	1.16	349.9	29.54	0.99
	4	216.8	46.97	1.57	232.2	46.80	1.56	320.4	38.92	1.29
	3	169.8	57.28	1.91	185.4	56.89	1.89	281.4	47.57	1.59
	2	112.5	63.67	2.12	128.5	64.30	2.14	233.9	59.87	1.99
	1	48.85	48.85	1.63	64.20	59.36	1.98	173.9	111.7	3.72
Soft Soil	6	405.9	29.51	0.98	484.1	34.30	1.14	728.4	38.23	1.27
	5	376.4	51.63	1.72	449.8	52.72	1.76	690.2	48.90	1.63
	4	324.8	70.91	2.36	397.1	69.21	2.31	641.3	59.13	1.97
	3	253.9	86.31	2.88	327.8	83.18	2.77	582.2	68.78	2.29
	2	167.6	95.16	3.17	244.7	96.25	3.21	513.4	83.13	2.77
	1	72.42	72.42	2.41	148.4	118.2	3.94	430.3	135.2	4.51

Table 4.15 Story displacements and drifts of stiff building with raft foundation on hard, medium, and soft soil

Soil	Story	Fixed			Spring			Direct		
		Disp. (mm)	Drift (mm)	Drift %	Disp. (mm)	Drift (mm)	Drift %	Disp. (mm)	Drift (mm)	Drift %
Hard Soil	6	31.36	2.19	0.07	34.47	2.27	0.08	36.96	2.53	0.08
	5	29.17	3.97	0.13	32.20	4.04	0.14	34.43	4.33	0.14
	4	25.20	5.53	0.18	28.16	5.64	0.19	30.10	5.95	0.19
	3	19.67	6.75	0.23	22.52	6.91	0.23	24.15	7.24	0.24
	2	12.92	7.38	0.25	15.61	7.76	0.26	16.91	8.03	0.27
	1	5.54	5.54	0.19	7.85	7.69	0.26	8.88	7.04	0.24
Medium Soil	6	36.62	2.56	0.09	42.43	2.91	0.09	59.03	3.84	0.13
	5	34.06	4.63	0.15	39.52	4.97	0.17	55.19	6.00	0.20
	4	29.43	6.46	0.22	34.55	6.84	0.23	49.19	7.96	0.27
	3	22.97	7.89	0.26	27.71	8.34	0.28	41.23	9.59	0.32
	2	15.08	8.60	0.29	19.37	9.35	0.31	31.64	10.67	0.36
	1	6.48	6.48	0.22	10.02	9.35	0.31	20.97	9.64	0.32
Soft Soil	6	44.45	3.11	0.10	61.02	4.63	0.15	152.9	8.72	0.29
	5	41.34	5.62	0.19	56.39	7.12	0.24	144.2	11.25	0.38
	4	35.72	7.85	0.26	49.27	9.39	0.31	132.9	13.66	0.46
	3	27.87	9.57	0.32	39.88	11.23	0.38	119.3	15.79	0.53
	2	18.30	10.40	0.35	28.65	12.49	0.42	103.5	17.37	0.58
	1	7.85	7.85	0.26	16.16	12.72	0.42	86.09	16.45	0.55

Table 4.16 Story displacements and drifts of medium building with raft foundation on hard, medium, and soft soil

Soil	Story	Fixed			Spring			Direct		
		Disp. (mm)	Drift (mm)	Drift %	Disp. (mm)	Drift (mm)	Drift %	Disp. (mm)	Drift (mm)	Drift %
Hard Soil	6	119.6	8.56	0.29	125.6	8.45	0.28	129.4	9.03	0.30
	5	111.1	15.22	0.51	117.1	14.82	0.49	120.4	15.28	0.51
	4	95.84	21.10	0.70	102.3	20.53	0.68	105.1	20.85	0.69
	3	74.74	25.65	0.86	81.76	25.09	0.84	84.24	25.32	0.84
	2	49.09	28.00	0.93	56.67	28.15	0.94	58.92	28.03	0.93
	1	21.09	21.01	0.70	28.52	27.95	0.93	30.89	24.61	0.82
Medium Soil	6	137.4	9.83	0.33	147.9	10.35	0.35	167.2	11.15	0.37
	5	127.6	17.49	0.58	137.6	17.47	0.58	156.0	17.27	0.58
	4	110.1	24.24	0.81	120.2	23.85	0.79	138.8	22.83	0.76
	3	85.88	29.46	0.98	96.30	28.98	0.97	115.9	27.44	0.92
	2	56.42	32.18	1.07	67.32	32.46	1.08	88.49	30.56	1.02
	1	24.24	24.24	0.81	34.86	32.54	1.09	57.93	27.66	0.92
Soft Soil	6	179.6	12.84	0.43	237.6	18.30	0.61	346.0	20.89	0.69
	5	166.8	22.86	0.76	219.3	27.92	0.93	325.1	26.91	0.89
	4	143.9	31.71	1.06	191.4	36.61	1.22	298.2	32.59	1.09
	3	112.2	38.54	1.29	154.8	43.64	1.46	265.6	37.58	1.25
	2	73.69	42.05	1.40	111.1	48.49	1.62	228.0	41.28	1.38
	1	31.64	31.64	1.06	62.64	49.39	1.65	186.8	39.04	1.30

Table 4.17 Story displacements and drifts of soft building with raft foundation on hard, medium, and soft soil

Soil	Story	Fixed			Spring			Direct		
		Disp. (mm)	Drift (mm)	Drift %	Disp. (mm)	Drift (mm)	Drift %	Disp. (mm)	Drift (mm)	Drift %
Hard Soil	6	236.8	17.36	0.58	249.6	17.20	0.57	256.8	18.34	0.61
	5	219.4	30.07	1.00	232.4	29.47	0.98	238.5	30.33	1.01
	4	189.4	41.07	1.37	202.9	40.16	1.34	208.1	40.76	1.36
	3	148.3	50.06	1.67	162.7	49.13	1.64	167.4	49.50	1.65
	2	98.22	55.60	1.85	113.6	55.93	1.86	117.9	55.62	1.85
	1	42.62	42.62	1.42	57.67	56.51	1.88	62.25	49.62	1.65
Medium Soil	6	271.1	19.90	0.66	293.9	21.05	0.70	330.5	22.54	0.75
	5	251.2	34.42	1.15	272.9	34.72	1.16	307.9	34.33	1.14
	4	216.8	46.97	1.57	238.2	46.62	1.55	273.6	44.65	1.49
	3	169.8	57.28	1.91	191.6	56.67	1.89	228.9	53.49	1.78
	2	112.5	63.67	2.12	134.9	64.46	2.15	175.5	60.18	2.01
	1	48.85	48.85	1.63	70.46	65.77	2.19	115.3	55.27	1.84
Soft Soil	6	405.9	29.51	0.98	477.1	37.27	1.24	679.2	41.82	1.39
	5	376.4	51.63	1.72	439.8	56.09	1.87	637.4	53.52	1.78
	4	324.8	70.91	2.36	383.7	72.75	2.43	583.9	64.43	2.15
	3	253.9	86.31	2.88	310.9	86.68	2.89	519.4	73.99	2.47
	2	167.6	95.16	3.17	224.3	97.20	3.24	445.5	81.28	2.71
	1	72.42	72.42	2.41	127.1	100.1	3.34	364.2	76.91	2.56

4.2.2.3 Foundation Displacement

Foundation vertical and lateral displacements of spring and direct models with different types of soil are presented in Table 4.18. Foundation displacements are given at three points (Loc. 1, 2, 3) in Table 4.18, such that Loc. 1 is leftmost point at the

bottom of the foundation, Loc. 2 is the center point at the bottom of the foundation, and Loc. 3 is the rightmost point at the bottom of the foundation. Foundation settlement (vertical displacement) is also plotted in Figures 4.25 and 4.26 for footing and raft foundations, respectively.

As the soil and/or structure gets softer, the foundation vertical and lateral displacements increase as expected. It is observed that spring models indicate lower vertical and lateral displacements compared to direct models, leading to less conservative results for foundation displacements. Spring models indicate a larger difference in foundation settlement between footing and raft foundations compared to direct models. Also, it is observed that spring models indicate larger foundation settlements in raft foundation for any soil and structure type whereas direct models indicate larger foundation settlements in raft foundation only for stiff structure.

Table 4.18 Foundation vertical and lateral displacements

Soil Type	Structure Type	Loc.	Spring Model				Direct Model			
			Footing		Raft		Footing		Raft	
			U_z (mm)	U_x (mm)	U_z (mm)	U_x (mm)	U_z (mm)	U_x (mm)	U_z (mm)	U_x (mm)
Hard Soil	Stiff	1	-0.23	0.09	-0.17	0.06	-0.87	2.01	-1.64	1.740
		2	-0.28	0.12	-0.32	0.06	-3.63	1.95	-4.02	1.770
		3	0.23	0.09	-0.17	0.10	-0.87	1.24	-1.64	1.570
	Medium	1	-0.15	0.34	-0.43	0.21	-5.35	6.24	-5.62	5.960
		2	-1.08	0.44	-1.16	0.22	-13.7	5.76	-13.0	6.030
		3	-0.15	0.35	-0.43	0.37	-5.35	3.35	-5.62	5.310
	Soft	1	-2.45	0.70	-1.81	0.26	-32.4	15.32	-32.5	12.61
		2	-4.25	0.88	-4.47	0.44	-53.7	11.55	-48.9	12.13
		3	-2.45	0.70	-1.81	0.89	-32.4	3.94	-32.5	10.10
Medium Soil	Stiff	1	0.14	0.52	-0.83	0.42	-3.95	10.48	-6.41	10.83
		2	-1.29	0.67	-1.24	0.54	-13.6	11.05	-15.8	11.10
		3	0.14	0.54	-0.83	0.42	-3.95	8.27	-6.41	10.90
	Medium	1	-0.40	1.88	1.94	1.49	-24.4	28.06	-25.3	28.94
		2	-4.93	2.38	-4.37	1.87	-51.3	28.11	-51.4	29.62
		3	-0.40	1.90	1.94	1.40	-24.4	19.63	-25.3	28.98
	Soft	1	-10.58	3.86	-7.46	3.17	-123	64.74	-130	57.54
		2	-19.41	4.84	-16.9	3.78	-201	56.61	-193	58.81
		3	-10.58	3.88	-7.46	2.75	-129	31.49	-130	57.49
Soft Soil	Stiff	1	-1.19	3.09	-3.46	2.76	-12.8	56.10	-22.5	67.65
		2	-5.62	3.90	-5.15	3.22	-51.5	61.72	-61.3	68.38
		3	-1.19	3.18	-3.46	2.71	-12.8	52.42	-22.5	68.23
	Medium	1	-2.62	11.94	12.80	10.74	-98.1	129.2	-105	143.
		2	-21.55	14.92	-18.2	12.41	-196	138.7	-200	144.8
		3	-2.62	12.03	12.80	10.24	-98.1	114.6	-105	144.5
	Soft	1	-36.36	24.36	-16.8	22.70	-525	272.2	-525	277.2
		2	-85.05	30.23	-70.0	25.29	-771	276.5	-753.	282
		3	-36.36	24.45	-16.8	20.40	-525	214.1	-525	282

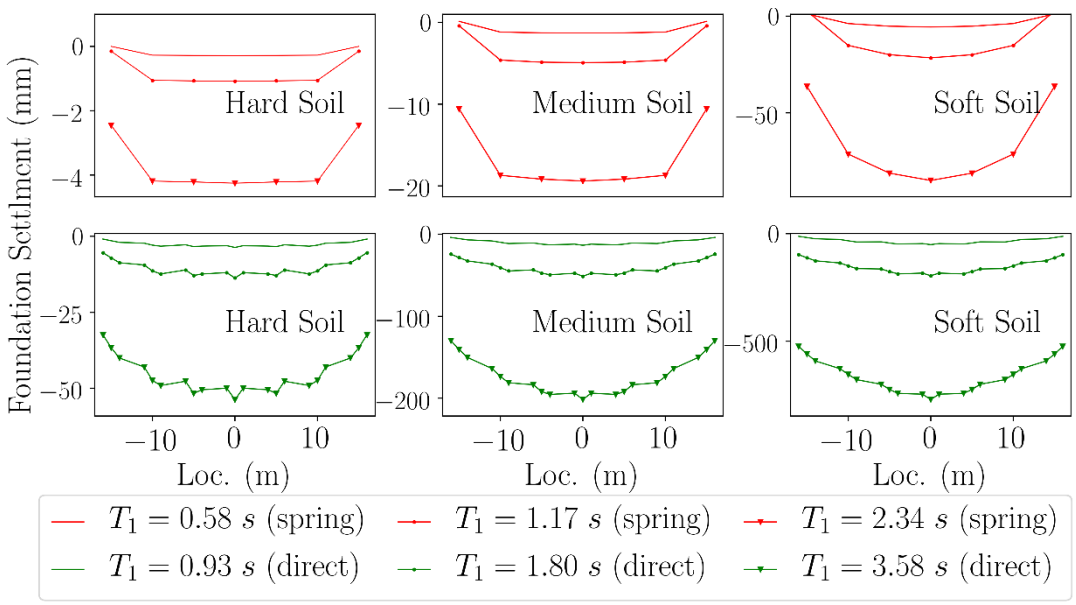

Figure 4.25 Foundation settlements of buildings with footing foundation on hard, medium, and soft soil

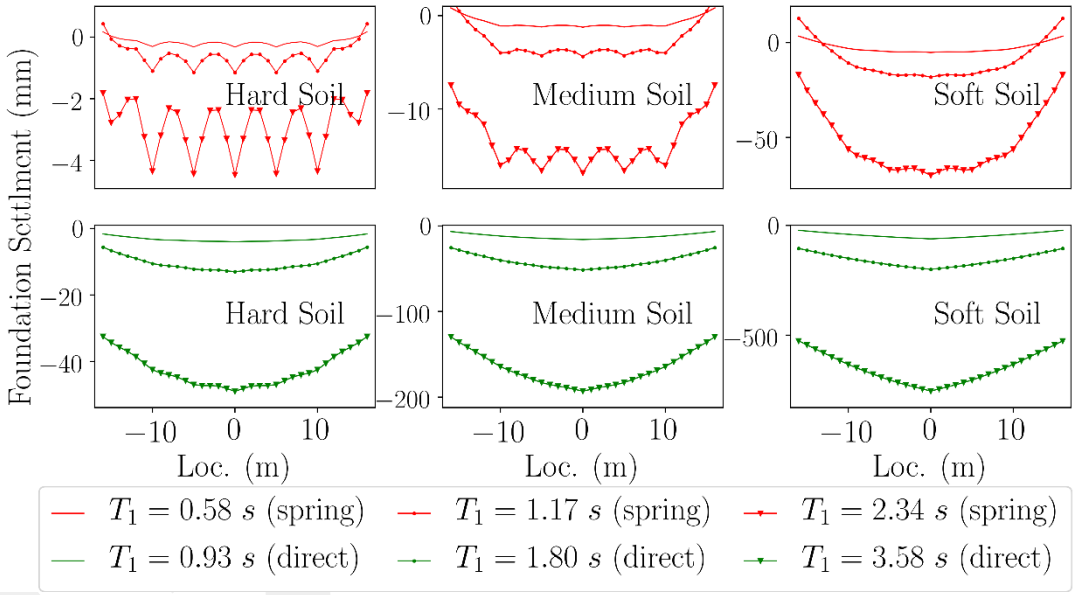

Figure 4.26 Foundation settlements of buildings with raft foundation on hard, medium, and soft soil

4.2.3 Time History Analysis Results

The time history analysis is carried out for the fixed base models and spring models using 1940 El Centro earthquake acceleration record. For the dynamic analysis, the natural periods and mode shapes, base and story shears, story displacements and drifts, and foundation displacements are presented in the following sections.

4.2.3.1 Base and Story Shears

Maximum story shears in the fixed base models and spring models on three types of soil (hard, medium, soft) are plotted in Figure 4.27 for footing foundation, and in Figure 4.29 for raft foundation. Sample base shear time histories are also plotted for fixed and spring models on soft soil in Figures 4.28 and 4.30 for footing foundation and raft foundation, respectively. Maximum values of base shears are also tabulated in Table 4.19.

From the figures below, it is observed that maximum story shears are very similar for all three buildings with footing foundation when they are on hard soil. As the soil gets softer, the maximum story shears start to differ more between the fixed base model and spring model, especially in soft building on soft soil. Similar trends can be observed in maximum story shears for buildings with raft foundation. In this case, the differences between fixed base and spring models are noticeable for medium and soft buildings on all three types of soil (hard, medium, soft) considered in this study.

From the figures and table below, it is observed that fixed based models have slightly lower (unconservative) base and story shears for the stiff structure on hard and medium soil. As the structure and underlying soil become softer, the fixed based models start to have higher (conservative) base and story shears. This effect becomes significant in spring models primarily for medium and soft buildings on soft soil. The dynamic base and story shear results are in general consistent with response spectrum analysis results, with minor discrepancies most likely due to using an unscaled ground acceleration for all soil types and effect of dominant frequency components in the ground motion record.

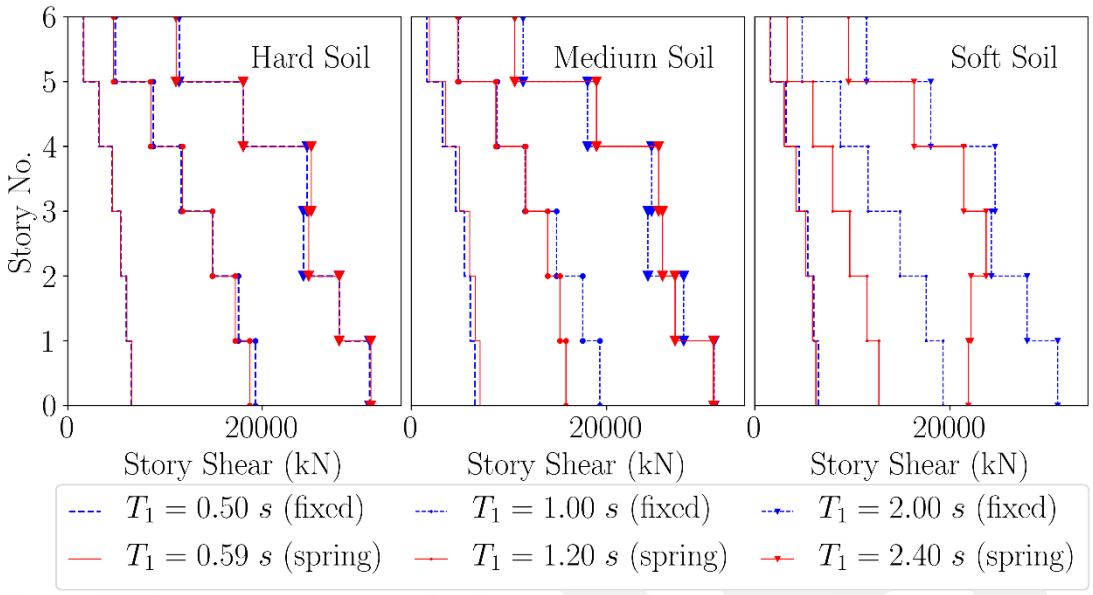

Figure 4.27 Maximum story shears of buildings with footing foundation on hard, medium, and soft soil under 1940 El Centro earthquake

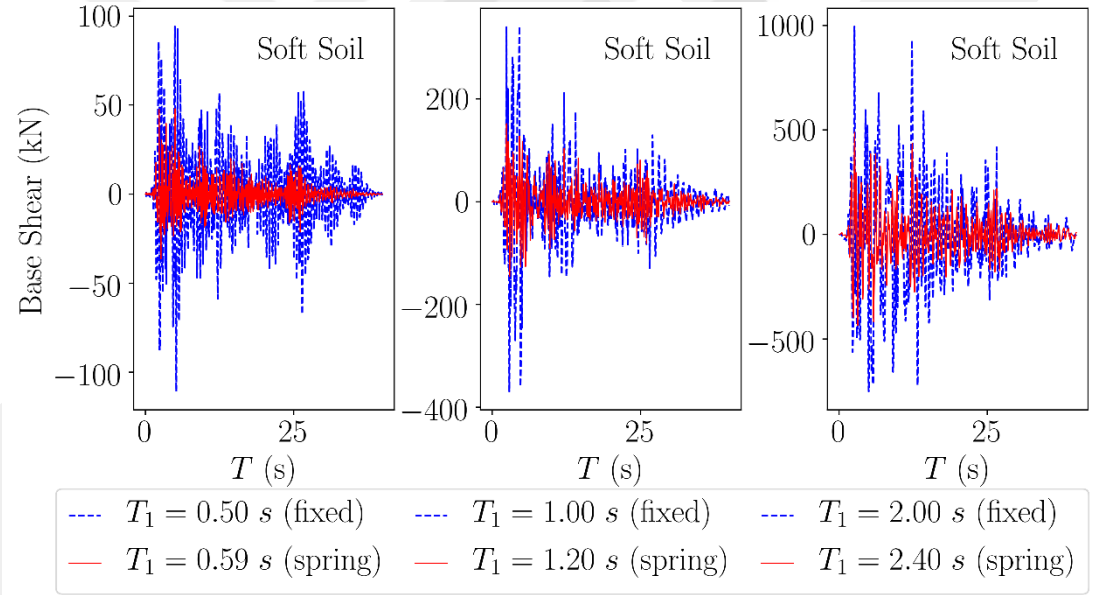

Figure 4.28 Base shear time-histories of buildings with footing foundation on soft soil under 1940 El Centro earthquake

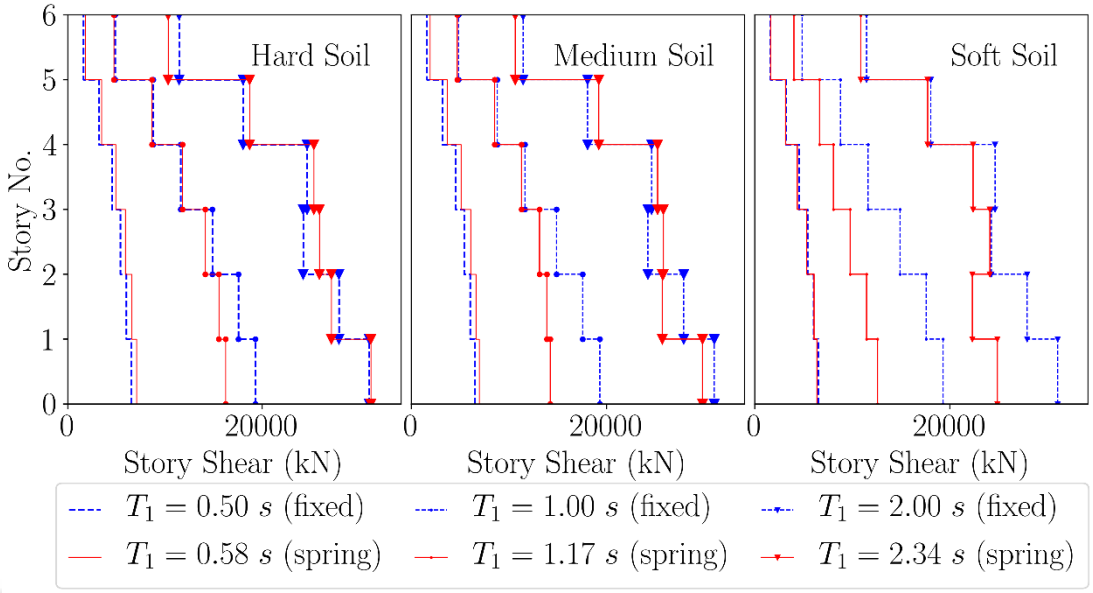

Figure 4.29 Maximum story shears of buildings with raft foundation on hard, medium, and soft soil under 1940 El Centro earthquake

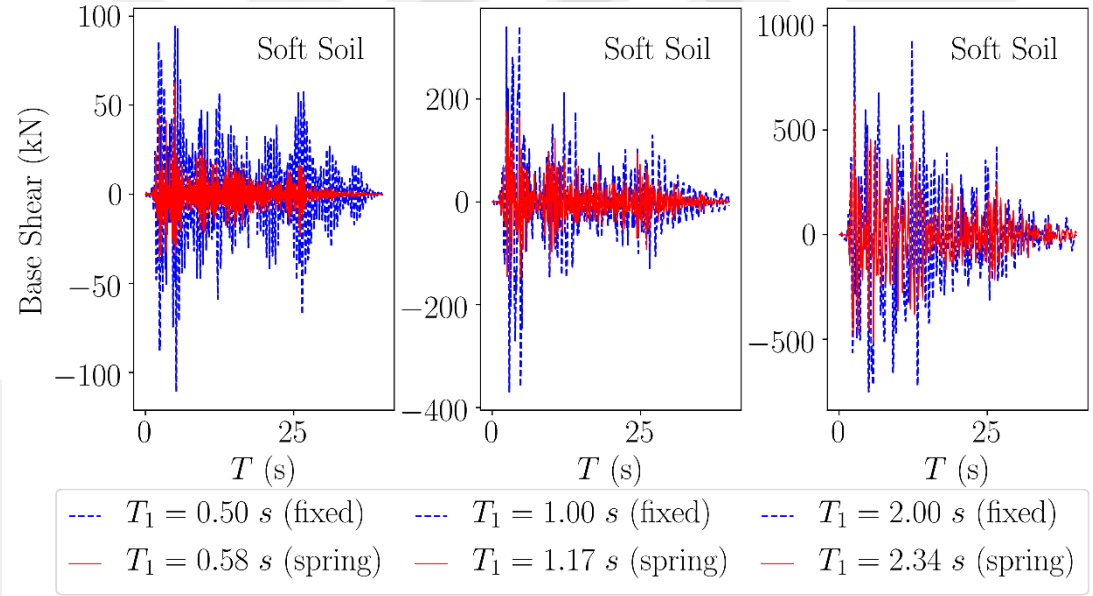

Figure 4.30 Base shear time-histories of buildings with raft foundation on soft soil under 1940 El Centro earthquake

Table 4.19 Maximum base shears of buildings on hard, medium, and soft soil

Structure Type	Fixed Model Base Shear (kN)	Soil Type	Spring Model Base Shear (kN)	
			Footing	Raft
Stiff	6519	Hard	6565	7080
		Medium	7031	6960
		Soft	6273	6381
Medium	19303	Hard	18691	16242
		Medium	15846	14238
		Soft	12718	12575
Soft	31035	Hard	31183	31208
		Medium	30949	29827
		Soft	21892	24871

4.2.3.2 Story Displacements and Drifts

Maximum story displacements and drifts of the fixed base and spring models are plotted in Figures 4.31, 4.33, 4.35, and 4.37 for footing and raft foundation cases on all three types of soil. Sample top floor displacement and first floor drift histories are plotted for footing and raft foundation cases on soft soil only in Figures 4.32, 4.34, 4.36, and 4.38. The values of story displacements and drifts are also tabulated in Tables 4.20 through 4.37.

For both footing and raft foundations, as building and soil become softer, maximum story displacements increase as expected due to two reasons, which are: (i) higher flexibility of building and soil, and (ii) higher design spectral acceleration for softer soil. For a given structure with footing or raft foundation, as soil becomes softer, the differences between the fixed model and spring model become more pronounced.

Similar to the story displacements, the story drift values increase as the structure and the soil get softer. For fixed base models, the largest story drift (maximum value) occurs in the second story columns. Spring models on hard and medium soil have the largest drift in the second story columns similar to the fixed models, but as the soil becomes softer, the largest drift occurs in the first story columns of the spring models. For a given structure as the soil gets softer, the story drifts of the spring model increase with respect to fixed based model story drifts for both footing and raft foundations.

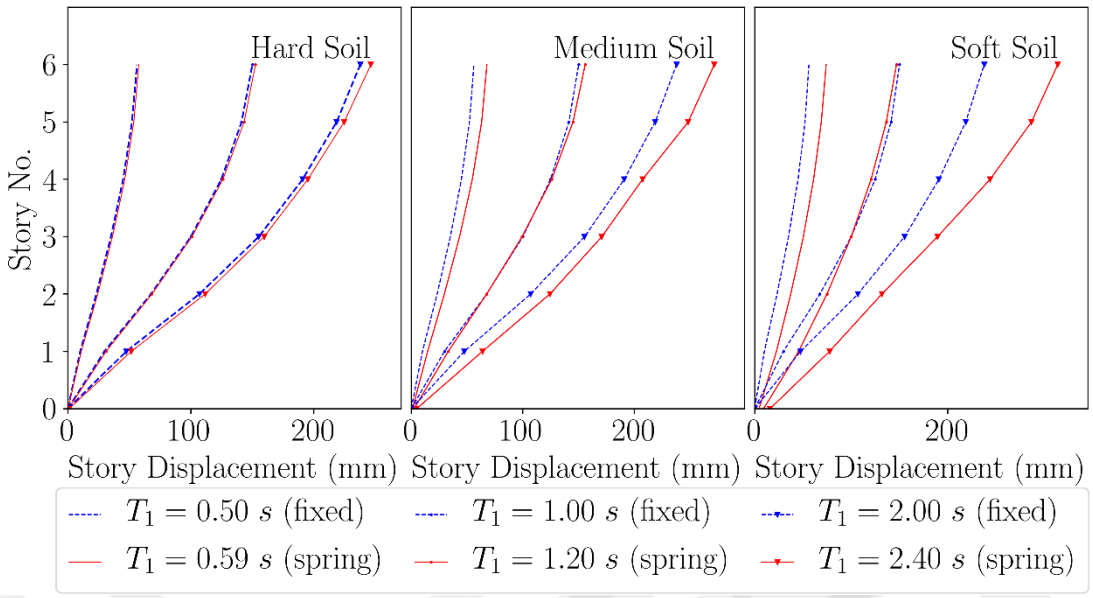

Figure 4.31 Maximum story displacements of buildings with footing foundation on hard, medium, and soft soil under 1940 El Centro earthquake

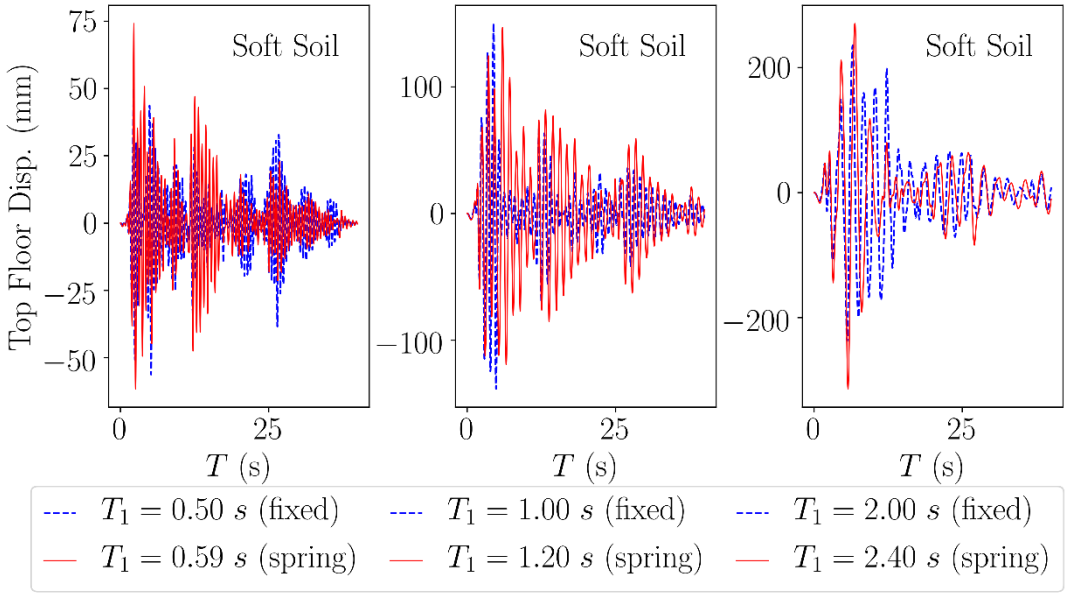

Figure 4.32 Top story displacement time-histories of buildings with footing foundation on soft soil under 1940 El Centro earthquake

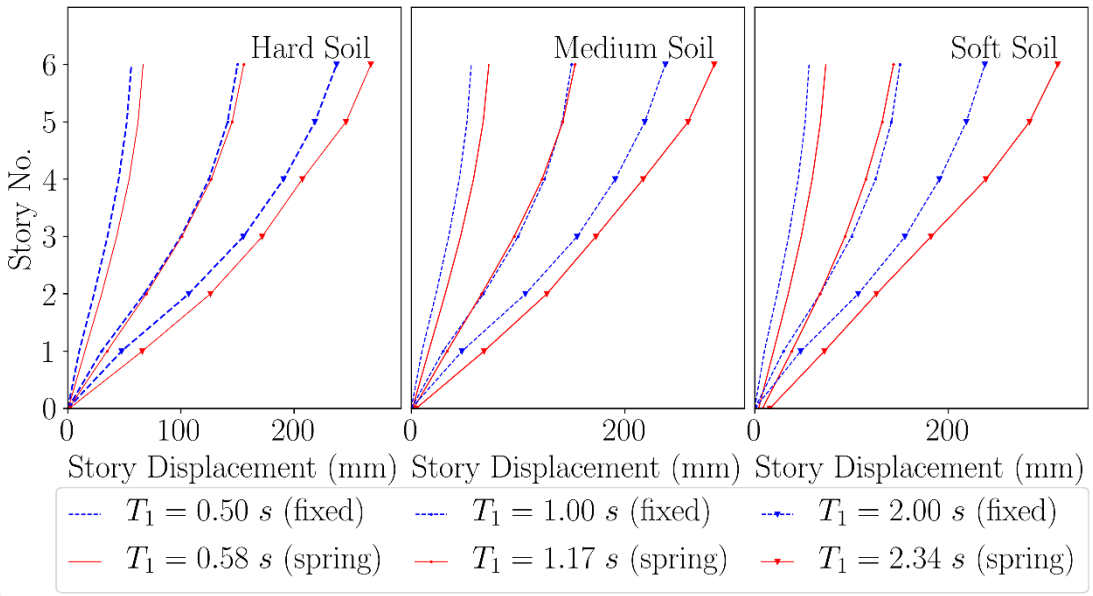

Figure 4.33 Maximum story displacements of buildings with raft foundation on hard, medium, and soft soil under 1940 El Centro earthquake

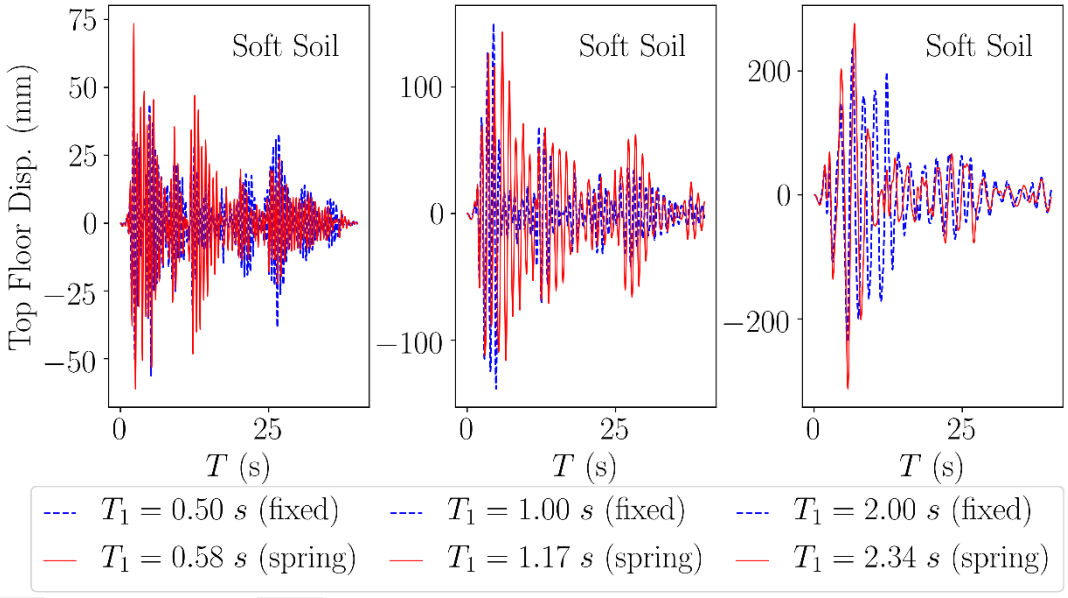

Figure 4.34 Top story displacement time-histories of buildings raft foundation on soft soil under 1940 El Centro earthquake

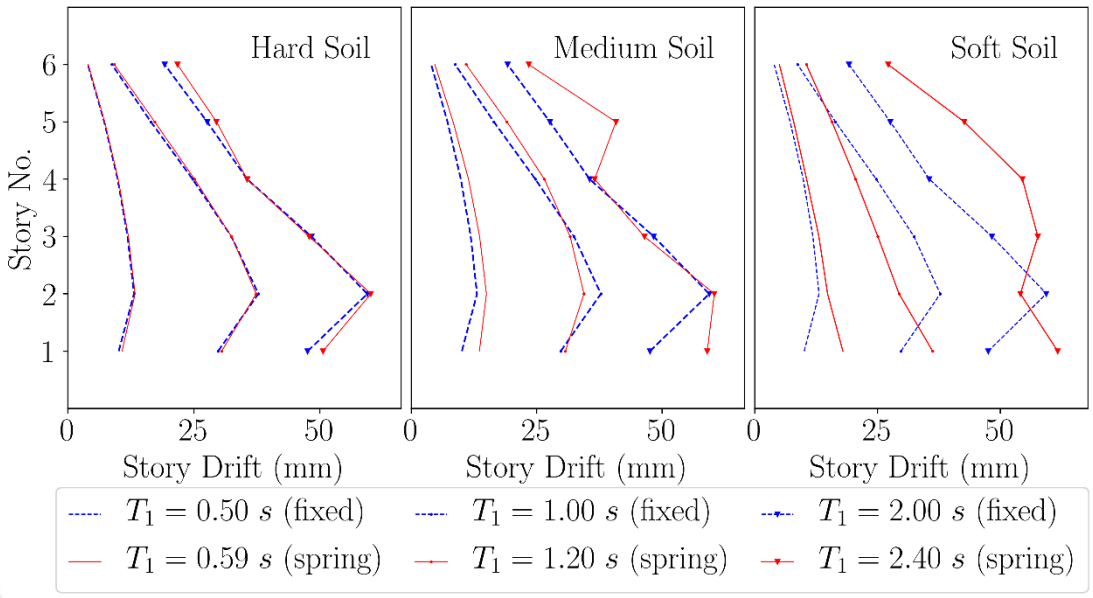

Figure 4.35 Maximum story drifts of buildings with footing foundation on hard, medium, and soft soil under 1940 El Centro earthquake

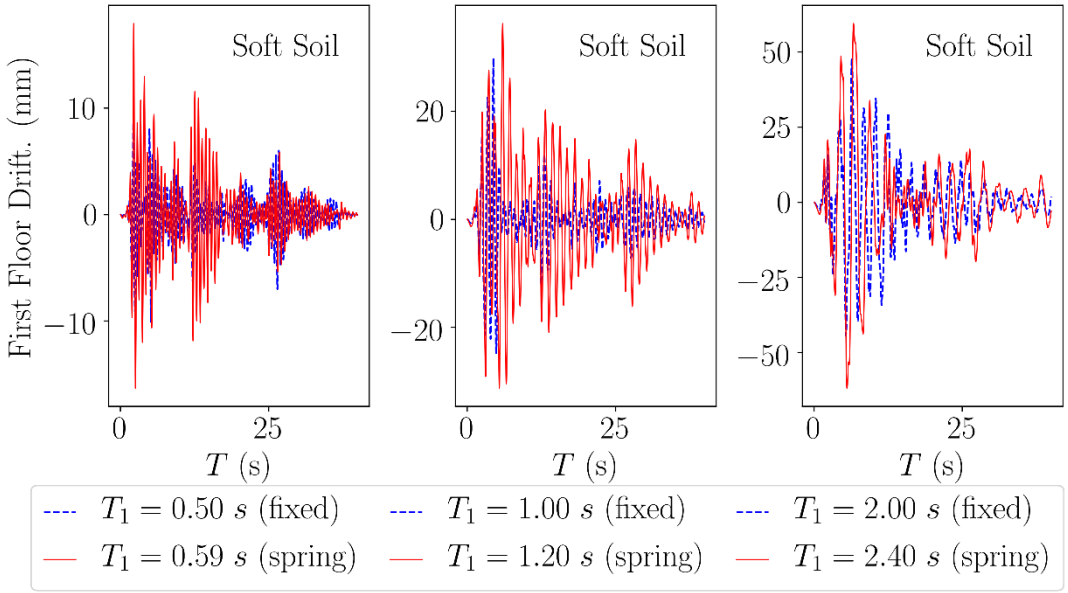

Figure 4.36 First story drift time-histories of buildings with footing foundation on soft soil under 1940 El Centro earthquake

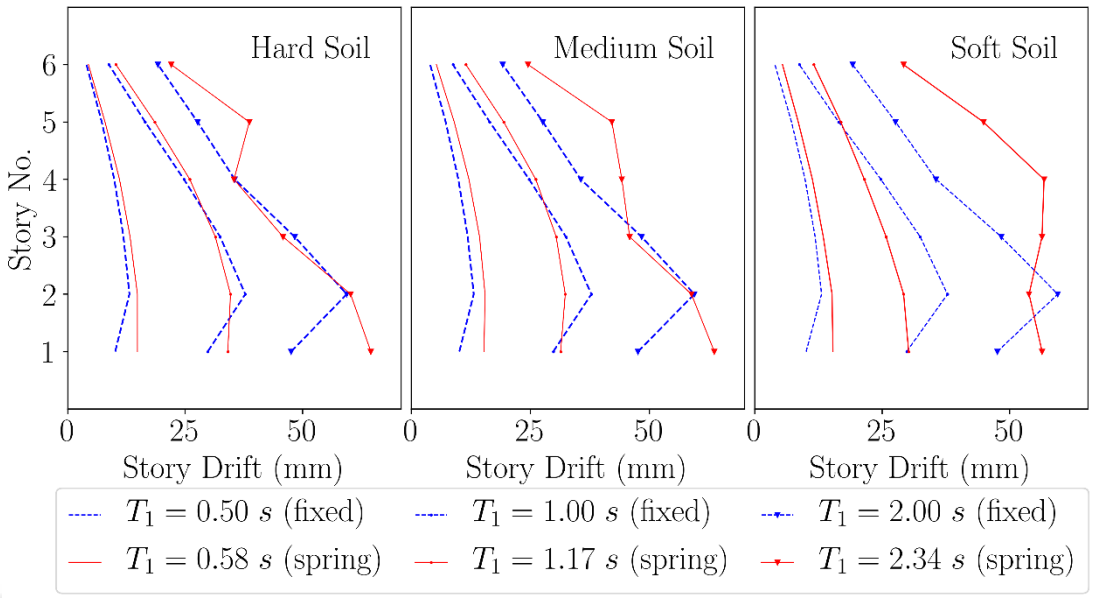

Figure 4.37 Maximum story drifts of buildings with raft foundation on hard, medium, and soft soil under 1940 El Centro earthquake

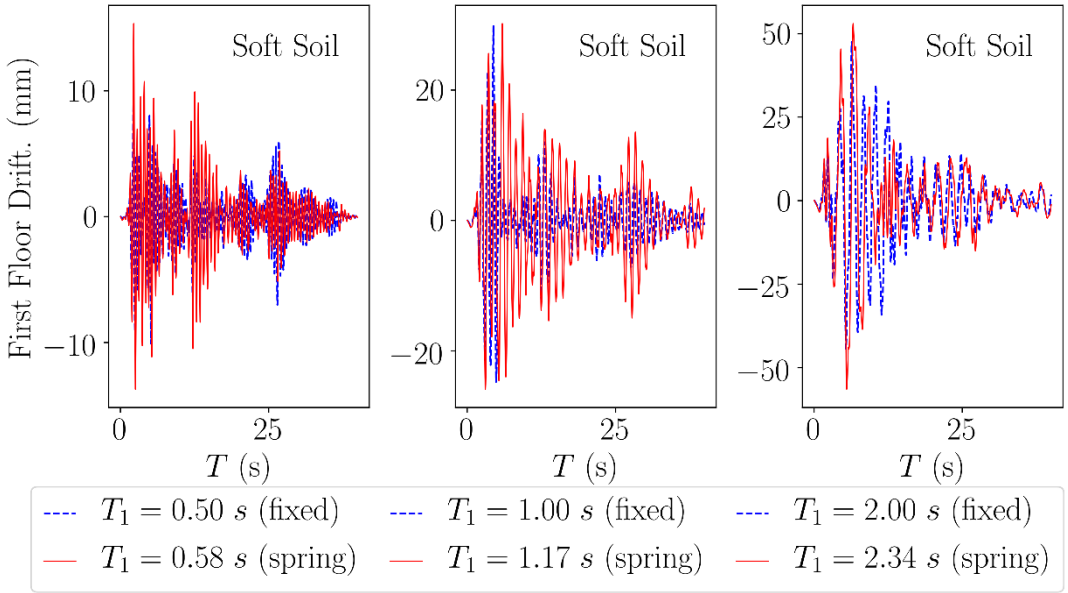

Figure 4.38 First story drift time-histories of buildings raft foundation on soft soil under 1940 El Centro earthquake

Table 4.20 Maximum story displacements and drifts of stiff building with footing foundation on hard soil

Story	Fixed			Spring		
	Disp. (mm)	Drift (mm)	Drift (%)	Disp. (mm)	Drift (mm)	Drift (%)
6	56.2	3.9	0.1	57.7	4.0	0.1
5	52.2	7.2	0.2	53.7	7.3	0.2
4	44.9	9.9	0.3	46.3	10.0	0.3
3	35.1	11.9	0.4	36.3	12.0	0.4
2	23.2	13.1	0.4	24.3	13.3	0.4
1	10.1	10.1	0.3	10.9	10.8	0.4

Table 4.21 Maximum story displacements and drifts of stiff building with footing foundation on medium soil

Story	Fixed			Spring		
	Disp. (mm)	Drift (mm)	Drift (%)	Disp. (mm)	Drift (mm)	Drift (%)
6	56.2	3.9	0.1	67.8	4.7	0.2
5	52.2	7.2	0.2	63.1	8.4	0.3
4	44.9	9.9	0.3	54.8	11.4	0.4
3	35.1	11.9	0.4	43.3	13.6	0.5
2	23.2	13.1	0.4	29.7	14.9	0.5
1	10.1	10.1	0.3	14.7	13.6	0.5

Table 4.22 Maximum story displacements and drifts of stiff building with footing foundation on soft soil

Story	Fixed			Spring		
	Disp. (mm)	Drift (mm)	Drift (%)	Disp. (mm)	Drift (mm)	Drift (%)
6	56.2	3.9	0.1	74.1	74.1	0.2
5	52.2	7.2	0.2	69.1	69.1	0.3
4	44.9	9.9	0.3	61.1	61.1	0.4
3	35.1	11.9	0.4	50.5	50.5	0.4
2	23.2	13.1	0.4	37.4	37.4	0.5
1	10.1	10.1	0.3	22.6	22.6	0.6

Table 4.23 Maximum story displacements and drifts of medium building with footing foundation on hard soil

Story	Fixed			Spring		
	Disp. (mm)	Drift (mm)	Drift (%)	Disp. (mm)	Drift (mm)	Drift (%)
6	150	8.8	0.3	152.5	9.2	0.3
5	141	16.5	0.5	143.3	17.2	0.6
4	124	24.8	0.8	126.1	25.2	0.8
3	100	32.5	1.1	100.9	32.5	1.1
2	67.6	37.8	1.3	68.5	37.4	1.2
1	29.8	29.8	0.9	31.1	30.5	1.0

Table 4.24 Maximum story displacements and drifts of medium building with footing foundation on medium soil

Story	Fixed			Spring		
	Disp. (mm)	Drift (mm)	Drift (%)	Disp. (mm)	Drift (mm)	Drift (%)
6	150	8.8	0.3	156	10.5	0.4
5	141	16.5	0.5	145	19.1	0.6
4	124	24.8	0.8	126	26.5	0.9
3	100	32.5	1.1	99.3	31.7	1.1
2	67.6	37.8	1.3	67.7	34.4	1.1
1	29.8	29.8	0.9	33.2	30.7	1.0

Table 4.25 Maximum story displacements and drifts of medium building with footing foundation on soft soil

Story	Fixed			Spring		
	Disp. (mm)	Drift (mm)	Drift (%)	Disp. (mm)	Drift (mm)	Drift (%)
6	150	8.8	0.3	147	10.5	0.4
5	141	16.5	0.5	136	15.8	0.5
4	124	24.8	0.8	121	20.6	0.7
3	100	32.5	1.1	100	25.1	0.8
2	67.6	37.8	1.3	74.9	29.4	0.9
1	29.8	29.8	0.9	45.5	36.3	1.2

Table 4.26 Maximum story displacements and drifts of soft building with footing foundation on hard soil

Story	Fixed			Spring		
	Disp. (mm)	Drift (mm)	Drift (%)	Disp. (mm)	Drift (mm)	Drift (%)
6	238	19.2	0.6	246	21.8	0.7
5	219	27.6	0.9	225	29.5	0.9
4	191	35.6	1.2	195	35.6	1.2
3	155	48.3	1.6	160	47.9	1.6
2	107	59.4	1.9	112	60.1	2.0
1	47.6	47.6	1.6	51.6	50.6	1.7

Table 4.27 Maximum story displacements and drifts of soft building with footing foundation on medium soil

Story	Fixed			Spring		
	Disp. (mm)	Drift (mm)	Drift (%)	Disp. (mm)	Drift (mm)	Drift (%)
6	238	19.2	0.6	272	23.4	0.8
5	219	27.6	0.9	248	40.8	1.4
4	191	35.6	1.2	207	36.6	1.2
3	155	48.3	1.6	171	46.5	1.6
2	107	59.4	1.9	124	60.4	2.0
1	47.6	47.6	1.6	63.9	59.0	1.9

Table 4.28 Maximum story displacements and drifts of soft building with footing foundation on soft soil

Story	Fixed			Spring		
	Disp. (mm)	Drift (mm)	Drift (%)	Disp. (mm)	Drift (mm)	Drift (%)
6	238	19.2	0.6	314	27.2	0.9
5	219	27.6	0.9	287	42.7	1.4
4	191	35.6	1.2	244	54.5	1.8
3	155	48.3	1.6	189	57.7	1.9
2	107	59.4	1.9	132	54.1	1.8
1	47.6	47.6	1.6	77.6	61.7	2.1

Table 4.29 Maximum story displacements and drifts of stiff building with raft foundation on hard soil

Story	Fixed			Spring		
	Disp. (mm)	Drift (mm)	Drift (%)	Disp. (mm)	Drift (mm)	Drift (%)
6	56.2	3.9	0.1	66.6	4.4	0.1
5	52.2	7.2	0.2	62.2	7.9	0.3
4	44.9	9.9	0.3	54.2	11.0	0.4
3	35.1	11.9	0.4	43.2	13.3	0.4
2	23.2	13.1	0.4	29.9	14.8	0.5
1	10.1	10.1	0.3	15.1	14.8	0.5

Table 4.30 Maximum story displacements and drifts of stiff building with raft foundation on medium soil

Story	Fixed			Spring		
	Disp. (mm)	Drift (mm)	Drift (%)	Disp. (mm)	Drift (mm)	Drift (%)
6	56.2	3.9	0.1	72.6	5.3	0.2
5	52.2	7.2	0.2	67.3	9.0	0.3
4	44.9	9.9	0.3	58.3	12.1	0.4
3	35.1	11.9	0.4	46.2	14.3	0.5
2	23.2	13.1	0.4	31.9	15.5	0.5
1	10.1	10.1	0.3	16.4	15.3	0.5

Table 4.31 Maximum story displacements and drifts of stiff building with raft foundation on soft soil

Story	Fixed			Spring		
	Disp. (mm)	Drift (mm)	Drift (%)	Disp. (mm)	Drift (mm)	Drift (%)
6	56.2	3.9	0.1	73.5	5.5	0.2
5	52.2	7.2	0.2	68.0	8.6	0.3
4	44.9	9.9	0.3	59.5	11.3	0.4
3	35.1	11.9	0.4	48.1	13.5	0.4
2	23.2	13.1	0.4	34.7	15.2	0.5
1	10.1	10.1	0.3	19.5	15.3	0.5

Table 4.32 Maximum story displacements and drifts of medium building with raft foundation on hard soil

Story	Fixed			Spring		
	Disp. (mm)	Drift (mm)	Drift (%)	Disp. (mm)	Drift (mm)	Drift (%)
6	150	8.8	0.3	156	10.3	0.3
5	141	16.5	0.5	145	18.5	0.6
4	125	24.8	0.8	127	25.9	0.9
3	100	32.5	1.1	101	31.4	1.0
2	67.6	37.8	1.3	69.4	34.7	1.2
1	29.8	29.8	0.9	34.8	34.1	1.1

Table 4.33 Maximum story displacements and drifts of medium building with raft foundation on medium soil

Story	Fixed			Spring		
	Disp. (mm)	Drift (mm)	Drift (%)	Disp. (mm)	Drift (mm)	Drift (%)
6	150	8.8	0.3	153	11.5	0.4
5	141	16.5	0.5	142	19.4	0.6
4	125	24.8	0.8	122	26.1	0.9
3	100	32.5	1.1	96.3	30.4	1.0
2	67.6	37.8	1.3	65.9	32.3	1.1
1	29.8	29.8	0.9	33.6	31.4	1.0

Table 4.34 Maximum story displacements and drifts of medium building with raft foundation on soft soil

Story	Fixed			Spring		
	Disp. (mm)	Drift (mm)	Drift (%)	Disp. (mm)	Drift (mm)	Drift (%)
6	150	8.8	0.3	143	11.6	0.4
5	141	16.5	0.5	132	16.9	0.6
4	125	24.8	0.8	115	21.5	0.7
3	100	32.5	1.1	93.3	25.8	0.9
2	67.6	37.8	1.3	67.5	29.2	1.0
1	29.8	29.8	0.9	38.3	30.2	1.0

Table 4.35 Maximum story displacements and drifts of soft building with raft foundation on hard soil

Story	Fixed			Spring		
	Disp. (mm)	Drift (mm)	Drift (%)	Disp. (mm)	Drift (mm)	Drift (%)
6	238	19.2	0.6	268	22.0	0.7
5	219	27.6	0.9	246	38.7	1.3
4	191	35.6	1.2	207	35.4	1.2
3	155	48.3	1.6	172	45.8	1.5
2	107	59.4	1.9	126	60.2	2.0
1	47.6	47.6	1.6	65.9	64.6	2.2

Table 4.36 Maximum story displacements and drifts of soft building with raft foundation on medium soil

Story	Fixed			Spring		
	Disp. (mm)	Drift (mm)	Drift (%)	Disp. (mm)	Drift (mm)	Drift (%)
6	238	19.2	0.6	284	24.5	0.8
5	219	27.6	0.9	259	42.1	1.4
4	191	35.6	1.2	217	44.2	1.5
3	155	48.3	1.6	173	45.8	1.5
2	107	59.4	1.9	127	58.8	1.9
1	47.6	47.6	1.6	68.2	63.6	2.1

Table 4.37 Maximum story displacements and drifts of soft building with raft foundation on soft soil

Story	Fixed			Spring		
	Disp. (mm)	Drift (mm)	Drift (%)	Disp. (mm)	Drift (mm)	Drift (%)
6	238	19.2	0.6	313	29.2	0.9
5	219	27.6	0.9	284	44.9	1.5
4	191	35.6	1.2	239	56.7	1.9
3	155	48.3	1.6	182	56.3	1.9
2	107	59.4	1.9	126	53.8	1.8
1	47.6	47.6	1.6	72.0	56.4	1.9

4.2.3.3 Foundation Displacement

Maximum values of the foundation vertical and lateral displacements of spring models on hard, medium and soft soils are presented in Tables 4.38 through 4.40. Foundation displacements are given at three points (Loc. 1, 2, 3) as described in Section 4.2.2.3. Maximum values of the foundation settlement (vertical displacement) is also plotted in Figures 4.39 through 4.40 for footing and raft foundations. As the soil and/or structure gets softer, the foundation vertical lateral displacements increase as expected.

Table 4.38 Maximum foundation vertical and lateral displacements in buildings on hard soil

Structure Type	Loc.	Spring Model			
		Footing		Raft	
		U_z (mm)	U_x (mm)	U_z (mm)	U_x (mm)
Stiff	1	-0.646	0.171	-1.214	0.170
	2	-0.282	0.212	-0.324	0.116
	3	-0.601	0.167	-1.113	0.133
Medium	1	-1.982	0.397	-2.968	0.367
	2	-1.078	0.493	-1.156	0.227
	3	-2.116	0.393	-3.401	0.212
Soft	1	-6.078	0.785	-8.752	0.926
	2	-4.251	0.966	-4.472	0.494
	3	-5.972	0.781	-8.775	0.302

Table 4.39 Maximum foundation vertical and lateral displacements in buildings on medium soil

Structure Type	Loc.	Spring Model			
		Footing		Raft	
		U_z (mm)	U_x (mm)	U_z (mm)	U_x (mm)
Stiff	1	-3.074	0.892	-5.009	0.669
	2	-1.289	1.107	-1.264	0.878
	3	-2.787	0.874	-4.535	0.669
Medium	1	-8.292	1.738	-11.634	1.180
	2	-4.925	2.140	-4.393	1.555
	3	-9.362	1.721	-13.185	1.266
Soft	1	-27.834	3.890	-36.625	2.722
	2	-19.414	4.751	-16.872	3.614
	3	-26.847	3.872	-35.525	3.150

Table 4.40 Maximum foundation vertical and lateral displacements in buildings on soft soil

Structure Type	Loc.	Spring Model			
		Footing		Raft	
		U_z (mm)	U_x (mm)	U_z (mm)	U_x (mm)
Stiff	1	-10.599	3.463	-14.752	3.073
	2	-5.618	4.205	-5.491	3.603
	3	-12.089	3.377	-16.932	3.124
Medium	1	-32.589	6.753	-39.119	5.492
	2	-21.556	8.150	-18.472	6.609
	3	-34.773	6.667	-42.659	5.997
Soft	1	-120.622	13.021	-135.706	11.928
	2	-85.055	15.903	-70.308	14.788
	3	-114.841	12.934	-128.899	14.234

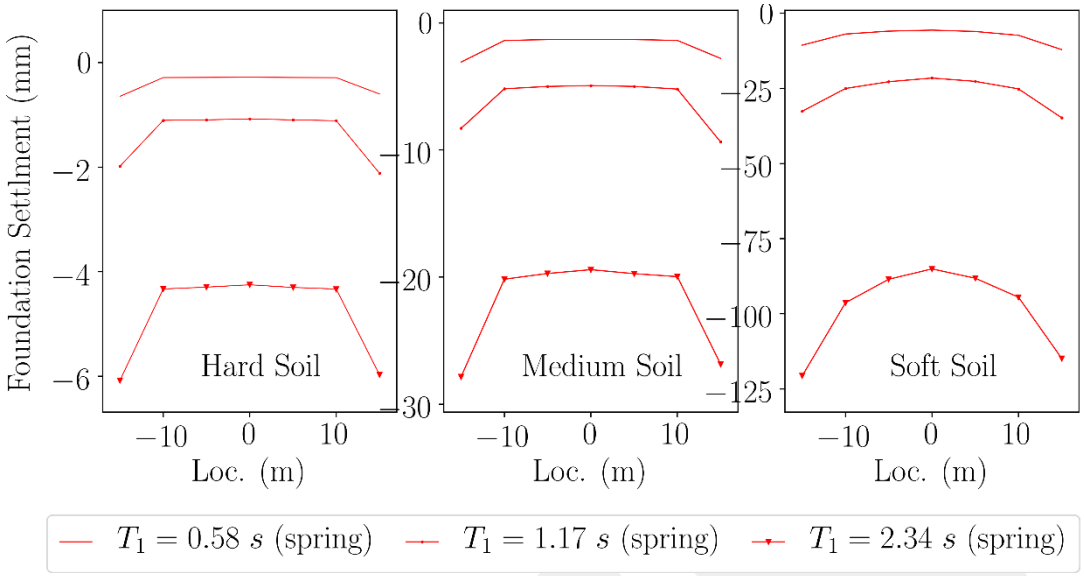

Figure 4.39 Maximum foundation settlements of buildings with footing foundation on hard, medium, and soft soil

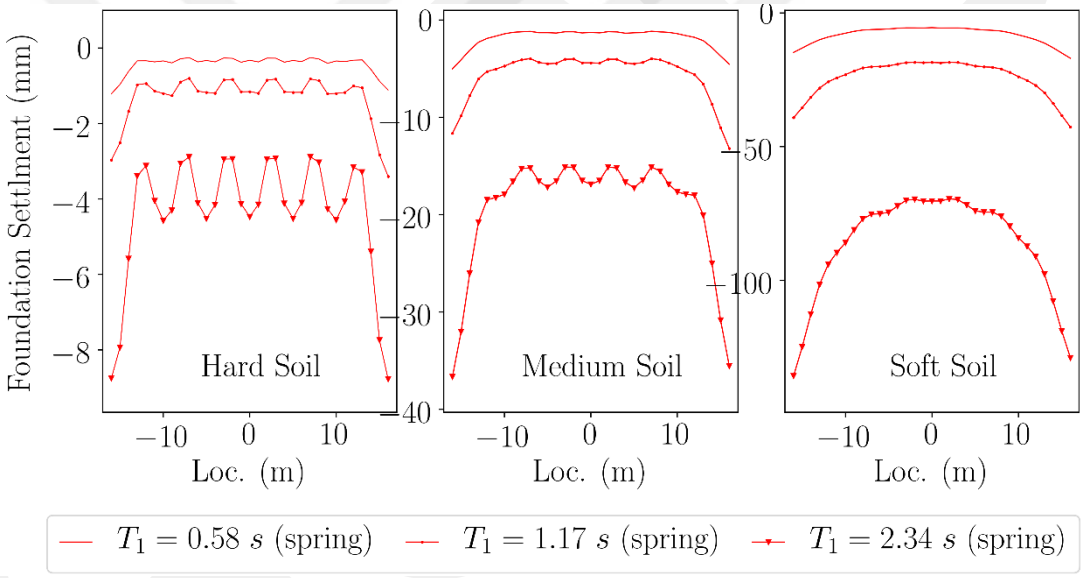

Figure 4.40 Maximum foundation settlements of buildings with raft foundation on hard, medium, and soft soil

CHAPTER 5

SOIL-STRUCTURE INTERACTION EFFECTS IN 3D MODEL

This chapter presents the description of the three-dimensional analysis models used to examine soil-structure interactions effects and discussion of the results obtained from those models.

5.1 Description of Soil-Structure Models

For the three-dimensional models, same dimensions and material properties are used to model and analyze the fixed, spring, and direct model. The floor and roof dead loads are 1.5 kN/m. The wall load is 10.5 kN/m. The building damping ratio is used equal to 5%. All models were subjected to three types of response spectrum according to the type of soil hard (C site class), medium (D site class), and soft (E site class), having S_s equal to 0.5g, S_1 equal to 0.4g, and T_L equal to 8. These response spectrums designed according to ASCE 7-10 code in 3.2.1 subchapter.

5.1.1 Fixed Base Model

The fixed base model is shown in Figure 5.1.

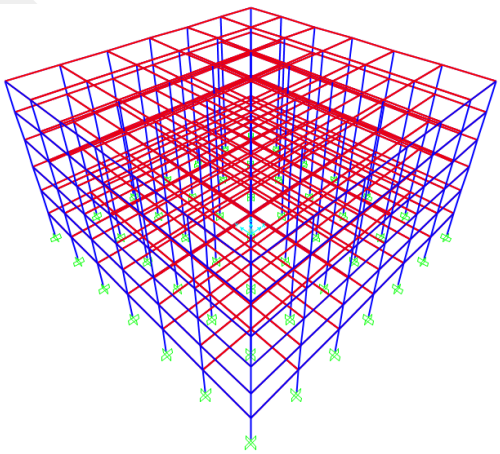

Figure 5.1 Fixed base model (3D)

5.1.2 Spring Model

The soil-structure interaction effects are represented by using equivalent Winkler springs with 6 DOF. The stiffnesses along these 6 degrees of freedoms are calculated as per Pais and Kuasel (1988) [76], and shown in Table 3.2. Two types of foundation footing and raft foundation are considered in this research to study the soil-structure interaction effects on buildings.

5.1.2.1 Footing Foundation

Footing foundation of size 4 m × 4 m with 0.8 m thickness is considered. The spring model for the footing foundation is shown in Figure 5.2. The shear modulus, G, is calculated for each type of soil by using Eq. (5.1).

$$G = \frac{E}{2(1+v)} \tag{5.1}$$

where

E = Soil modulus of elasticity

v = Poisson ratio.

The values of static and dynamic spring stiffness and dashpots coefficients for the hard, medium and soft soil are calculated and presented as follows:

Table 5.1 Static spring stiffness values for footing foundation

DOF	Stiffness of equivalent soil spring (kN/m)		
	Hard Soil	Medium Soil	Soft Soil
K_z	5711810	1250660	285357
K_y	4680230	964400	209464
K_x	4680230	964400	209464
K_{zz}	7271200	1437320	302721
K_{yy}	481110	1064390	242857
K_{xx}	481110	1064390	242857

Table 5.2 Dynamic spring stiffness values for footing foundation

DOF	Stiffness of equivalent soil spring (kN/m)		
	Hard Soil	Medium Soil	Soft Soil
K_z	5711670	1250530	285264
K_y	4680230	964400	209464
K_x	4680230	964400	209464
K_{zz}	7267270	1434060	300403
K_{yy}	486059	1063920	242496
K_{xx}	486059	1063920	242496

Table 5.3 Radiation damping ratios for footing foundation

DOF	Radiation damping ratios		
	Hard Soil	Medium Soil	Soft Soil
β_z	1.09×10^{-2}	2.3×10^{-2}	4.6×10^{-2}
β_y	7.36×10^{-3}	1.4×10^{-2}	2.56×10^{-2}
β_x	7.36×10^{-3}	1.4×10^{-2}	2.56×10^{-2}
β_{zz}	8.74×10^{-7}	7.35×10^{-6}	4.52×10^{-5}
β_{yy}	9.21×10^{-7}	8.05×10^{-6}	5.41×10^{-5}
β_{xx}	9.21×10^{-7}	8.05×10^{-6}	5.41×10^{-5}

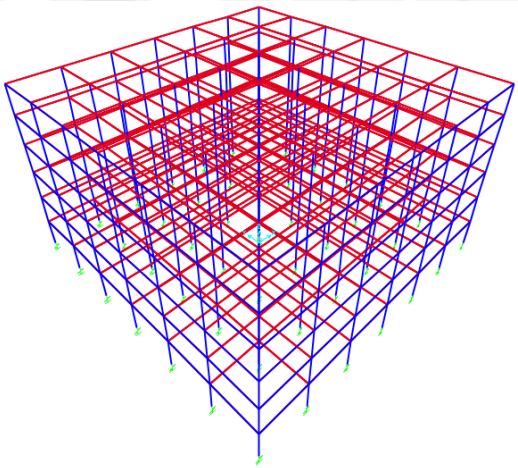

Figure 5.2 Spring model with footing foundation (3D)

5.1.2.2 Raft Foundation

For the second case of the spring model, a raft foundation of size 32m × 32m with thickness 0.8 m is considered. The raft foundation is assumed to have the same properties as the 2-D model. The raft foundation with spring supports is shown in Figure 5.4. To determine the stiffnesses along 6 DOF, a special calculation should be made, using Pais and Kuasel (1988) [76] formulas. For the corner springs, the horizontal K_x, horizontal K_y, and the vertical K_z should be divided by the tributary area of the spring. At the side of the raft, the horizontal K_x, horizontal K_y, and the

vertical K_z involved in the SSI representation. Whereas, at the center side springs of the raft, four components are involved the horizontal K_x, horizontal K_y , the vertical K_z, and the rocking K_{xx} or the rocking K_{yy}, depending on which axis the springs are stiffness. Moreover, the center spring has six involved spring stiffnesses. The raft foundation stiffnesses and radiation damping ratios along 6 degrees of freedoms are shown in Tables 5.4 through 5.12. Springs distribution is shown in Figure 5.3.

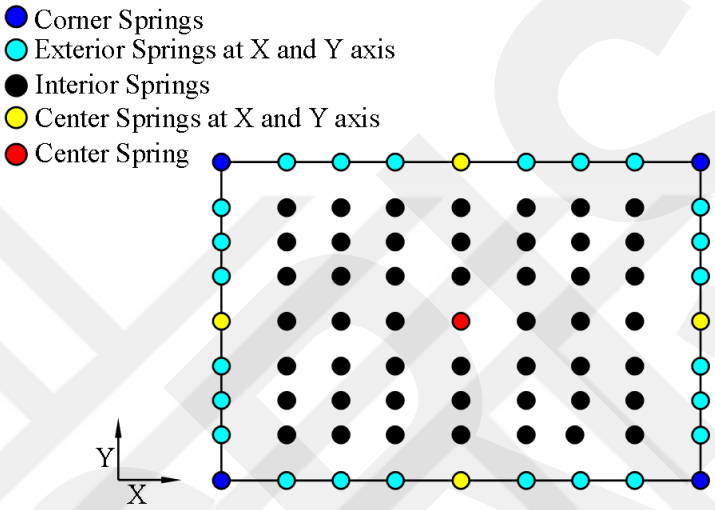

Figure 5.3 Springs distribution

Table 5.4 Static spring stiffness values for raft foundation on hard soil

Soil type	Spring Location	K_x (kN/m)	K_y (kN/m)	K_z (kN/m)	K_{zz} (kN.m/rad)	K_{yy} (kN.m/rad)	K_{xx} (kN.m/rad)
Hard	Corner Springs	18282.1	18282.1	22311.7	-	-	-
	Exterior x Spring	36564.3	36564.3	44623.4	-	-	-
	Exterior y Spring	36564.3	36564.3	44623.4	-	-	-
	Interior Spring	73128.6	73128.6	89246.9	-	-	-
	Center x Spring	36564.3	36564.3	44623.4	-	-	4.97×10^9
	Center y Spring	36564.3	36564.3	44623.4	-	4.9×10^9	-
	Center Spring	73128.6	73128.6	89246.9	2.9×10^{10}	9.9×10^9	9.9×10^9

Table 5.5 Static spring stiffness values for raft foundation on medium soil

Soil type	Spring Location	K_x (kN/m)	K_y (kN/m)	K_z (kN/m)	K_{zz} (kN.m/rad)	K_{yy} (kN.m/rad)	K_{xx} (kN.m/rad)
Medium	Corner Springs	3767.2	3767.2	4885.4	-	-	-
	Exterior x Spring	7534.4	7534.4	9770.7	-	-	-
	Exterior y Spring	7534.4	7534.4	9770.7	-	-	-
	Interior Spring	15068.7	15068.7	19541.5	-	-	-
	Center x Spring	7534.4	7534.4	9770.7	-	-	1.1×10^9
	Center y Spring	7534.4	7534.4	9770.7	-	1.1×10^9	-
	Center Spring	15068.7	15068.7	19541.5	5.9×10^9	2.2×10^9	2.2×10^9

Table 5.6 Static spring stiffness values for raft foundation on soft soil

Soil type	Spring Location	K_x (kN/m)	K_y (kN/m)	K_z (kN/m)	K_{zz} (kN.m/rad)	K_{yy} (kN.m/rad)	K_{xx} (kN.m/rad)
Soft	Corner Springs	818.2	818.2	1114.7	-	-	-
	Exterior x Spring	1636.4	1636.4	2229.4	-	-	-
	Exterior y Spring	1636.4	1636.4	2229.4	-	-	-
	Interior Spring	3272.8	3272.8	4458.7	-	-	-
	Center x Spring	1636.4	1636.4	2229.4	-	-	2.4×10^8
	Center y Spring	1636.4	1636.4	2229.4	-	2.4×10^8	-
	Center Spring	3272.8	3272.8	4458.7	1.2×10^9	4.9×10^8	4.9×10^8

Table 5.7 Dynamic spring stiffness values for raft foundation on hard soil

Soil type	Spring Location	K_x (kN/m)	K_y (kN/m)	K_z (kN/m)	K_{zz} (kN.m/rad)	K_{yy} (kN.m/rad)	K_{xx} (kN.m/rad)
Hard	Corner Springs	18282.1	18282.1	22371.1	-	-	-
	Exterior x Spring	36564.3	36564.3	44742.2	-	-	-
	Exterior y Spring	36564.3	36564.3	44474.2	-	-	-
	Interior Spring	73128.6	73128.6	88948.4	-	-	-
	Center x Spring	36564.3	36564.3	44474.2	-	-	4.9×10^9
	Center y Spring	36564.3	36564.3	44474.2	-	4.9×10^9	-
	Center Spring	73128.6	73128.6	88948.4	2.7×10^{10}	9.8×10^9	9.8×10^9

Table 5.8 Dynamic spring stiffness values for raft foundation on medium soil

Soil type	Spring Location	K_x (kN/m)	K_y (kN/m)	K_z (kN/m)	K_{zz} (kN.m/rad)	K_{yy} (kN.m/rad)	K_{xx} (kN.m/rad)
Medium	Corner Springs	3767.2	3767.2	4823.9	-	-	-
	Exterior x Spring	7534.4	7534.4	9647.8	-	-	-
	Exterior y Spring	7534.4	7534.4	9647.8	-	-	-
	Interior Spring	15068.7	15068.7	19295.6	-	-	-
	Center x Spring	7534.4	7534.4	9647.8	-	-	1.0×10^9
	Center y Spring	7534.4	7534.4	9647.8	-	1.0×10^9	-
	Center Spring	15068.7	15068.7	19295.6	4.1×10^9	2.1×10^9	2.1×10^9

Table 5.9 Dynamic spring stiffness values for raft foundation on soft soil

Soil type	Spring Location	K_x (kN/m)	K_y (kN/m)	K_z (kN/m)	K_{zz} (kN.m/rad)	K_{yy} (kN.m/rad)	K_{xx} (kN.m/rad)
Soft	Corner Springs	818.2	818.2	1078.4	-	-	-
	Exterior x Spring	1636.4	1636.4	2156.8	-	-	-
	Exterior y Spring	1636.4	1636.4	2156.8	-	-	-
	Interior Spring	3272.8	3272.8	4313.7	-	-	-
	Center x Spring	1636.4	1636.4	2156.8	-	-	2.2×10^8
	Center y Spring	1636.4	1636.4	2156.8	-	2.2×10^8	-
	Center Spring	3272.8	3272.8	4313.7	4.4×10^8	4.4×10^8	4.4×10^8

Table 5.10 Radiation damping ratios for raft foundation on hard soil

Soil type	Spring Location	β_x	β_y	β_z	β_{zz}	β_{yy}	β_{xx}
Hard	Corner Springs	8.4×10^{-8}	8.4×10^{-8}	3.2×10^{-5}	-	-	-
	Exterior x Spring	1.7×10^{-7}	1.7×10^{-7}	6.4×10^{-5}	-	-	-
	Exterior y Spring	1.7×10^{-7}	1.7×10^{-7}	6.4×10^{-5}	-	-	-
	Interior Spring	3.4×10^{-7}	3.4×10^{-7}	1.3×10^{-4}	-	-	-
	Center x Spring	1.7×10^{-7}	1.7×10^{-7}	6.4×10^{-5}	-	-	2.3×10^{-11}
	Center y Spring	1.6×10^{-7}	1.6×10^{-7}	6.3×10^{-5}	-	3.8×10^{-4}	-
	Center Spring	3.4×10^{-7}	3.4×10^{-7}	1.3×10^{-4}	8.0×10^{-11}	7.6×10^{-4}	4.6×10^{-11}

Table 5.11 Radiation damping ratios for raft foundation on medium soil

Soil type	Spring Location	β_x	β_y	β_z	β_{zz}	β_{yy}	β_{xx}
Medium	Corner Springs	1.6×10^{-7}	1.6×10^{-7}	6.4×10^{-5}	-	-	-
	Exterior x Spring	3.2×10^{-7}	3.2×10^{-7}	1.3×10^{-4}	-	-	-
	Exterior y Spring	3.2×10^{-7}	3.2×10^{-7}	1.3×10^{-4}	-	-	-
	Interior Spring	6.3×10^{-7}	6.3×10^{-7}	2.6×10^{-4}	-	-	-
	Center x Spring	3.2×10^{-7}	3.2×10^{-7}	1.3×10^{-4}	-	-	1.6×10^{-10}
	Center y Spring	3.2×10^{-7}	3.2×10^{-7}	1.3×10^{-4}	-	2.6×10^{-3}	-
	Center Spring	6.3×10^{-7}	6.3×10^{-7}	2.6×10^{-4}	4.1×10^{-10}	5.3×10^{-3}	3.1×10^{-10}

Table 5.12 Radiation damping ratios for raft foundation on soft soil

Soil type	Spring Location	β_x	β_y	β_z	β_{zz}	β_{yy}	β_{xx}
Soft	Corner Springs	2.5×10^{-7}	2.5×10^{-7}	1.1×10^{-4}	-	-	-
	Exterior x Spring	5.0×10^{-7}	5.0×10^{-7}	2.2×10^{-4}	-	-	-
	Exterior y Spring	5.0×10^{-7}	5.0×10^{-7}	2.2×10^{-4}	-	-	-
	Interior Spring	1.0×10^{-6}	1.0×10^{-6}	4.5×10^{-4}	-	-	-
	Center x Spring	5.0×10^{-7}	5.0×10^{-7}	2.2×10^{-4}	-	-	5.9×10^{-10}
	Center y Spring	5.0×10^{-7}	5.0×10^{-7}	2.2×10^{-4}	-	9.8×10^{-3}	-
	Center Spring	1.0×10^{-6}	1.0×10^{-6}	4.5×10^{-4}	4.0×10^{-10}	1.9×10^{-2}	1.2×10^{-9}

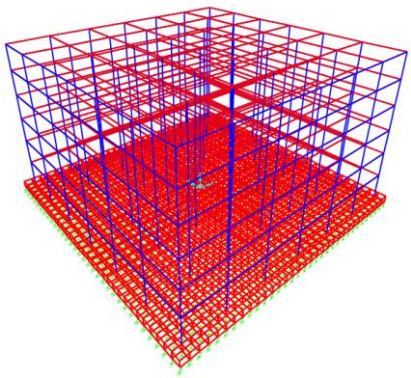

Figure 5.4 Spring model with a raft foundation (3D)

5.1.3 Direct Model

The direct model is considered to have the same dimensions and material properties as the 2D model. The direct footing and raft foundation are shown in Figures 5.5 and 5.6, respectively.

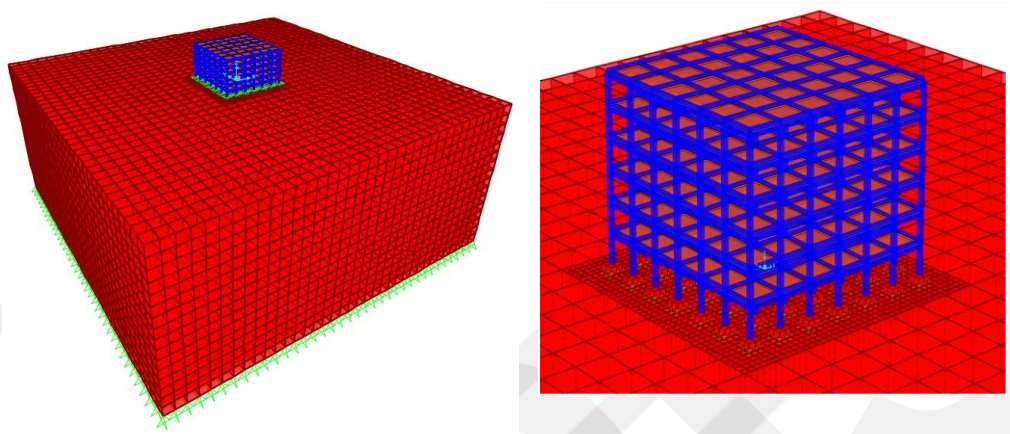

Figure 5.5 Direct model with footing foundation (3D)

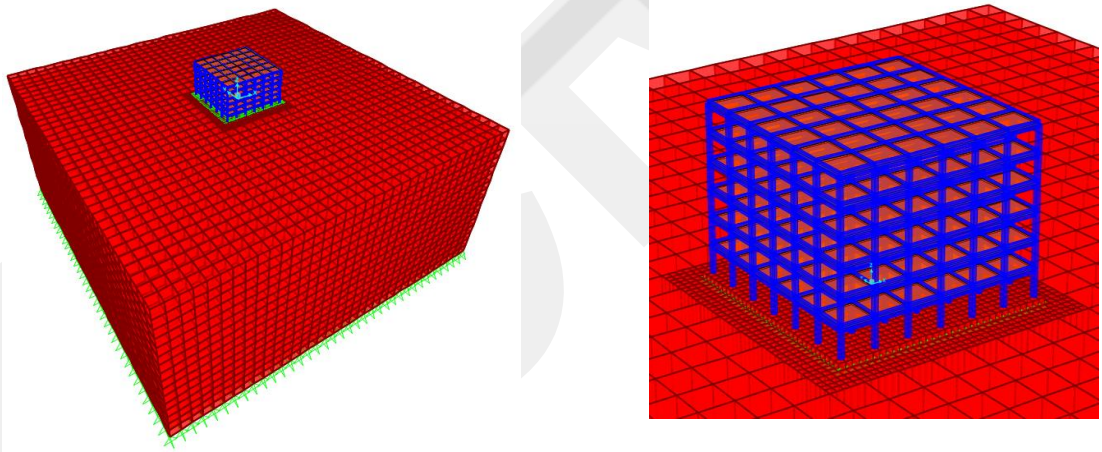

Figure 5.6 Direct model with raft foundation (3D)

5.2 Results and Discussions

The results of the two-dimensional analysis models (i.e., natural periods and mode shapes, base shear, story displacements, story drifts and foundation settlement) of fixed, spring, and direct model are presented and discussed below.

5.2.1 Natural Periods and Mode Shapes

5.2.1.1 Natural Periods and Mode Shapes from Static Analysis

The fundamental periods (first mode natural periods) of the fixed base, spring and direct models, having three types of soils (i.e., hard, medium and soft) are shown in Table 5.13. For medium building only, the first mode shapes of the fixed base, spring, and direct models are shown in Figures 5.7 through 5.12. From Table 5.13, it is observed that the fundamental periods of the spring models (using static spring stiffnesses given by Pais [78]) are lower than the fundamental periods of the corresponding direct models for the footing foundation, whereas, the fundamental periods of the direct models are lower than fundamental periods of the corresponding spring models for the raft foundation. In direct models, footing foundation leads to higher fundamental periods (i.e., softer system) for all soil types and structure types, whereas, footing foundation leads to lower fundamental periods in spring models for all soil types and structure types. For structures on hard, medium, and soft soil, spring models with footing foundation are stiffer than the ones with raft foundation.

Table 5.13 The natural periods of the three types of structures with three types of soils

Structure Type	Fixed Model Fundamental Period (s)	Soil Type	Spring Model Fundamental Period (s)		Direct Model Fundamental Period (s)	
			Footing	Raft	Footing	Raft
Stiff	0.497	Hard	0.504	0.664	0.657	0.655
		Medium	0.525	0.700	0.679	0.675
		Soft	0.599	0.830	0.768	0.759
Medium	1.001	Hard	1.013	1.327	1.313	1.310
		Medium	1.056	1.402	1.356	1.350
		Soft	1.203	1.659	1.534	1.512
Soft	2.000	Hard	2.026	2.649	2.619	2.614
		Medium	2.111	2.797	2.706	2.693
		Soft	2.403	3.310	3.060	3.014

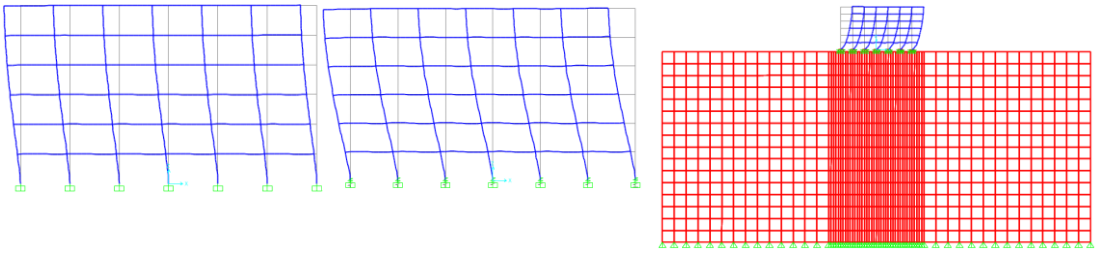

Figure 5.7 First natural mode shapes for medium building with footing foundation on hard soil: fixed (T_1= 1 sec), spring (T_1= 1.01 sec), and direct (T_1= 1.31 sec) model

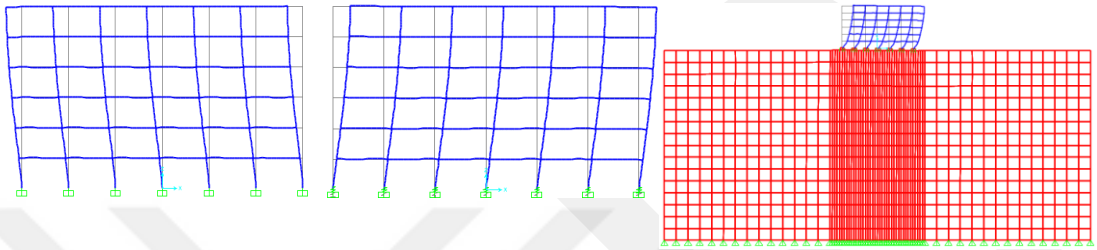

Figure 5.8 First natural mode shapes for medium building with footing foundation on medium soil: fixed (T_1= 1 sec), spring (T_1= 1.05 sec), and direct (T_1= 1.35 sec) model

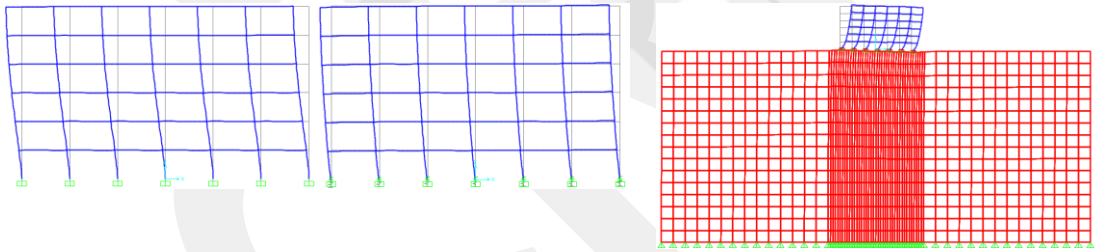

Figure 5.9 First natural mode shapes for medium building with footing foundation on soft soil: fixed (T_1= 1 sec), spring (T_1= 1.2 sec), and direct (T_1= 1.53 sec) model

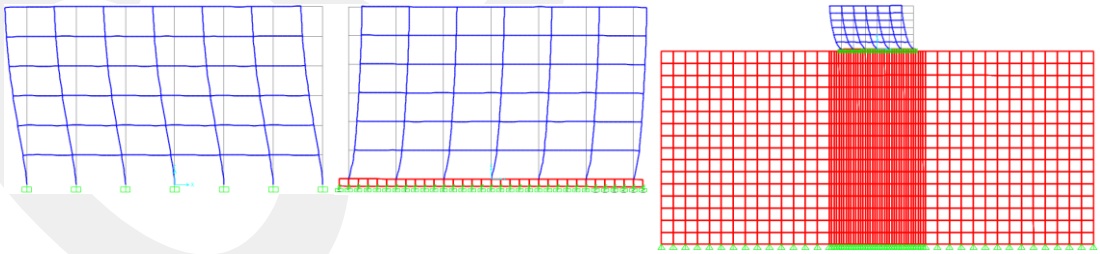

Figure 5.10 First natural mode shapes for medium building with raft foundation on hard soil: fixed (T_1= 1 sec), spring (T_1= 1.32 sec), and direct (T_1= 1.31 sec) model

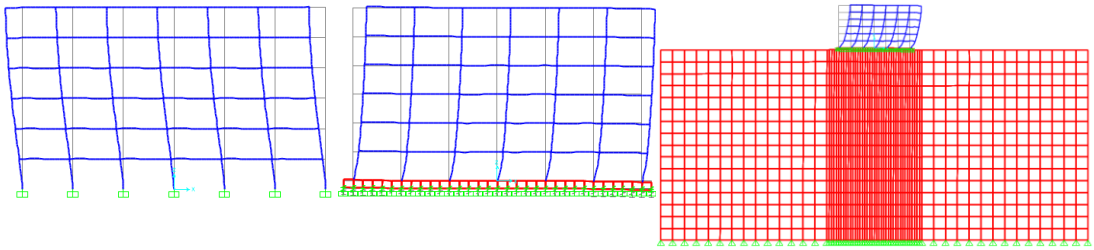

Figure 5.11 First natural mode shapes for medium building with raft foundation on medium soil: fixed (T_1= 1 sec), spring (T_1= 1.4 sec), and direct (T_1= 1.35 sec) model

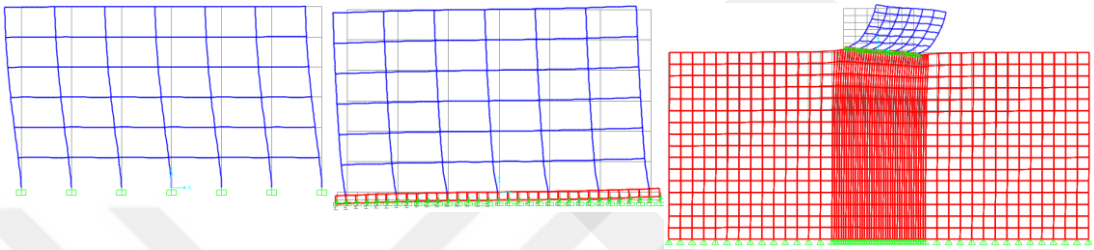

Figure 5.12 First natural mode shapes for medium building with raft foundation on soft soil: fixed (T_1= 1 sec), spring (T_1= 1.65 sec), and direct (T_1= 1.51 sec) model

5.2.1.2 Natural periods and Mode Shapes from Dynamic Analysis

The fundamental periods of the fixed base and spring models subjected to 1940 El Centro earthquake, having three types of soils (hard, medium and soft) are shown in Table 5.14. For medium building only, the first mode shapes of the fixed base, spring, and direct models are shown in Figures 5.13 through 5.18. For both footing foundation and raft foundation, the fundamental periods of spring models (using dynamic spring stiffnesses given by Pais [78]) are almost identical to the values presented in Table 5.13 (based on static spring stiffnesses given by Pais [78]).

Table 5.14 The natural periods of the three types of structures with three types of soils

Structure Type	Fixed Model Fundamental Period (s)	Soil Type	Spring Model Fundamental Period (s)	
			Footing	Raft
Stiff	0.497	Hard	0.504	0.664
		Medium	0.525	0.701
		Soft	0.599	0.834
Medium	1.001	Hard	1.013	1.327
		Medium	1.056	1.402
		Soft	1.203	1.661
Soft	2.000	Hard	2.026	2.649
		Medium	2.111	2.797
		Soft	2.403	3.311

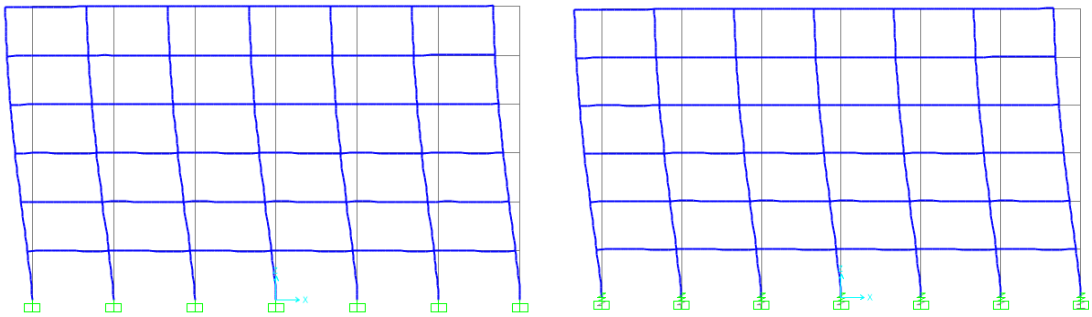

Figure 5.13 First natural mode shapes for medium building with footing foundation on hard soil: fixed (T_1= 1 sec) and spring (T_1= 1.01 sec) model

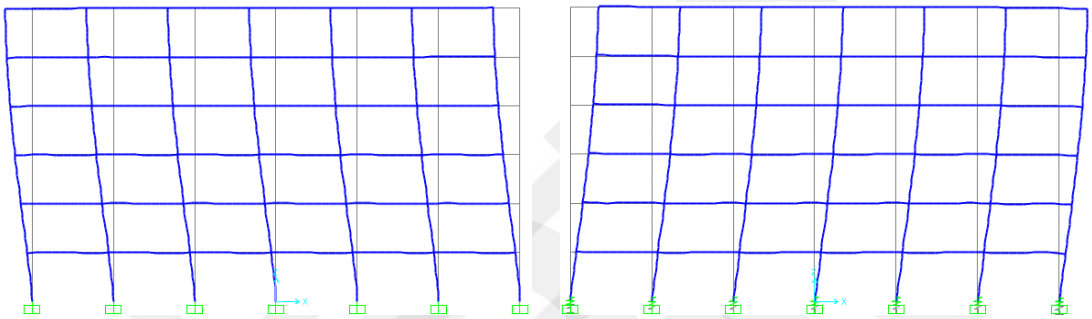

Figure 5.14 First natural mode shapes for medium building with footing foundation on medium soil: fixed (T_1= 1 sec) and spring (T_1= 1.05 sec) model

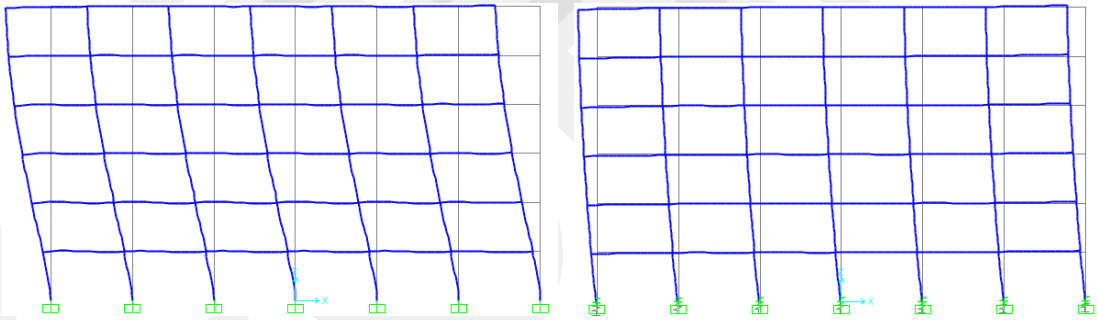

Figure 5.15 First natural mode shapes for medium building with footing foundation on soft soil: fixed (T_1= 1 sec) and spring (T_1= 1.20 sec) model

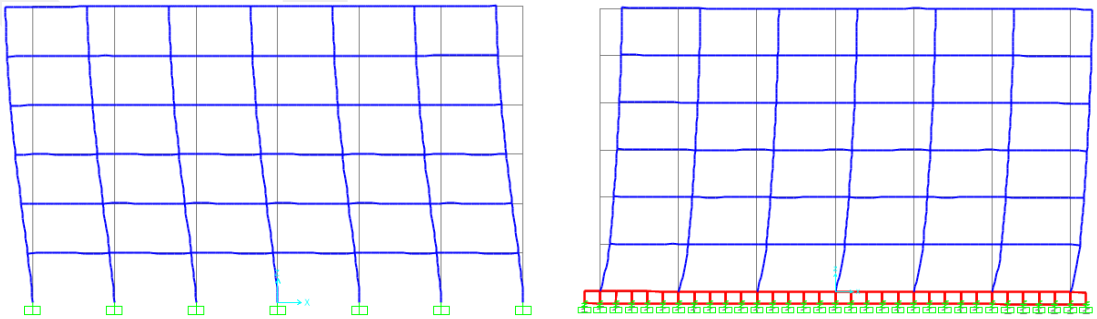

Figure 5.16 First natural mode shapes for medium building with raft foundation on hard soil: fixed (T_1= 1 sec) and spring (T_1= 1.32 sec) model

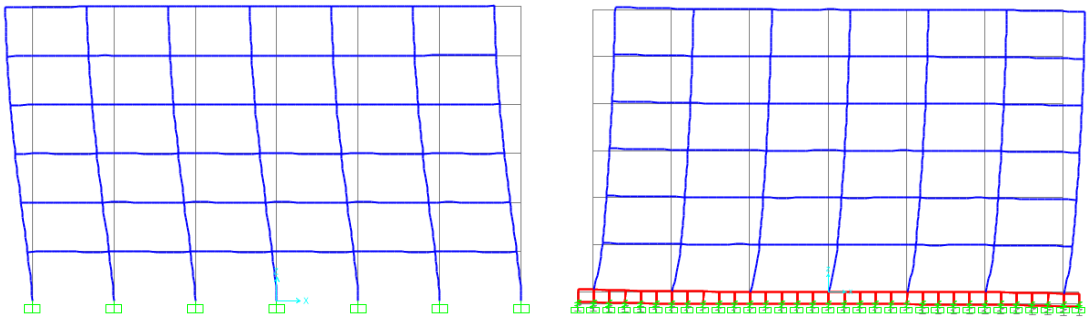

Figure 5.17 First natural mode shapes for medium building with raft foundation on medium soil: fixed (T_1= 1 sec) and spring (T_1= 1.40 sec) model

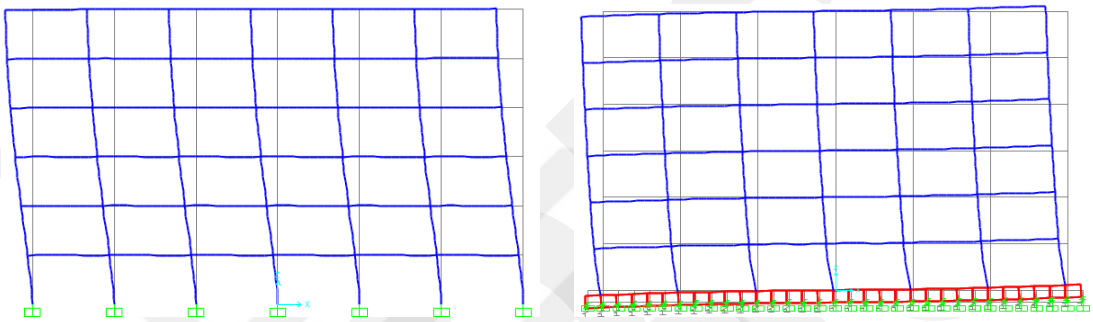

Figure 5.18 First natural mode shapes for medium building with raft foundation on soft soil: fixed (T_1= 1 sec) and spring (T_1= 1.66 sec) model

5.2.2 Response Spectrum Analysis Results

For the three-dimensional analysis, models are subjected to the same response spectrum as the two-dimensional models in the previous chapter.

5.2.2.1 Base and Story Shears

Story shear results of buildings with footing and raft foundations on different type soils are plotted in Figures 5.19 and 5.20, respectively. Base shear values are also tabulated in Table 5.15. From the figures and table below, it is observed that fixed based models have lower (unconservative) base and story shears for the stiff structure on all three types of soil (i.e., hard, medium, soft). As the structure and underlying soil become softer, the fixed based models start to have higher (conservative) base and story shears. This effect is more pronounced for direct (footing and raft) and spring (raft) models of medium and soft buildings on all soil types whereas it becomes significant in spring footing models only for soft building on soft soil.

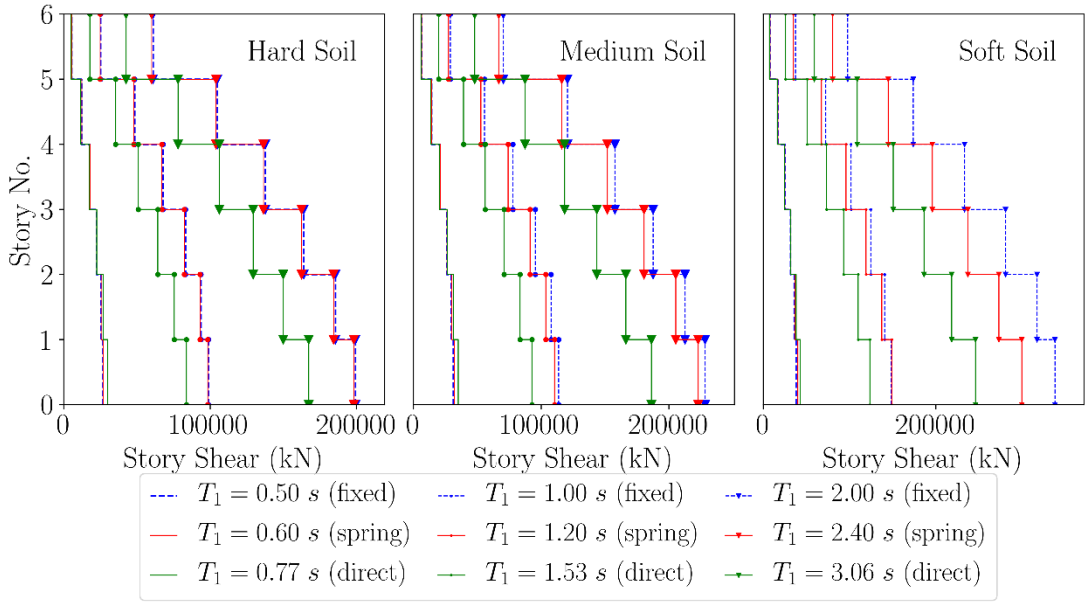

Figure 5.19 Story shears of buildings with footing foundation on hard, medium, and soft soil

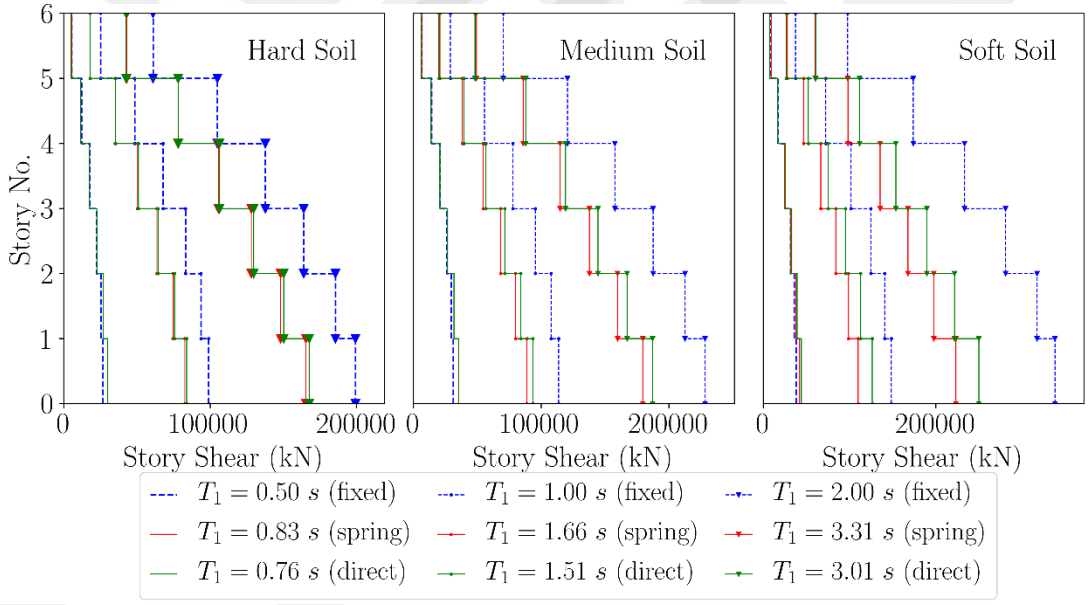

Figure 5.20 Story shears of buildings with raft foundation on hard, medium, and soft soil

Table 5.15 The base shear of the three types of structures with three types of soils

Structure Type	Soil Type	Fixed Model Base Shear (kN)	Spring Model Base Shear (kN)		Direct Model Base Shear (kN)	
			Footing	Raft	Footing	Raft
Stiff	Hard	26704	26871	29891	29904	29971
	Medium	31188	31967	35039	35071	35421
	Soft	37804	40243	42168	42929	44318
Medium	Hard	98866	98324	82554	83680	83901
	Medium	113629	110532	88790	92800	93535
	Soft	148327	148973	110140	123457	126270
Soft	Hard	199290	198163	165473	167416	167746
	Medium	228488	223010	179583	186395	187400
	Soft	337880	299697	223440	246022	249767

5.2.2.2 Story Displacements and Drifts

Story displacements and drifts of the fixed base, spring and direct models are plotted in Figures 5.21 through 5.24 for footing and raft foundation cases. The values of story displacements and drifts are also tabulated in Tables 5.16 through 5.21.

For both footing and raft foundations, as building and soil become softer, story displacements increase as expected due to two reasons, which are: (i) higher flexibility of building and soil, and (ii) higher design spectral acceleration for softer soil.

For a given structure with footing or raft foundation, as soil becomes softer, the differences between the fixed model and SSI models (spring and direct) become more pronounced. For any given soil, the difference between fixed model and SSI models increases as the structure becomes stiffer. This effect is more visible in direct models (compared to the spring models) and in spring raft models. Furthermore, this effect is more visible in spring footing models on soft soil.

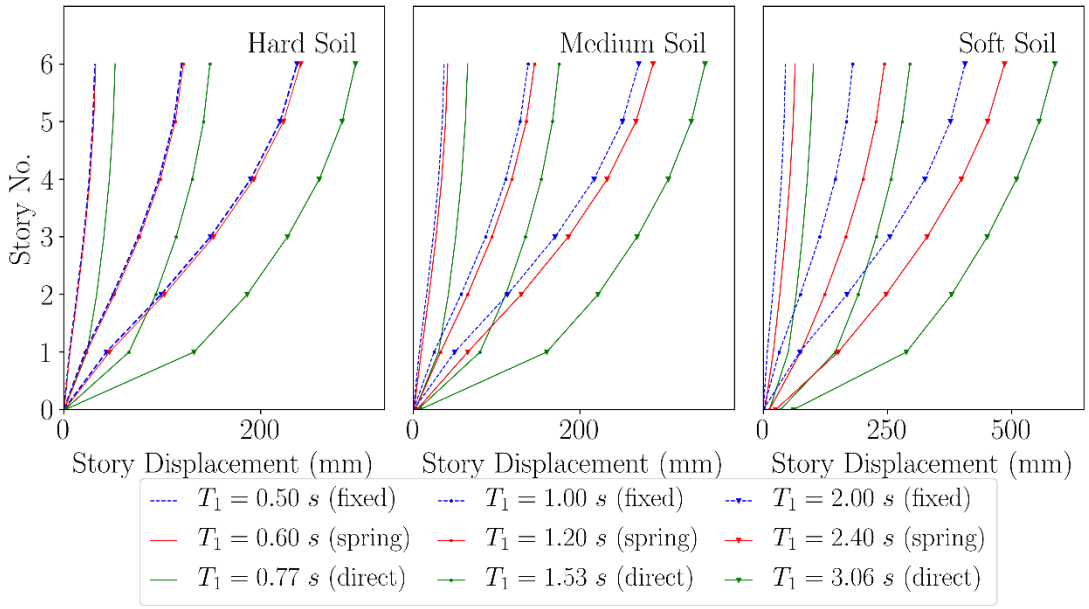

Figure 5.21 Story displacements of buildings with footing foundation on hard, medium, and soft soil

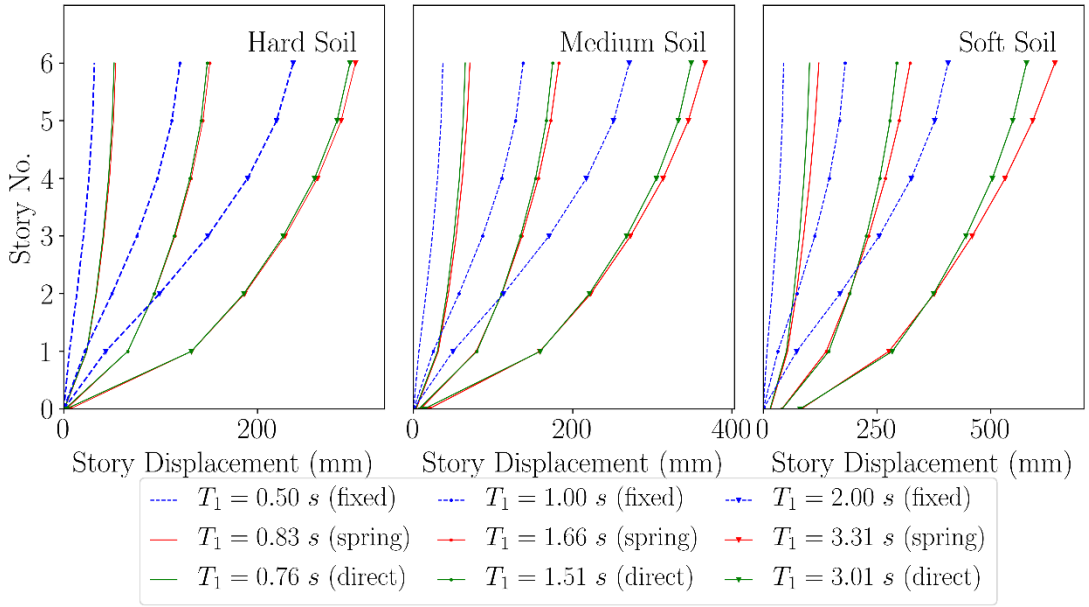

Figure 5.22 Story displacements of buildings with raft foundation on hard, medium, and soft soil

Figures 5.23 and 5.24 show the story drifts. Tables 5.16 through 5.21 present the story drifts both in mm and as percentage of the story height. Similar to the story displacements, the story drifts increase as the structure and the soil gets softer. For fixed base models, the largest story drift occurs in the second story columns, whereas the largest story drift occurs in the first story columns for direct models with footing or raft foundation. Spring footing models on hard and medium soil have the largest

drift in the second story columns similar to the fixed models, but as the soil becomes softer, the largest drift occurs in the first story columns of the spring models. Spring models with raft foundation have largest story drift occurs in the first story columns.

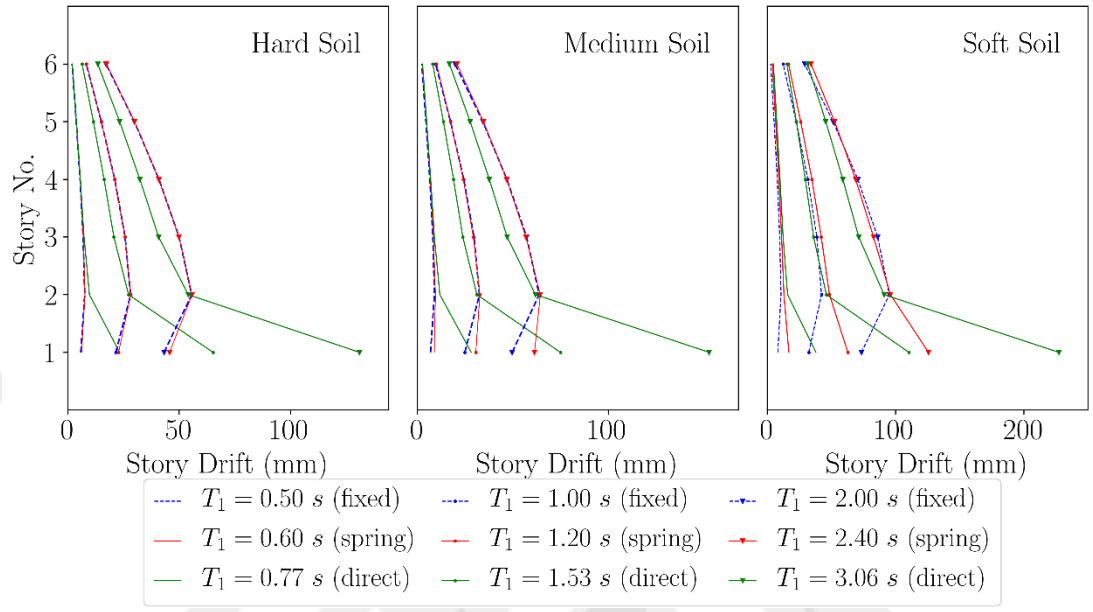

Figure 5.23 Story drifts of buildings with footing foundation on hard, medium, and soft soil

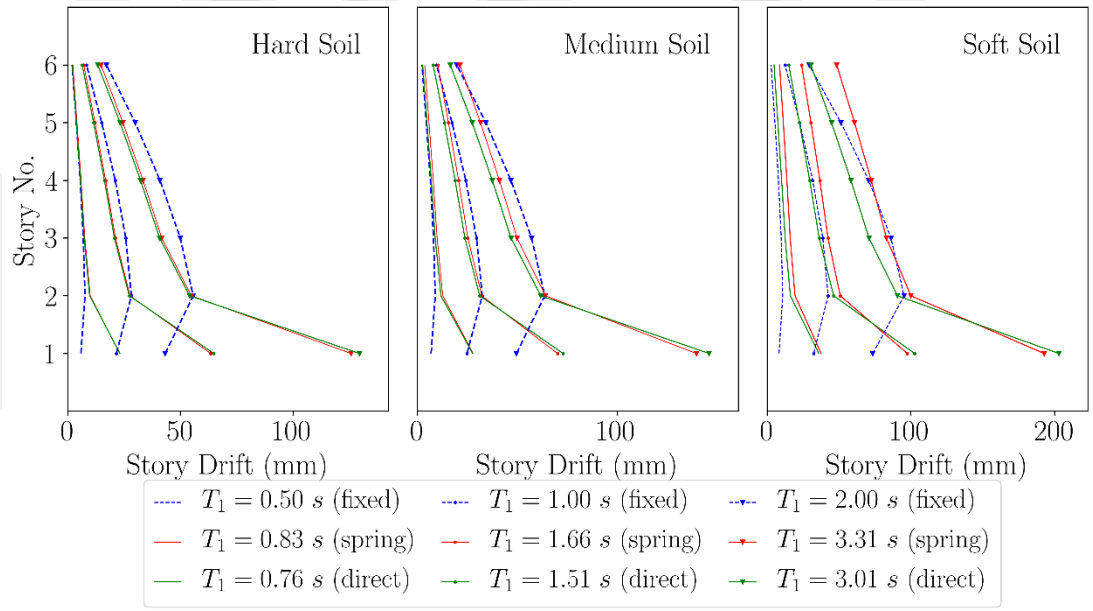

Figure 5.24 Story drifts of buildings with raft foundation on hard, medium, and soft soil

Table 5.16 Story displacements and drifts of stiff building with footing foundation on hard, medium, and soft soil

Soil	Story	Fixed			Spring			Direct		
		Disp. (mm)	Drift (mm)	Drift %	Disp. (mm)	Drift (mm)	Drift %	Disp. (mm)	Drift (mm)	Drift %
Hard Soil	6	31.57	1.93	0.06	32.39	1.97	0.07	52.06	1.99	0.07
	5	29.64	3.81	0.13	30.42	3.86	0.13	50.07	3.82	0.13
	4	25.83	5.53	0.18	26.56	5.59	0.19	46.25	5.63	0.19
	3	20.30	6.87	0.23	20.97	6.94	0.23	40.62	7.28	0.24
	2	13.43	7.61	0.25	14.03	7.71	0.26	33.34	9.71	0.32
	1	5.82	5.82	0.19	6.32	6.22	0.21	23.63	23.25	0.78
Medium Soil	6	36.86	2.25	0.08	41.10	2.51	0.08	65.05	2.64	0.09
	5	34.61	4.44	0.15	38.59	4.70	0.16	62.41	4.79	0.16
	4	30.17	6.46	0.22	33.89	6.73	0.22	57.62	6.90	0.23
	3	23.71	8.03	0.27	27.16	8.35	0.28	50.72	8.84	0.29
	2	15.68	8.88	0.29	18.81	9.41	0.31	41.88	11.69	0.39
	1	6.80	6.80	0.23	9.40	8.82	0.29	30.19	28.11	0.94
Soft Soil	6	44.74	2.73	0.09	64.26	3.99	0.13	101.0	4.86	0.16
	5	42.01	5.39	0.18	60.27	6.62	0.22	96.16	7.44	0.25
	4	36.62	7.85	0.26	53.65	9.11	0.30	88.72	9.99	0.33
	3	28.77	9.75	0.33	44.54	11.21	0.37	78.73	12.37	0.41
	2	19.02	10.78	0.36	33.33	13.02	0.43	66.36	15.91	0.53
	1	8.24	8.24	0.28	20.31	16.89	0.56	50.45	37.97	1.27

Table 5.17 Story displacements and drifts of medium building with footing foundation on hard, medium, and soft soil

Soil	Story	Fixed			Spring			Direct		
		Disp. (mm)	Drift (mm)	Drift %	Disp. (mm)	Drift (mm)	Drift %	Disp. (mm)	Drift (mm)	Drift %
Hard Soil	6	119.9	8.29	0.28	121.6	8.39	0.28	148.3	6.43	0.21
	5	111.6	15.04	0.50	113.2	15.06	0.50	141.9	11.48	0.38
	4	96.56	21.06	0.70	98.13	21.02	0.70	130.4	16.28	0.54
	3	75.50	25.72	0.86	77.11	25.67	0.86	114.1	20.68	0.69
	2	49.78	28.22	0.94	51.44	28.30	0.94	93.45	27.28	0.91
	1	21.56	21.56	0.72	23.14	22.78	0.76	66.17	65.19	2.17
Medium Soil	6	137.8	9.52	0.32	145.6	9.97	0.33	175.2	7.99	0.27
	5	128.2	17.29	0.58	135.7	17.33	0.58	167.2	13.56	0.45
	4	110.9	24.19	0.81	118.3	23.95	0.79	153.6	18.85	0.63
	3	86.75	29.55	0.99	94.37	29.21	0.97	134.8	23.73	0.79
	2	57.20	32.42	1.08	65.16	32.64	1.09	111.0	31.08	1.04
	1	24.78	24.78	0.83	32.52	30.54	1.02	79.94	74.84	2.49
Soft Soil	6	180.1	12.44	0.42	243.6	16.58	0.55	295.2	15.41	0.51
	5	167.7	22.60	0.75	227.0	26.12	0.87	279.8	22.71	0.76
	4	145.1	31.65	1.06	200.9	34.87	1.16	257.0	29.69	0.99
	3	113.4	38.66	1.29	166.1	42.16	1.41	227.4	36.17	1.21
	2	74.74	42.38	1.41	123.9	48.56	1.62	191.2	46.11	1.54
	1	32.36	32.36	1.08	75.33	62.82	2.09	145.1	110.4	3.68

Table 5.18 Story displacements and drifts of soft building with footing foundation on hard, medium, and soft soil

Soil	Story	Fixed			Spring			Direct		
		Disp. (mm)	Drift (mm)	Drift %	Disp. (mm)	Drift (mm)	Drift %	Disp. (mm)	Drift (mm)	Drift %
Hard Soil	6	236.8	17.17	0.57	240.4	17.38	0.58	296.1	13.44	0.45
	5	219.6	29.91	0.99	223.0	29.99	1.00	282.7	23.28	0.78
	4	189.7	40.91	1.36	193.0	40.90	1.36	259.4	32.36	1.08
	3	148.8	49.94	1.67	152.1	49.88	1.66	227.0	40.79	1.36
	2	98.87	55.64	1.86	102.2	55.82	1.86	186.2	54.07	1.80
	1	43.23	43.23	1.44	46.41	45.69	1.52	132.2	130.9	4.37
Medium Soil	6	271.1	19.68	0.66	288.2	20.66	0.69	350.8	16.69	0.56
	5	251.4	34.24	1.14	267.5	34.57	1.15	334.1	27.58	0.92
	4	217.2	46.79	1.56	232.9	46.64	1.56	306.5	37.59	1.25
	3	170.4	57.13	1.90	186.3	56.73	1.89	268.9	46.94	1.57
	2	113.3	63.71	2.12	129.6	64.32	2.14	222.0	61.79	2.06
	1	49.56	49.56	1.65	65.25	61.25	2.04	160.2	152.7	5.09
Soft Soil	6	405.9	29.19	0.97	485.5	34.16	1.14	586.7	31.51	1.05
	5	376.8	51.34	1.71	451.4	52.56	1.75	555.2	45.68	1.52
	4	325.5	70.65	2.36	398.8	68.94	2.29	509.5	58.94	1.97
	3	254.8	86.10	2.87	329.9	82.90	2.76	450.5	71.35	2.38
	2	168.7	95.24	3.18	246.9	96.07	3.20	379.2	91.09	3.04
	1	73.46	73.46	2.45	150.9	125.7	4.19	288.1	227.2	7.58

Table 5.19 Story displacements and drifts of stiff building with raft foundation on hard, medium, and soft soil

Soil	Story	Fixed			Spring			Direct		
		Disp. (mm)	Drift (mm)	Drift %	Disp. (mm)	Drift (mm)	Drift %	Disp. (mm)	Drift (mm)	Drift %
Hard Soil	6	31.57	1.93	0.06	53.58	2.24	0.08	51.95	1.97	0.07
	5	29.64	3.81	0.13	51.34	4.08	0.14	49.98	3.81	0.13
	4	25.83	5.53	0.18	47.26	5.89	0.19	46.17	5.62	0.19
	3	20.30	6.87	0.23	41.37	7.54	0.25	40.55	7.28	0.24
	2	13.43	7.61	0.25	33.83	9.96	0.33	33.27	9.70	0.32
	1	5.82	5.82	0.19	23.87	23.03	0.77	23.57	23.13	0.77
Medium Soil	6	36.86	2.25	0.08	70.83	3.61	0.12	65.04	2.60	0.09
	5	34.61	4.44	0.15	67.22	5.76	0.19	62.44	4.78	0.16
	4	30.17	6.46	0.22	61.46	7.88	0.26	57.66	6.90	0.23
	3	23.71	8.03	0.27	53.58	9.82	0.33	50.76	8.86	0.29
	2	15.68	8.88	0.29	43.76	12.64	0.42	41.90	11.73	0.39
	1	6.80	6.80	0.23	31.12	27.81	0.93	30.17	27.60	0.92
Soft Soil	6	44.74	2.73	0.09	122.4	8.62	0.29	101.8	4.76	0.16
	5	42.01	5.39	0.18	113.7	11.21	0.37	97.07	7.43	0.25
	4	36.62	7.85	0.26	102.5	13.71	0.46	89.64	10.04	0.34
	3	28.77	9.75	0.33	88.81	15.99	0.53	79.60	12.48	0.42
	2	19.02	10.78	0.36	72.82	19.37	0.65	67.12	16.10	0.54
	1	8.24	8.24	0.28	53.45	37.50	1.25	51.02	35.94	1.19

Table 5.20 Story displacements and drifts of medium building with raft foundation on hard, medium, and soft soil

Soil	Story	Fixed			Spring			Direct		
		Disp. (mm)	Drift (mm)	Drift %	Disp. (mm)	Drift (mm)	Drift %	Disp. (mm)	Drift (mm)	Drift %
Hard Soil	6	119.9	8.29	0.28	150.7	7.08	0.24	148.1	6.39	0.21
	5	111.6	15.04	0.50	143.6	12.06	0.40	141.7	11.45	0.38
	4	96.56	21.06	0.70	131.6	16.79	0.56	130.2	16.26	0.54
	3	75.50	25.72	0.86	114.8	21.15	0.71	113.9	20.68	0.69
	2	49.78	28.22	0.94	93.61	27.63	0.92	93.30	27.28	0.91
	1	21.56	21.56	0.72	65.98	63.39	2.11	66.02	64.76	2.16
Medium Soil	6	137.8	9.52	0.32	182.6	10.18	0.34	174.7	7.88	0.26
	5	128.2	17.29	0.58	172.4	15.51	0.52	166.9	13.49	0.45
	4	110.9	24.19	0.81	156.9	20.57	0.69	153.4	18.83	0.63
	3	86.75	29.55	0.99	136.3	25.21	0.84	134.5	23.74	0.79
	2	57.20	32.42	1.08	111.1	32.21	1.07	110.8	31.13	1.04
	1	24.78	24.78	0.83	78.9	70.14	2.34	79.67	72.92	2.43
Soft Soil	6	180.1	12.44	0.42	322.8	23.92	0.79	293.5	14.96	0.49
	5	167.7	22.60	0.75	298.8	30.47	1.02	278.6	22.41	0.75
	4	145.1	31.65	1.06	268.4	36.67	1.22	256.2	29.55	0.99
	3	113.4	38.66	1.29	231.7	42.30	1.41	226.6	36.18	1.21
	2	74.74	42.38	1.41	189.4	50.86	1.69	190.4	46.21	1.54
	1	32.36	32.36	1.08	138.5	97.51	3.25	144.2	102.6	3.42

Table 5.21 Story displacements and drifts of soft building with raft foundation on hard, medium, and soft soil

Soil	Story	Fixed			Spring			Direct		
		Disp. (mm)	Drift (mm)	Drift %	Disp. (mm)	Drift (mm)	Drift %	Disp. (mm)	Drift (mm)	Drift %
Hard Soil	6	236.8	17.17	0.57	301.1	14.75	0.49	295.4	13.34	0.45
	5	219.6	29.91	0.99	286.3	24.46	0.82	282.1	23.21	0.77
	4	189.7	40.91	1.36	261.9	33.39	1.11	258.9	32.30	1.08
	3	148.8	49.94	1.67	228.5	41.71	1.39	226.6	40.76	1.36
	2	98.87	55.64	1.86	186.8	54.82	1.83	185.8	54.05	1.80
	1	43.23	43.23	1.44	131.9	125.7	4.19	131.8	129.5	4.32
Medium Soil	6	271.1	19.68	0.66	366.5	21.17	0.71	349.1	16.43	0.55
	5	251.4	34.24	1.14	345.3	31.56	1.05	332.7	27.38	0.91
	4	217.2	46.79	1.56	313.7	41.02	1.37	305.3	37.46	1.25
	3	170.4	57.13	1.90	272.7	49.86	1.66	267.9	46.86	1.56
	2	113.3	63.71	2.12	222.9	64.10	2.14	221.0	61.74	2.06
	1	49.56	49.56	1.65	158.8	139.7	4.66	159.3	146.1	4.87
Soft Soil	6	405.9	29.19	0.97	640.7	48.35	1.61	578.6	30.36	1.01
	5	376.8	51.34	1.71	592.4	60.80	2.03	548.3	44.77	1.49
	4	325.5	70.65	2.36	531.6	72.35	2.41	503.5	58.23	1.94
	3	254.8	86.10	2.87	459.2	82.98	2.77	445.3	70.83	2.36
	2	168.7	95.24	3.18	376.2	100.0	3.33	374.4	90.64	3.02
	1	73.46	73.46	2.45	276.2	192.6	6.42	283.8	202.9	6.77

5.2.2.3 Foundation Displacements

Foundation vertical and lateral displacements of spring and direct models with different types of soil are presented in Tables 5.22 through 5.24. Four points are considered to report foundation vertical and horizontal displacements. First point is the

center point of the foundation, second point is one of the four corner points of the foundation with the maximum value, third point is one of the center points of the foundation sides parallel to x axis with the maximum value, fourth point is one of the center points of the foundation sides parallel to y axis with the maximum value. Foundation settlement (vertical displacement) is also plotted in Figures 5.25 and 5.26 for footing and raft foundations, respectively.

As the soil and/or structure gets softer, the foundation vertical lateral displacements increase as expected. It is observed that spring models indicate lower foundation vertical and lateral displacements compared to direct models, leading to less conservative results for foundation displacements. Spring models indicate a larger difference in foundation settlement between footing and raft foundations compared to direct models.

Table 5.22 Foundation displacements of buildings on hard soil

Structure Type	Loc.	Spring Model				Direct Model			
		Footing		Raft		Footing		Raft	
		U_z (mm)	U_x (mm)	U_z (mm)	U_x (mm)	U_z (mm)	U_x (mm)	U_z (mm)	U_x (mm)
Stiff	1	-0.34	0.12	-1.25	0.45	-1.34	0.47	-1.35	0.45
	2	-0.06	0.10	-1.04	0.22	-0.04	0.30	-0.17	0.36
	3	-0.01	0.10	-0.43	0.35	-0.20	0.47	-0.40	0.45
	4	-0.25	0.12	-1.66	0.48	-0.95	0.47	-0.99	0.45
Medium	1	-1.17	0.46	-3.68	1.23	-4.68	1.33	-4.19	1.26
	2	-0.10	0.36	-1.17	0.40	-1.08	0.78	-1.27	0.98
	3	-0.16	0.36	-0.46	1.06	-1.52	1.38	-1.74	1.28
	4	-1.07	0.45	-6.39	1.32	-3.68	1.33	-3.42	1.26
Soft	1	-4.45	0.92	-13.4	2.46	-17.9	2.65	-15.5	2.50
	2	-2.49	0.72	-23.2	0.03	-8.02	1.02	-8.21	1.70
	3	-2.53	0.73	-13.3	2.72	-10.0	3.30	-9.68	2.82
	4	-4.35	0.91	-25.2	2.64	-14.5	2.65	-13.1	2.50

Table 5.23 Foundation displacements of buildings on medium soil

Structure Type	Loc.	Spring Model				Direct Model			
		Footing		Raft		Footing		Raft	
		U_z (mm)	U_x (mm)	U_z (mm)	U_x (mm)	U_z (mm)	U_x (mm)	U_z (mm)	U_x (mm)
Stiff	1	-1.56	0.72	-5.12	2.54	-5.18	2.63	-5.55	2.50
	2	-0.38	0.58	-2.80	1.97	-0.34	1.91	-0.84	2.40
	3	-0.09	0.59	-1.55	2.18	-0.96	2.49	-1.74	2.39
	4	-1.17	0.71	-6.07	2.57	-3.73	2.63	-4.10	2.50
Medium	1	-5.33	2.49	-14.9	6.40	-18.2	6.97	-17.3	6.56
	2	-0.21	1.98	-4.32	4.54	-4.81	4.81	-5.38	6.25
	3	-0.45	2.00	-2.16	5.75	-6.68	6.83	-7.48	6.29
	4	-4.93	2.47	-21.9	6.46	-14.2	6.97	-13.8	6.56
Soft	1	-20.3	5.02	-53.8	12.87	-70.0	13.96	-63.8	13.08
	2	-10.8	4.00	-67.4	7.86	-31.9	7.79	-32.2	12.39
	3	-10.9	4.03	-44.6	12.89	-40.3	15.54	-39.7	12.62
	4	-19.9	4.98	-85.0	13.01	-55.9	13.96	-52.4	13.08

Table 5.24 Foundation displacements of buildings on soft soil

Structure Type	Loc.	Spring Model				Direct Model			
		Footing		Raft		Footing		Raft	
		U_z (mm)	U_x (mm)	U_z (mm)	U_x (mm)	U_z (mm)	U_x (mm)	U_z (mm)	U_x (mm)
Stiff	1	-6.73	4.20	-22.16	13.99	-20.5	14.7	-22.5	14.64
	2	1.92	3.42	-10.33	12.97	-0.95	11.8	-3.14	14.53
	3	-0.94	3.45	-8.14	13.23	-2.86	13.2	-6.03	14.14
	4	-5.39	4.17	-23.85	13.97	-15.8	14.70	-17.9	14.64
Medium	1	-23.2	15.57	-67.84	35.36	-73.1	42.03	-70.6	40.20
	2	-3.16	12.51	-0.57	32.12	-15.8	33.00	-18.5	39.80
	3	2.39	12.59	-3.21	33.80	-21.6	38.24	-25.3	38.86
	4	-21.9	15.46	-81.79	35.30	-59.8	42.03	-59.6	40.20
Soft	1	-88.9	31.27	-249.5	71.00	-282	83.37	-262	78.68
	2	-37.4	25.16	-170.7	62.92	-128	60.51	-129	78.50
	3	-37.9	25.32	-135.1	70.02	-157	80.92	-156	75.42
	4	-87.5	31.05	-312.1	70.96	-234	83.37	-225	78.68

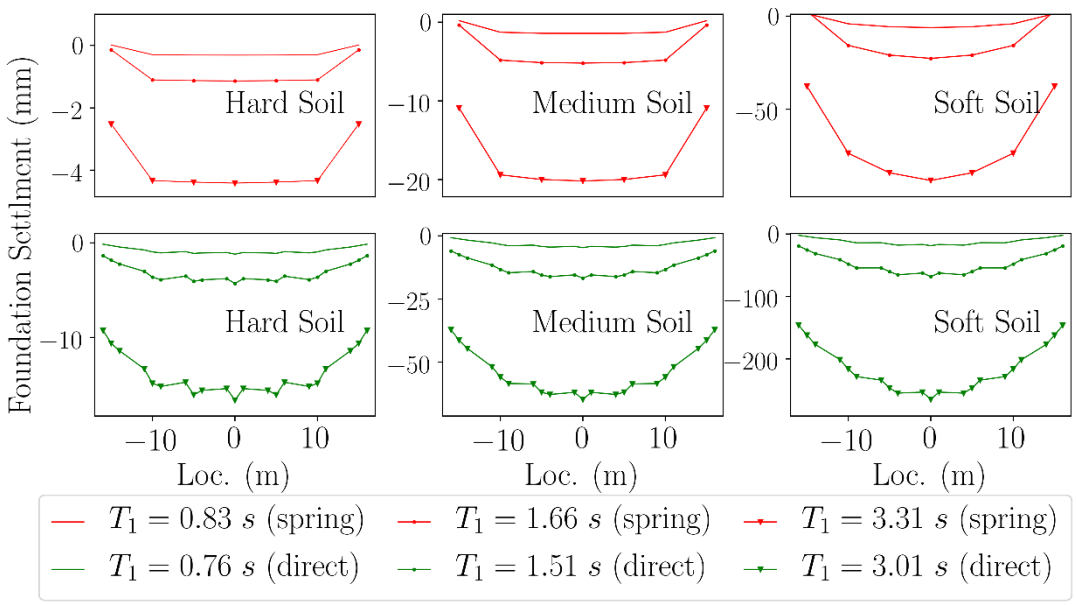

Figure 5.25 Foundation settlements of buildings with footing foundation on hard, medium, and soft soil

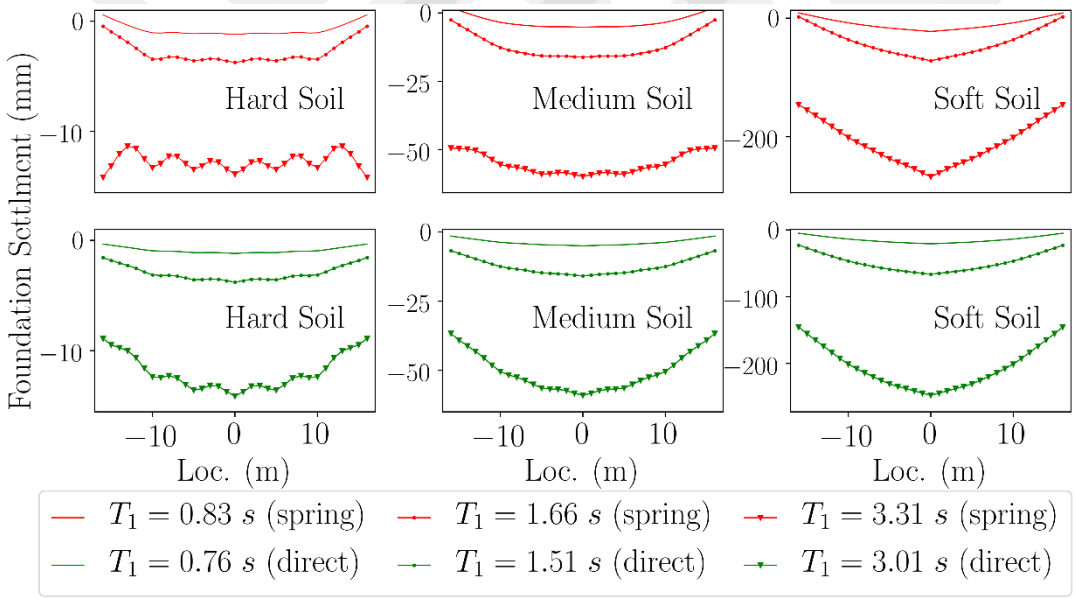

Figure 5.26 Foundation settlements of buildings with raft foundation on hard, medium, and soft soil

5.2.3 Time History Analysis Results

For the three-dimensional analysis, models are subjected to the 1940 El Centro earthquake as the two-dimensional models in the previous chapter.

5.2.3.1 Base and Story Shears

Maximum story shears in the fixed base models and spring models on three types of soil (hard, medium, soft) are plotted in Figure 5.27 for footing foundation, and in Figure 5.29 for raft foundation. Sample base shear time histories are also plotted for fixed and spring models on soft soil in Figures 5.28 and 5.30 for footing foundation and raft foundation, respectively. Maximum values of base shears are also tabulated in Table 5.25.

From the figures below, it is observed that maximum story shears are very similar for all three buildings with footing foundation when they are on hard soil. As the soil gets softer, the maximum story shears start to differ more between the fixed base model and spring model, especially in soft building on soft soil. Similar trends can be observed in maximum story shears for buildings with raft foundation. In this case, the differences between fixed base and spring models are noticeable for medium and soft buildings on all three types of soil (hard, medium, soft) considered in this study.

From the figures and table below, it is observed that fixed based models have slightly lower (unconservative) base and story shears for the stiff structure on hard and medium soil for building with footing foundation. As the structure and underlying soil become softer, the fixed based models start to have higher (conservative) base and story shears. This effect is more pronounced for spring models of medium and soft buildings on all soil types whereas it becomes significant in spring models primarily for medium and soft buildings on soft soil. For buildings with raft foundation, it is observed that fixed base models have larger (conservative) base and story shears in all types of structure and soil. The dynamic base and story shear results are in general consistent with response spectrum analysis results, with minor discrepancies most likely due to using an unscaled ground acceleration for all soil types and effect of dominant frequency components in the ground motion record.

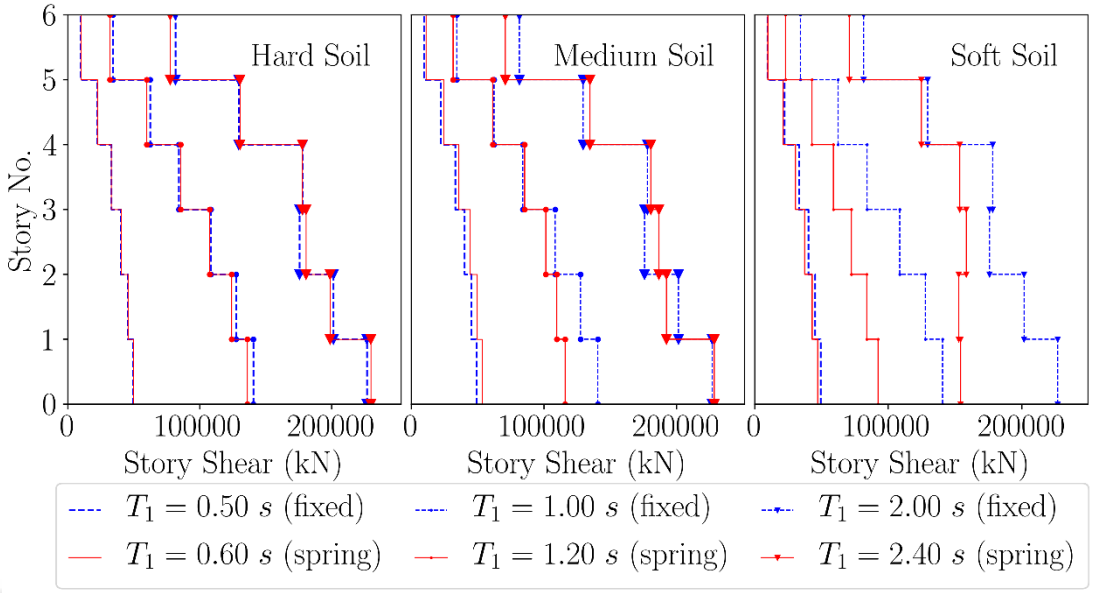

Figure 5.27 Maximum story shears of buildings with footing foundation on hard, medium, and soft soil under 1940 El Centro earthquake

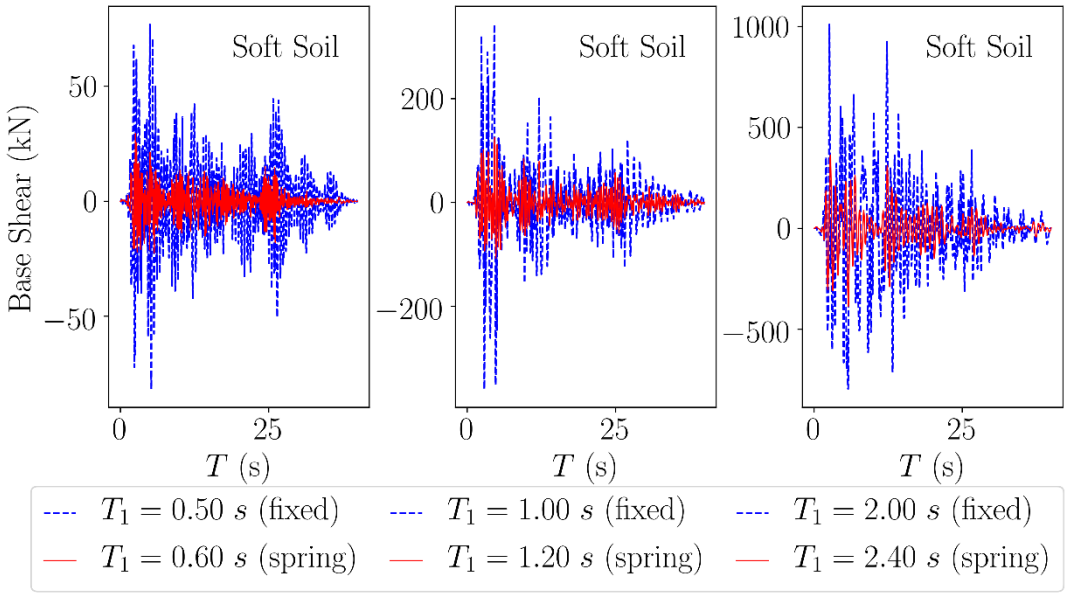

Figure 5.28 Base shear time-histories of buildings with footing foundation on soft soil under 1940 El Centro earthquake

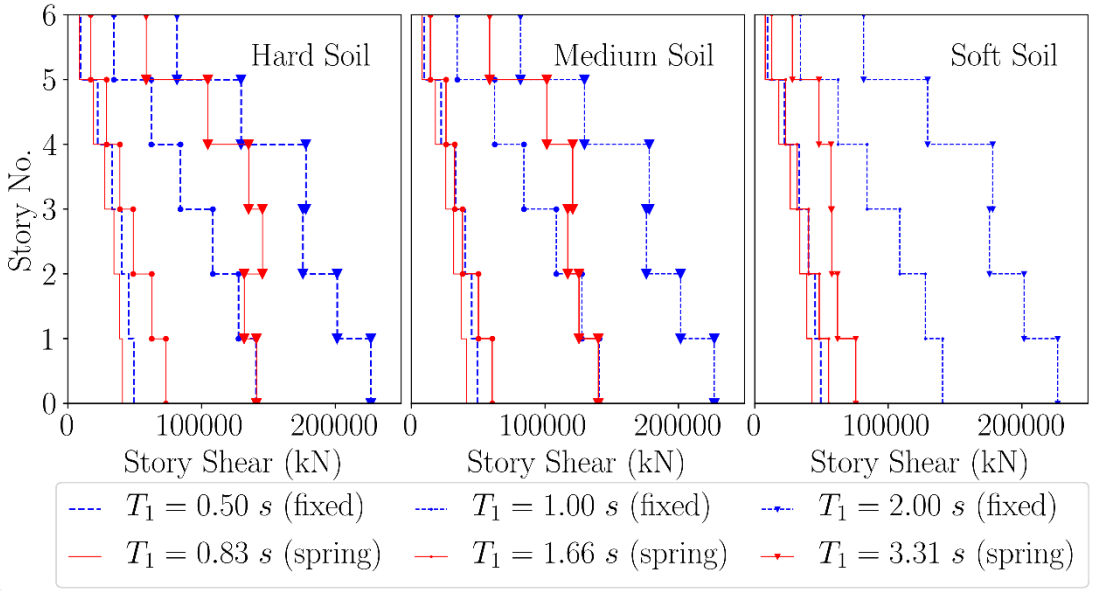

Figure 5.29 Maximum story shears of buildings with raft foundation on hard, medium, and soft soil under 1940 El Centro earthquake

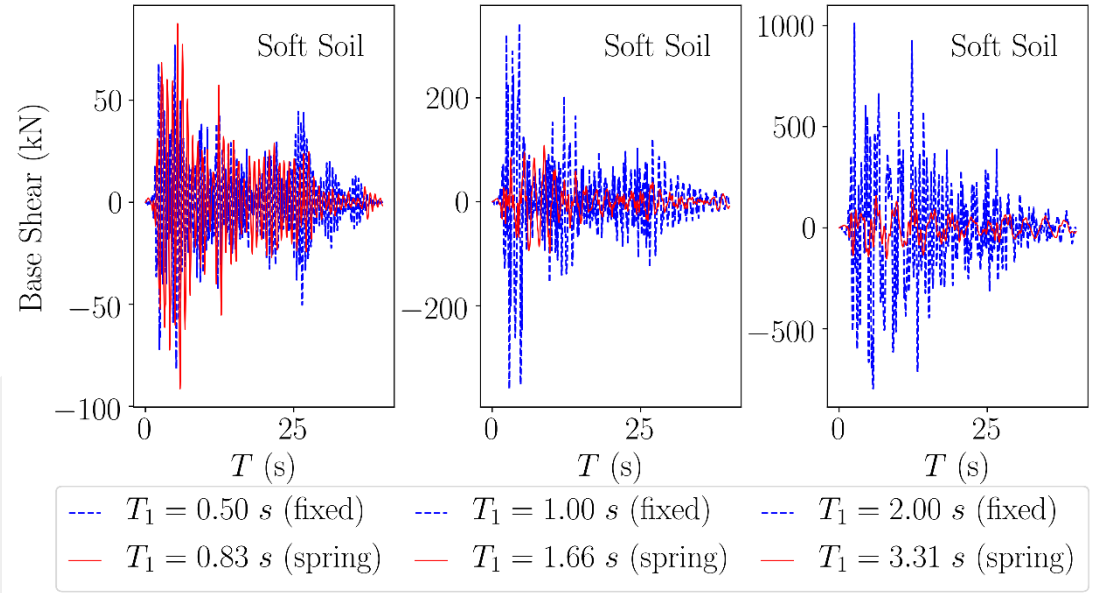

Figure 5.30 Base shear time-histories of buildings raft footing foundation on soft soil under 1940 El Centro earthquake

Table 5.25 Maximum base shears of buildings on hard, medium, and soft soil

Structure Type	Fixed Model Base Shear (kN)	Soil Type	Spring Model Base Shear (kN)	
			Footing	Raft
Stiff	49285	Hard	49664	40848
		Medium	53323	41200
		Soft	47161	42848
Medium	140672	Hard	136191	73369
		Medium	115988	60537
		Soft	92354	55305
Soft	226736	Hard	229880	141140
		Medium	228393	140004
		Soft	154064	75766

5.2.3.2 Story Displacement and Drift

Maximum story displacements and drifts of the fixed base, spring and direct models are plotted in Figures 5.31, 5.33, 5.35, and 5.37 for footing and raft foundation cases on all three types of soil. Sample top floor displacement and first floor drift histories are plotted for footing and raft foundation cases on soft soil only in Figures 5.32, 5.34, 5.36, and 5.38. The values of story displacements and drifts are also tabulated in Tables 5.26 through 5.43.

For both footing and raft foundations, as building and soil become softer, maximum story displacements increase as expected due to two reasons, which are: (i) higher flexibility of building and soil, and (ii) higher design spectral acceleration for softer soil. For a given structure with footing or raft foundation, as soil becomes softer, the differences between the fixed model and spring model become more pronounced.

Similar to the story displacements, the story drift values increase as the structure and the soil get softer. For fixed base models, the largest story drift (maximum value) occurs in the second story columns. Spring footing models on hard and medium soil have the largest drift in the second story columns similar to the fixed models, but as the soil becomes softer, the largest drift occurs in the first story columns of the spring models. Whereas, the largest drift occurs in the first story columns of raft spring models for different types of structure and soil. For a given structure as the soil gets softer, the story drifts of the spring model increase with respect to fixed based model story drifts for both footing and raft foundations.

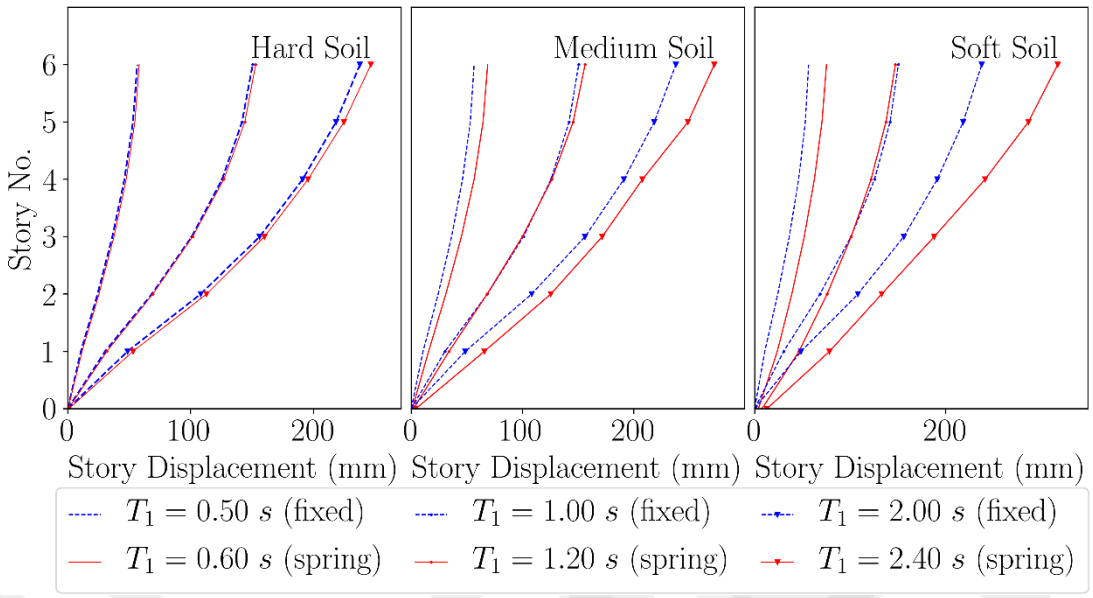

Figure 5.31 Maximum story displacements of buildings with footing foundation on hard, medium, and soft soil under 1940 El Centro earthquake

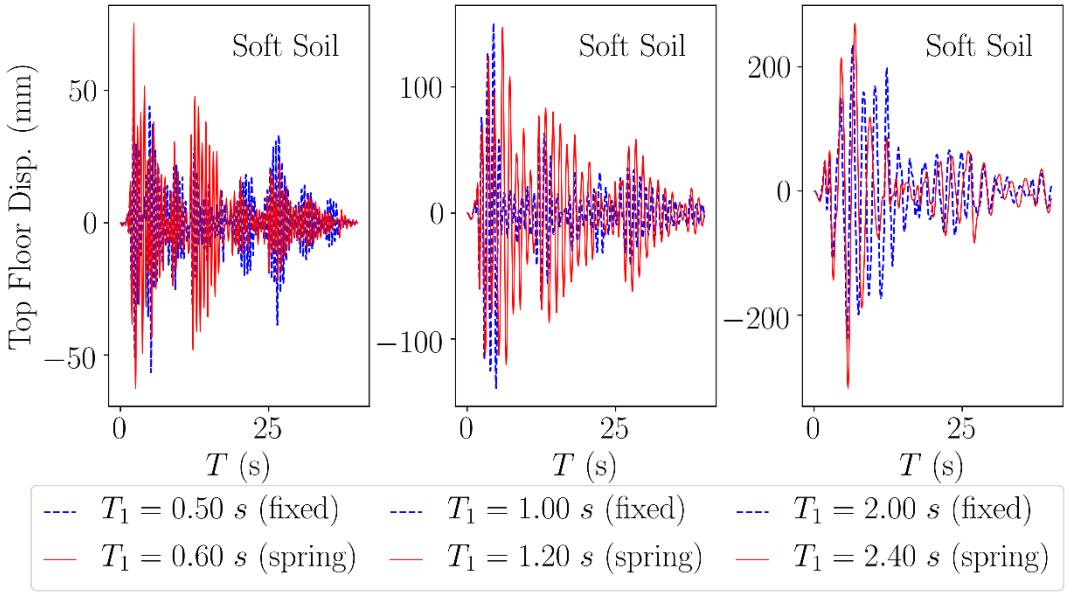

Figure 5.32 Top story displacement time-histories of buildings with footing foundation on soft soil under 1940 El Centro earthquake

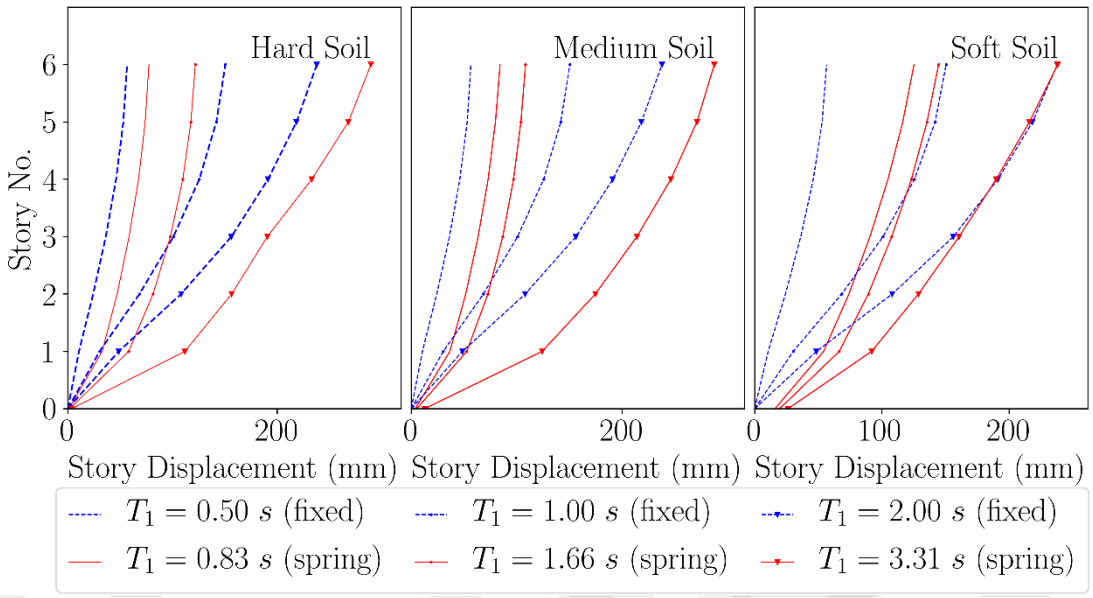

Figure 5.33 Maximum story displacements of buildings with raft foundation on hard, medium, and soft soil under 1940 El Centro earthquake

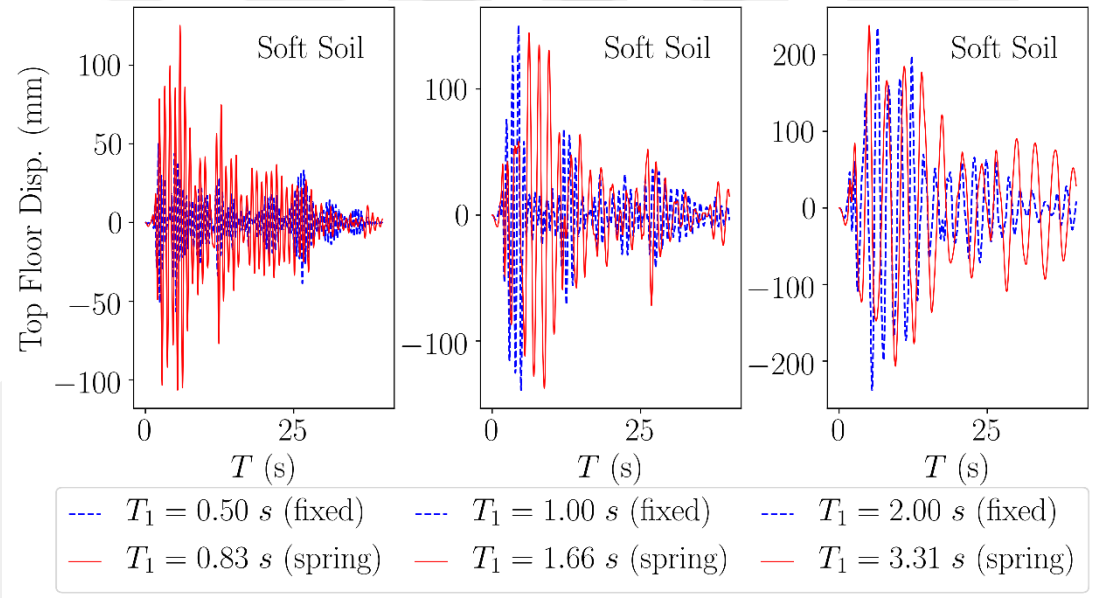

Figure 5.34 Top story displacement time-histories of buildings raft footing foundation on soft soil under 1940 El Centro earthquake

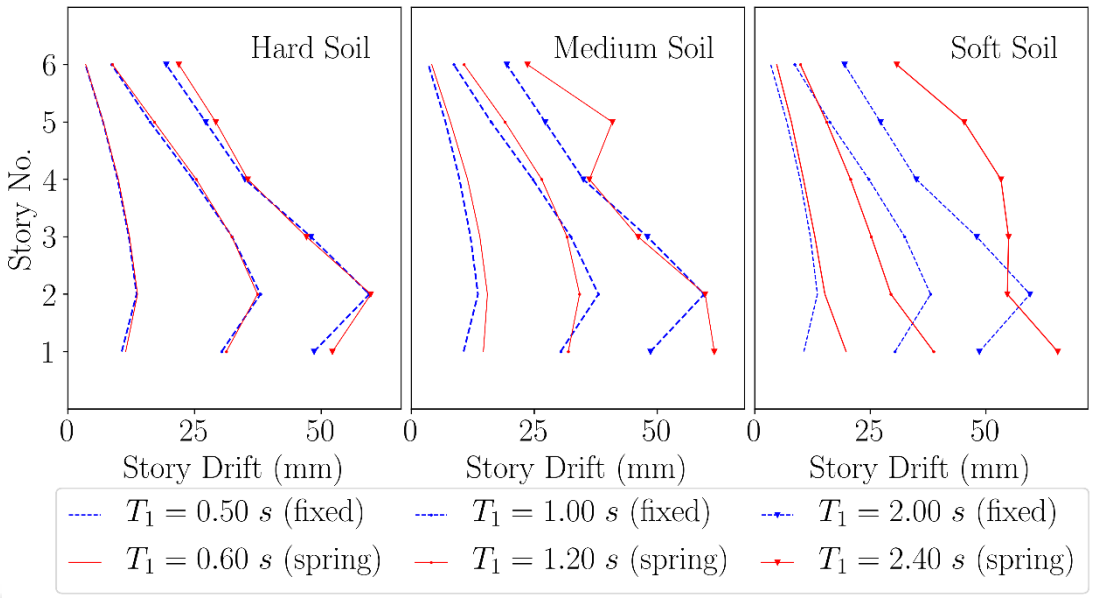

Figure 5.35 Maximum story drifts of buildings with footing foundation on hard, medium, and soft soil under 1940 El Centro earthquake

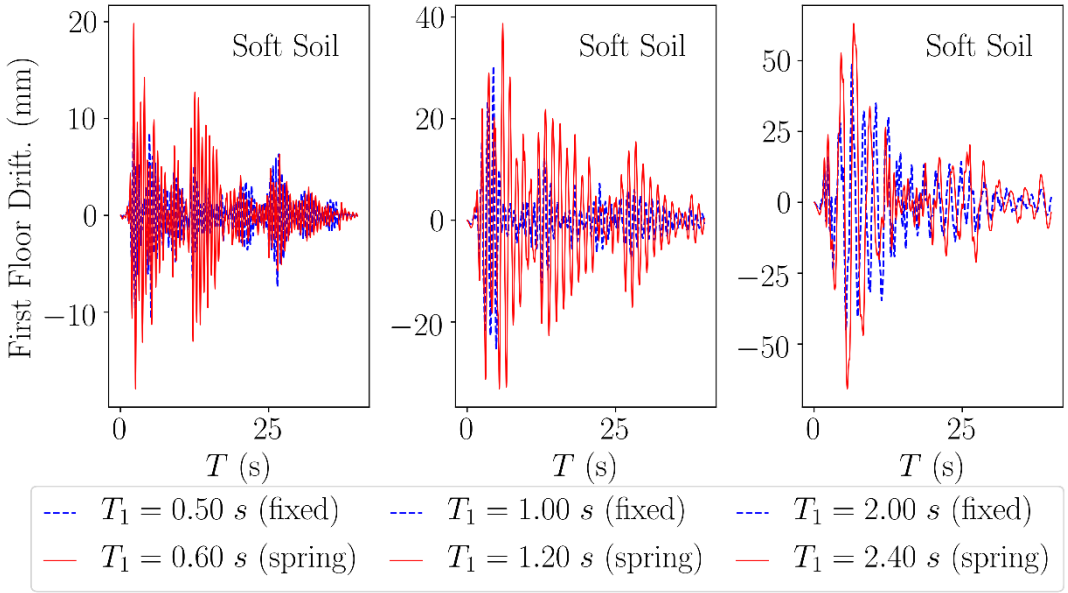

Figure 5.36 First story drift time-histories of buildings with footing foundation on soft soil under 1940 El Centro earthquake

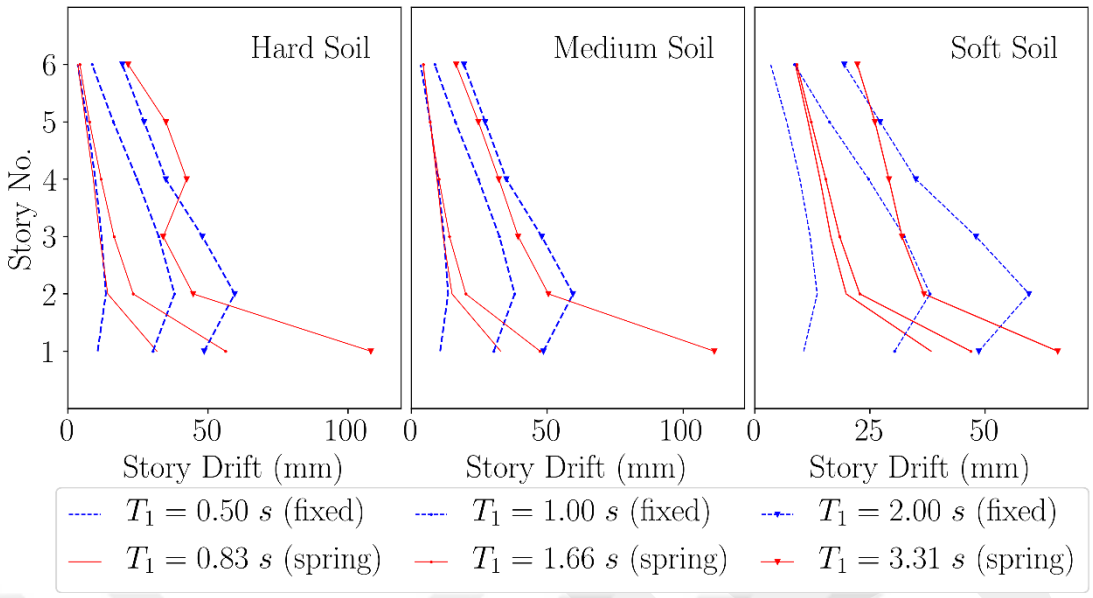

Figure 5.37 Maximum story drifts of buildings with raft foundation on hard, medium, and soft soil under 1940 El Centro earthquake

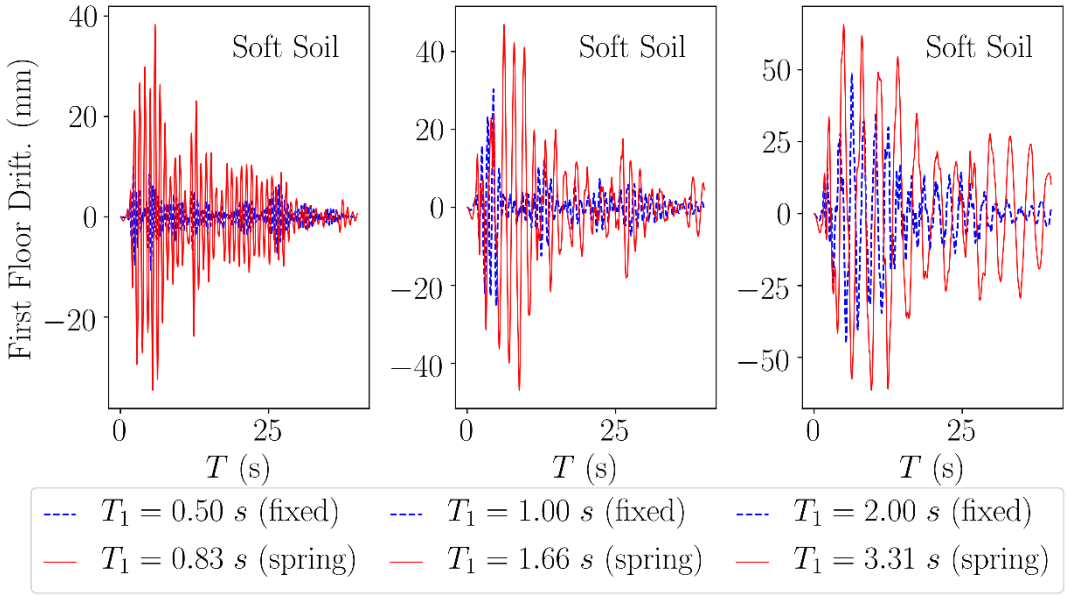

Figure 5.38 First story drift time-histories of buildings raft foundation on soft soil under 1940 El Centro earthquake

Table 5.26 Maximum story displacements and drifts of stiff building with footing foundation on hard soil

Story	Fixed			Spring		
	Disp. (mm)	Drift (mm)	Drift (%)	Disp. (mm)	Drift (mm)	Drift (%)
6	56.6	3.5	0.1	58.1	3.5	0.1
5	53.1	6.9	0.2	54.6	7.0	0.2
4	46.1	9.8	0.3	47.6	9.9	0.3
3	36.3	12.0	0.4	37.6	12.2	0.4
2	24.2	13.6	0.5	25.4	13.8	0.5
1	10.6	10.6	0.4	11.6	11.4	0.4

Table 5.27 Maximum story displacements and drifts of stiff building with footing foundation on medium soil

Story	Fixed			Spring		
	Disp. (mm)	Drift (mm)	Drift (%)	Disp. (mm)	Drift (mm)	Drift (%)
6	56.6	3.5	0.1	68.7	4.2	0.1
5	53.1	6.9	0.2	64.5	7.9	0.3
4	46.1	9.8	0.3	56.5	11.5	0.4
3	36.3	12.0	0.4	45.1	13.9	0.5
2	24.2	13.6	0.5	31.1	15.5	0.5
1	10.6	10.6	0.4	15.6	14.7	0.5

Table 5.28 Maximum story displacements and drifts of stiff building with footing foundation on soft soil

Story	Fixed			Spring		
	Disp. (mm)	Drift (mm)	Drift (%)	Disp. (mm)	Drift (mm)	Drift (%)
6	56.6	3.5	0.1	75.3	4.8	0.2
5	53.1	6.9	0.2	70.5	7.9	0.3
4	46.1	9.8	0.3	62.5	10.6	0.4
3	36.3	12.0	0.4	51.9	13.0	0.4
2	24.2	13.6	0.5	38.9	15.2	0.5
1	10.6	10.6	0.4	23.7	19.8	0.7

Table 5.29 Maximum story displacements and drifts of medium building with footing foundation on hard soil

Story	Fixed			Spring		
	Disp. (mm)	Drift (mm)	Drift (%)	Disp. (mm)	Drift (mm)	Drift (%)
6	151	8.7	0.3	153	8.8	0.3
5	141	16.3	0.5	144	17.1	0.6
4	126	24.7	0.8	127	25.4	0.8
3	101	32.4	1.1	102	32.4	1.1
2	68.4	38.1	1.3	69.2	37.5	1.2
1	30.4	30.4	1.0	31.8	31.3	1.0

Table 5.30 Maximum story displacements and drifts of medium building with footing foundation on medium soil

Story	Fixed			Spring		
	Disp. (mm)	Drift (mm)	Drift (%)	Disp. (mm)	Drift (mm)	Drift (%)
6	151	8.7	0.3	156	10.7	0.4
5	141	16.3	0.5	146	19.1	0.6
4	126	24.7	0.8	126	26.5	0.9
3	101	32.4	1.1	99.9	31.7	1.1
2	68.4	38.1	1.3	68.2	34.2	1.1
1	30.4	30.4	1.0	33.9	31.9	1.1

Table 5.31 Maximum story displacements and drifts of medium building with footing foundation on soft soil

Story	Fixed			Spring		
	Disp. (mm)	Drift (mm)	Drift (%)	Disp. (mm)	Drift (mm)	Drift (%)
6	151	8.7	0.3	147	9.9	0.3
5	141	16.3	0.5	137	15.6	0.5
4	126	24.7	0.8	122	20.7	0.7
3	101	32.4	1.1	101	25.2	0.8
2	68.4	38.1	1.3	75.9	29.5	0.9
1	30.4	30.4	1.0	46.5	38.7	1.3

Table 5.32 Maximum story displacements and drifts of soft building with footing foundation on hard soil

Story	Fixed			Spring		
	Disp. (mm)	Drift (mm)	Drift (%)	Disp. (mm)	Drift (mm)	Drift (%)
6	238	19.4	0.6	247	21.9	0.7
5	218	27.2	0.9	225	29.2	0.9
4	191	34.9	1.2	196	35.6	1.2
3	156	48.0	1.6	160	47.1	1.6
2	108	59.5	1.9	113	59.8	1.9
1	48.6	48.6	1.6	53.1	52.3	1.7

Table 5.33 Maximum story displacements and drifts of soft building with footing foundation on medium soil

Story	Fixed			Spring		
	Disp. (mm)	Drift (mm)	Drift (%)	Disp. (mm)	Drift (mm)	Drift (%)
6	238	19.4	0.6	247	21.9	0.7
5	218	27.2	0.9	225	29.2	0.9
4	191	34.9	1.2	196	35.6	1.2
3	156	48.0	1.6	160	47.1	1.6
2	108	59.5	1.9	113	59.8	1.9
1	48.6	48.6	1.6	53.1	52.3	1.7

Table 5.34 Maximum story displacements and drifts of soft building with footing foundation on soft soil

Story	Fixed			Spring		
	Disp. (mm)	Drift (mm)	Drift (%)	Disp. (mm)	Drift (mm)	Drift (%)
6	238	19.4	0.6	317	30.7	1.0
5	218	27.2	0.9	287	45.3	1.5
4	191	34.9	1.2	241	53.3	1.8
3	156	48.0	1.6	188	54.9	1.8
2	108	59.5	1.9	133	54.7	1.8
1	48.6	48.6	1.6	78.4	65.5	2.2

Table 5.35 Maximum story displacements and drifts of stiff building with raft foundation on hard soil

Story	Fixed			Spring		
	Disp. (mm)	Drift (mm)	Drift (%)	Disp. (mm)	Drift (mm)	Drift (%)
6	56.5	3.5	0.1	77.5	3.6	0.1
5	53.1	6.9	0.2	73.9	6.3	0.2
4	46.1	9.8	0.3	67.6	9.1	0.3
3	36.3	12.0	0.4	58.5	11.4	0.4
2	24.2	13.6	0.5	47.1	14.3	0.5
1	10.6	10.6	0.4	32.8	31.8	1.1

Table 5.36 Maximum story displacements and drifts of stiff building with raft foundation on medium soil

Story	Fixed			Spring		
	Disp. (mm)	Drift (mm)	Drift (%)	Disp. (mm)	Drift (mm)	Drift (%)
6	56.5	3.5	0.1	84.3	4.4	0.1
5	53.1	6.9	0.2	79.9	6.9	0.2
4	46.1	9.8	0.3	72.9	9.5	0.3
3	36.3	12.0	0.4	63.5	11.7	0.4
2	24.2	13.6	0.5	51.7	15.0	0.5
1	10.6	10.6	0.4	36.7	32.9	1.1

Table 5.37 Maximum story displacements and drifts of stiff building with raft foundation on soft soil

Story	Fixed			Spring		
	Disp. (mm)	Drift (mm)	Drift (%)	Disp. (mm)	Drift (mm)	Drift (%)
6	56.5	3.5	0.1	125	8.8	0.3
5	53.1	6.9	0.2	116	11.6	0.4
4	46.1	9.8	0.3	105	14.2	0.5
3	36.3	12.0	0.4	90.6	16.5	0.6
2	24.2	13.6	0.5	74.1	19.9	0.7
1	10.6	10.6	0.4	54.2	38.3	1.2

Table 5.38 Maximum story displacements and drifts of medium building with raft foundation on hard soil

Story	Fixed			Spring		
	Disp. (mm)	Drift (mm)	Drift (%)	Disp. (mm)	Drift (mm)	Drift (%)
6	151	8.7	0.3	122	4.3	0.1
5	142	16.3	0.5	118	7.7	0.3
4	126	24.7	0.8	110	11.9	0.4
3	101	32.4	1.1	97.9	16.5	0.5
2	68.4	38.1	1.3	81.4	23.3	0.8
1	30.4	30.4	1.0	58.1	56.3	1.9

Table 5.39 Maximum story displacements and drifts of medium building with raft foundation on medium soil

Story	Fixed			Spring		
	Disp. (mm)	Drift (mm)	Drift (%)	Disp. (mm)	Drift (mm)	Drift (%)
6	151	8.7	0.3	108	4.4	0.1
5	142	16.3	0.5	104	6.9	0.2
4	126	24.7	0.8	97.0	10.2	0.3
3	101	32.4	1.1	86.8	14.1	0.5
2	68.4	38.1	1.3	72.8	20.1	0.7
1	30.4	30.4	1.0	52.7	47.4	1.6

Table 5.40 Maximum story displacements and drifts of medium building with raft foundation on soft soil

Story	Fixed			Spring		
	Disp. (mm)	Drift (mm)	Drift (%)	Disp. (mm)	Drift (mm)	Drift (%)
6	151	8.7	0.3	145	9.2	0.3
5	142	16.3	0.5	135	12.3	0.4
4	126	24.7	0.8	123	15.4	0.5
3	101	32.4	1.1	108	18.4	0.6
2	68.4	38.1	1.3	89.3	22.8	0.8
1	30.4	30.4	1.0	66.5	46.9	1.6

Table 5.41 Maximum story displacements and drifts of soft building with raft foundation on hard soil

Story	Fixed			Spring		
	Disp. (mm)	Drift (mm)	Drift (%)	Disp. (mm)	Drift (mm)	Drift (%)
6	238	19.4	0.6	289	21.5	0.7
5	218	27.2	0.9	268	34.9	1.2
4	191	34.9	1.2	233	42.4	1.4
3	156	48.0	1.6	191	34.1	1.1
2	108	59.5	1.9	156	44.7	1.5
1	48.6	48.6	1.6	112	108	3.6

Table 5.42 Maximum story displacements and drifts of soft building with raft foundation on medium soil

Story	Fixed			Spring		
	Disp. (mm)	Drift (mm)	Drift (%)	Disp. (mm)	Drift (mm)	Drift (%)
6	238	19.4	0.6	287	16.5	0.6
5	218	27.2	0.9	271	24.7	0.8
4	191	34.9	1.2	246	32.2	1.1
3	156	48.0	1.6	214	39.4	1.3
2	108	59.5	1.9	175	50.5	1.7
1	48.6	48.6	1.6	124	111	3.7

Table 5.43 Maximum story displacements and drifts of soft building with raft foundation on soft soil

Story	Fixed			Spring		
	Disp. (mm)	Drift (mm)	Drift (%)	Disp. (mm)	Drift (mm)	Drift (%)
6	238	19.4	0.6	238	22.3	0.7
5	218	27.2	0.9	216	26.1	0.9
4	191	34.9	1.2	190	29.1	0.9
3	156	48.0	1.6	161	31.9	1.1
2	108	59.5	1.9	129	36.7	1.2
1	48.6	48.6	1.6	91.9	65.7	2.2

5.2.3.3 Foundation Displacement

Maximum values of the foundation vertical and lateral displacements of spring models on hard, medium and soft soils are presented in Tables 5.44 through 5.46. Foundation displacements are given at four points (Loc. 1, 2, 3, 4) as described in Section 5.2.2.3. Maximum values of the foundation settlement (vertical displacement) is also plotted in Figures 5.39 through 5.40 for footing and raft foundations. As the soil and/or structure gets softer, the foundation vertical lateral displacements increase as expected.

Table 5.44 Maximum foundation displacements in buildings on hard soil

Structure Type	Loc.	Spring Model			
		Footing		Raft	
		U_z (mm)	U_x (mm)	U_z (mm)	U_x (mm)
Stiff	1	-0.34	0.23	-1.25	0.58
	2	-0.60	0.18	-6.02	0.30
	3	-0.69	0.19	-4.51	0.33
	4	-0.25	0.23	-1.67	0.62
Medium	1	-1.17	0.51	-3.69	0.92
	2	-1.98	0.39	-15.97	0.28
	3	-2.08	0.40	-10.78	0.38
	4	-1.07	0.50	-6.39	0.98
Soft	1	-4.45	0.99	-13.38	2.09
	2	-6.198	0.79	-58.02	0.06
	3	-6.32	0.80	-37.59	0.38
	4	-4.35	0.98	-25.20	2.24

Table 5.45 Maximum foundation displacements in buildings on medium soil

Structure Type	Loc.	Spring Model			
		Footing		Raft	
		U_z (mm)	U_x (mm)	U_z (mm)	U_x (mm)
Stiff	1	-1.56	1.20	-5.19	2.99
	2	-2.91	0.96	-18.18	2.32
	3	-3.27	0.97	-15.32	2.34
	4	-1.17	1.19	-6.14	3.03
Medium	1	-5.33	2.20	-14.96	3.77
	2	-8.29	1.77	-43.33	2.58
	3	-8.69	1.79	-33.17	2.65
	4	-4.93	2.18	-21.99	3.82
Soft	1	-20.30	4.91	-53.85	10.06
	2	-28.44	3.98	-168.01	5.69
	3	-28.94	4.01	-122.53	5.89
	4	-19.91	4.87	-85.06	10.16

Table 5.46 Maximum foundation displacements in buildings on soft soil

Structure Type	Loc.	Spring Model			
		Footing		Raft	
		U_z (mm)	U_x (mm)	U_z (mm)	U_x (mm)
Stiff	1	-6.73	4.49	-22.91	13.49
	2	-10.13	3.69	-59.16	12.61
	3	-11.40	3.72	-55.14	12.59
	4	-5.39	4.46	-24.61	13.48
Medium	1	-23.24	8.38	-68.46	17.81
	2	-32.83	6.89	-137.93	16.04
	3	-34.28	6.94	-120.63	16.02
	4	-21.89	8.32	-82.43	17.82
Soft	1	-88.86	16.14	-250.06	23.39
	2	-123.83	12.94	-447.36	18.92
	3	-125.45	13.02	-380.21	18.83
	4	-87.52	16.03	-312.76	23.47

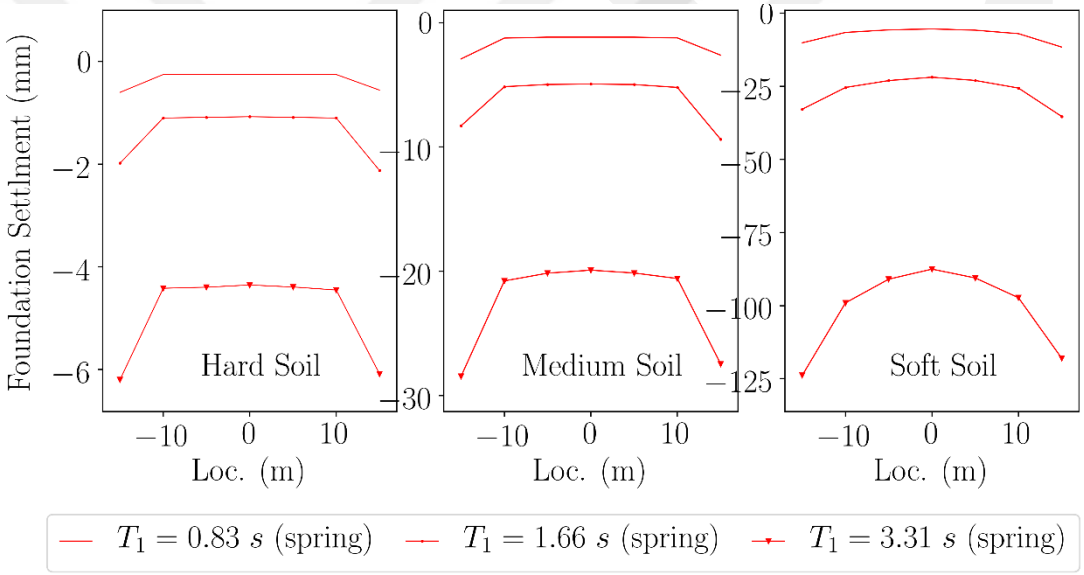

Figure 5.39 Maximum foundation settlements of buildings with footing foundation on hard, medium, and soft soil

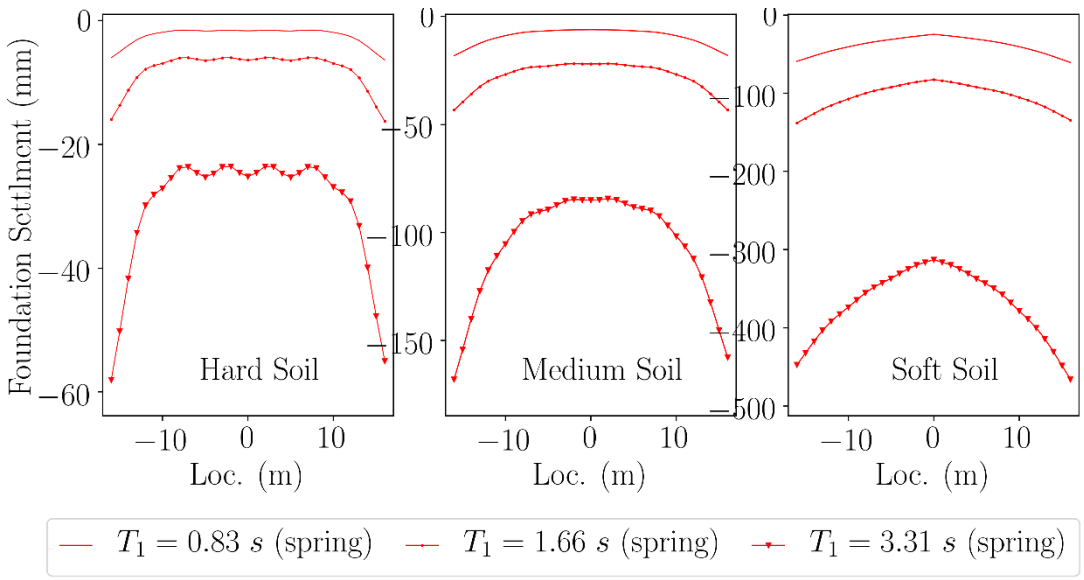

Figure 5.40 Maximum foundation settlements of buildings with raft foundation on hard, medium, and soft soil

CHAPTER 6

CONCLUSION

6.1 Summary

Soil-structure interaction effects in buildings are studied in this thesis using relatively simple models prepared by a general-purpose structural analysis software (SAP2000). A symmetrical, 6-story, 6-bay reinforced concrete moment resisting frame is considered for both 2D and 3D building models. Seismic responses of three different building structures (with varying dynamic characteristics) on three different homogeneous, elastic soil mediums are computed and compared with the responses of the corresponding fixed base models. Soil-structure interaction effects are modeled by two approaches: (i) defining soil springs representing the soil impedance functions (substructure method), and (ii) modeling the soil medium directly along with the structure and the foundation (direct analysis method). Two types of foundation are considered in the models: footing foundation (i.e., isolated footings) and raft foundation. ASCE 7-10 acceleration response spectra are determined based on the soil properties and used to examine the seismic response of the models considered. A limited study is also performed by time-history analyses using an actual earthquake ground acceleration record (1940 El Centro).

6.2 Concluding Remarks

The main conclusions of this study are as follows:

1. Including soil-structure interaction effects cause a period lengthening in the fundamental mode. This is a well-known fact stated by many publications in the literature and major design codes.

2. Among the SSI models, it is observed that the direct models lead to a larger period lengthening in the fundamental period compared to the spring models. This effect is more pronounced in footing foundation than raft foundation, especially as the soil gets softer.
3. Base shear increases as the soil gets softer due to higher design spectral acceleration for softer soil. For a given structure and soil, consideration of soil-structure interaction effects through a spring model or a direct model decrease the base shear (and the story shears) due to period lengthening, compared to the fixed base model. This effect is again more pronounced in direct models.
4. Story displacements increase as the building and soil become softer due to higher flexibility of building and soil, and higher design spectral acceleration for softer soil. For a given structure with footing or raft foundation, as soil becomes softer, the differences between the fixed model and SSI models (spring and direct) become more pronounced. For any given soil, the difference between fixed model and SSI models increases as the structure becomes stiffer. This effect is more visible in direct models (compared to the spring models) and in spring models on soft soil.
5. Similar to the story displacements, the story drift values increase as the structure and the soil get softer. For fixed base models, the largest story drift occurs in the second story columns, whereas the largest story drift occurs in the first story columns for direct models with footing or raft foundation. Spring models on hard and medium soil have the largest drift in the second story columns similar to the fixed models, but as the soil becomes softer, the largest drift occurs in the first story columns of the spring models.
6. For a given structure as the soil gets softer, the story drifts of the SSI models (spring and direct) increases with respect to fixed based model story drifts for both footing and raft foundations. This effect is higher in direct models. For a given soil, as the structure gets softer, the drifts of the SSI models decrease with respect to fixed base model drifts for both footing and raft foundations.
7. Vertical and lateral displacements of the foundation increase as the soil and/or structure gets softer. It is observed that spring models indicate lower vertical and lateral displacements compared to direct models, leading to less conservative

results for foundation displacements. Spring models indicate a larger difference in foundation settlement between footing and raft foundations compared to direct models. Also, it is observed that spring models indicate larger foundation settlements in raft foundation for any soil and structure type whereas direct models indicate larger foundation settlements in raft foundation only for stiff structure.

8. A limited study using time-history response analysis with a single ground acceleration record indicates that the dynamic responses are in general consistent with response spectrum analysis results summarized above, with minor discrepancies most likely due to using an unscaled ground acceleration for all soil types and effect of dominant frequency components in the ground motion record. A more detailed study including many ground acceleration records that are scaled to be representative of the design acceleration spectrum is required for a more rational analysis of dynamic soil-structure interaction effects.

REFERENCES

[1] Okabe, S., "General Theory of Earth Pressure," Jour. of the Japanese Society of Civil Engineers, Tokyo, Japan, 1926.

[2] Mononobe N., Matsuo H., "On the Determination of Earth Pressure During Earthquakes," in Proc. of the World Eng. Conf., 1929, 176 pp.

[3] Roesset JM., "Soil Structure Interaction: The Status of Current Analysis Methods and Research (Seismic Safety Margins Research Program)," in NUREG/CR-1780. Lawrence Live more Laboratory, University of California, California, 1980.

[4] Sezawa K., Kanai K., "Decay in The Seismic Vibration of a Simple or Tall Structure by Dissipation of Their Energy into The Ground," in Bull. Of the Earthquake. Research Inst., University of Tokyo, Japan, 1935.

[5] Sezawa K., Kanai K., "Energy Dissipation in Seismic Vibrations of a Framed Structure," in Bull. of the Earthquake Research Inst, University of Tokyo, Japan, 1935.

[6] Sezawa K., Kanai K., "Energy Dissipation in Seismic Vibrations of Actual Buildings," in Bull. of the Earthquake Research Inst, University of Tokyo, Japan, 1935.

[7] Martel, R. R., "Effect of Foundation on Earthquake Motion," Civil Engineering, Jan 1940.

[8] Merritt R.G. and Housner G.W., "Effects of Foundation Compliance on Earthquake Stress in Multi-Story Buildings," bulletin of the seismological society of America journal, Vol. 44, No. 4, 1954, pp. 551–570.

[9] Housner G.W., "Interaction of Building and Ground During an Earthquake," Bulletin of The Seismological Society of America, Vol. 47 (3), pp. 179-186, 1957.

[10] Parmelee R.A., "Building-Foundation Interaction Effects," Jour. Eng. Mech Div. ASCE, Vol. 93, No. EM2, pp. 131-152, 1967.

[11] Parmelee R.A., Perelman D.S., Lee S. and Keer L., "Seismic Response of Structure-Foundation Systems," Jour. Eng. Mech Div. ASCE, Vol. 94, No. EM6, pp. 1295- 1315, 1968.

[12] Biggs, "J. M., Introduction to Structural Dynamics," New York City, McGraw-Hill College, 1964.

[13] Bycroft G. N., "Forced Vibrations of a Rigid Circular Plate on A Semi-infinite Elastic Space and on an Elastic Stratum," Phil. Trans. of The Roy. Soc Of London, Vol. 248, 327 pp., 1956.

[14] Sarrazin M.A., "Soil-Structure Interaction in Earthquake Resistant Design," Massachusetts Institute of Technology, School of Engineering, Department of Civil Engineering, 1970, 744 pp.

[15] Maccalden PB, Matthiesen RB., "Coupled Response of Two Foundations," In: Proceedings of the fifth World Conference on Earthquake Engineering, Rome, Italy, 1973, pp. 1913–22.

[16] Luco JE, Contesse L., "Dynamic Structure–Soil–Structure Interaction," Bulletin of The Seismological Society of America, Vol. 63, No. 4, pp.1289–1303, 1973.

[17] Triantafyllidis Th., Neidhart Th., "Diffraction Effects Between Foundations Due to Incident Rayleigh Waves," Earthquake Engineering and Structural Dynamics Vol. 18, pp. 815-36, 1989.

[18] S. C. Dutta, R. Rana, "A Critical Review on Idealization and Modeling for Interaction Among Soil-Foundation-Structure System," Elsevier journal, Computers and Structures 80, pp. 1579-1594, 2002.

[19] Elsabee F. and Morray J. P., "Dynamic Behavior of Embedded Foundations," Massachusetts Institute of Technology, School of Engineering, Department of Civil Engineering, 1977.

[20] Luco, J. E. and Wong H. L., "Seismic Response of Foundations Embedded in A Layered Half-Space," Earthquake Engineering and Structural Dynamics journal, Vol. 15, pp. 233-247, 1987.

[21] Scanlan R. H., "Seismic Wave Effects in Soil Structure Interaction," Earthquake Engineering and Structural Dynamics journal, Vol. 4, pp. 379-388, 1976.

[22] Seed HB., Lysmer J., Hwang R, "Soil–Structure Interaction Analysis for Seismic Response," ASCE Library, Vol. 101, pp. 439–57, 1975.

[23] Gonzalez JJ., "Dynamic Interaction Between Adjacent Structures,", Department of Civil Engineering, Massachusetts Institute of Technology, Cambridge, Mass, 1977.

[24] Roesset JM, Gonzalez JJ., "Dynamic Interaction Between Adjacent Structures," Earthquake Engineering & Structural Dynamics journal, Vol. 15, 1978, pp. 323-343.

[25] Solari G, Stura D., Vardanega C., "Accuracy of Numerical Models In 3-D Soil–Structure Interaction," in Proceedings of The Seventh World Conference on Earthquake Engineering., 1980, pp. 237-44.

[26] Menglin Lou, Huaifeng Wang, Xi Chen, and Yongmei Zhai., "Soil-Structure Interaction: Literature Review," Elsevier Soil Dynamics and Earthquake Engineering, Vol. 31, pp. 1724–173, 2011.

[27] Roesset JM., “Soil Structure Interaction: The Status of Current Analysis Methods and Research (Seismic Safety Margins Research Program),” in NUREG/CR-1780. Lawrence Live more Laboratory, University of California, California, 1980.

[28] Dominguez J., “Dynamic Stiffness of Rectangular Foundations,” Massachusetts Institute of Technology, Department of Civil Engineering, 1978, pp. 120.

[29] Gazetas G., “Formulas and Charts for Impedances of Surface and Embedded Foundations,” Journal of Geotechnical Engineering, Vol. 117, pp. 1363–1381, 1991.

[30] Kausel E., “An Explicit Solution for The Green’s Functions for Dynamic Loads in Layered Media,” Research Report R81-13, Massachusetts Institute of Technology, Department of Civil Engineering, 1981.

[31] Luco J. E. and Apsel R. J., “On the Green’s Functions for A Layered Half Space Part I,” Bulletin of the Seismological Society of America., Vol. 73, Pp. 931□951, 1983.

[32] Seed H.B., Whitman R.V., and Lysmer J., “Soil Structure Interaction Effects in The Design of Nuclear Power Plants,” Structural and Geotechnical Mechanics, A Volume Honoring N. M. Newmark (W. J. Hall Editor) Prentice Hall, 1977.

[33] Nelson I., and Isenberg J., “Soil Island Approach to Structure Media Interaction,” in Desai C.S., Ed., “Numerical Methods in Geomechanics”, ASCE, N.Y., pp. 41-57, 1976.

[34] Kausel E. and Roesset J. M., “Soil Structure Interaction Problems for Nuclear Containment Structures,” Electric Power and The Civil Engineer, Proc. Of the ASCE Power Div. Conf., Boulder, Colorado, 1974.

[35] Veletsos A. S. (1977). "Dynamics of structure-foundation systems." Structural and geotechnical mechanic, Prentice-Hall, Englewood Cliffs, N.J., 33, pp. 333-361, 1977.

[36] Luco, J. E., “Linear Soil Structure Interaction: A Review,” ASME Earthquake Ground Motion and Its Effects on Structures, Winter Annual Meeting, Vol. 53, pp. 41-57, 1982.

[37] Lysmer J., Tabatabaie M., Tajirian F., Vahduni, S., and Ostradan F., “SASSI A System for Analysis of Soil Structure Interaction,” Geotechnical Engineering Group Reoprt, University of California, Berkeley, 1981.

[38] Wolf J. P., “Dynamic Soil-Structure-Interaction,” Prentice-Hall, Englewood Cliffs (NJ), 1985, pp. 466.

[39] Wolf J. P., Song Ch., “Some Cornerstones of Dynamic Soil-Structure Interaction,” ELSEVIER, Engineering Structures, Vol. 24, pp.13-28, 2002.

[40] E. Çelebi, S. Fırat, and İ. Çankaya, "The Evaluation of Impedance Functions in The Analysis of Foundations Vibrations Using Boundary Element Method," Elsevier Applied Mathematics and Computation, Vol 173, pp 636-667, 2006.

[41] Wolf J.P., Ch. Song, "Finite Element Modeling of Unbounded Media", West Sussex: John Wiley & Sons, 1996, 331 pp.

[42] Wolf J.P., "Simple Physical Models for Foundation Vibration," Department of Civil Engineering, Swiss Federal Institute of Technology Lausanne, Switzerland, pp. 663-668, 1994.

[43] Beskos DE., "Boundary Element Methods in Dynamic Analysis," ASME, Vol. 40, pp.1-23, 1987.

[44] Kausel E., "Thin Layer Method: Formulation in The Time Domain," International Journal for Numerical Methods in Engineering, Vol. 37, pp. 927-941, 1994.

[45] Wolf JP., "Spring-Dashpot-Mass Models for Foundation Vibrations," Earthquake Engineering and Structural Dynamics, Vol. 26, pp. 931-949, 1997.

[46] Walker W. and Holland J. A., "Modulus of Subgrade Reaction - Which One Should be Used?, " Structural Services Inc. , USA, 2016.

[47] Terzaghi K., "Evaluation of Coefficient of Subgrade Reaction," Thomas Telford Limited, Vol. 5, pp. 297-326, 1955.

[48] Ghalimath A.G., More Sheetal.A, Hatti Mantesh.A, Jamadar Chaitrali.A, "Analytical Approaches for Soil-Structure Interaction," International Research Journal of Engineering and Technology (IRJET), Vol. 02, pp. 595-600, 2015.

[49] Ray W. Clough, and Joseph Penzien, "Dynamics of Structures," Book 3nd Edition, University Ave Berkeley, CA, USA, 1995.

[50] Kramer S. L., "GEOTHECNICAL EARTHQUAKE ENGNERRING," Prentice Hall, New jersey, 1996, pp. 637.

[51] Mehmet Celebi, "Radiation Damping Observed from Seismic Responses of Buildings," 12th World Conference on Earthquake Engineering, 2000, 2634 pp.

[52] Mordai V., "Investigating Parameters Affecting the Dynamic Soil-Structure Interaction Analysis," MSc Dissertaion, Urmia University, Urmia, Iran, 2011.

[53] Lysmer J. & Kuhlemeyer R.L., "Finite Dynamic Model for Infinite Media," Journal of The Engineering Mechanics Division, ASCE, Vol.95, No.4, pp. 859-877, 1969.

[54] Zienkiewicz O. C., Bicanic N., and Shen F. Q., "Earthquake Input Definition and The Transmitting Boundary Conditions," Proceedings Advances in Computational Nonlinear Mechanics I, Springer-Verlag, pp. 109-138, 1989.

[55] Wolf J.P., "Soil-Structure Interaction Analysis in Time Domain," Prentice Hall, 1988, 446 pp.

[56] Kocak S and Mengi Y., "A Simple Soil–Structure Interaction Model," Appl Math Model 2000, 24(8–9), pp. 607–35, 2000.

[57] Bardet JP, Ichii K, and Lin CH, "A Computer Program for Equivalent Linear Earthquake Site Response Analysis of Layered Soils Deposits," University of Southern California, Los Angeles, 2000.

[58] Schnabel, P.B., Lysmer, J. and Seed, H.B., "SHAKE - A computer program for earthquake analysis of horizontally layered sites," Earthquake Engineering Research Center, University of California, Berkeley, Report No. EERC 72-12, 1972.

[59] Hudson M., Idriss I. M., and Beikae M., "QUAD4M—A computer program to evaluate the seismic response of soil structures using finite element procedures and incorporation a compliant base," Center for Geotechnical Modeling, Department of Civil and Environmental Engineering, University of California, Davis, 1994.

[60] Lysmer J., Udaka T., Tsai, C.F. and Seed, H.B., "FLUSH a computer program for approximate 3-D analysis of soil-structure interaction problems", EERC,75-30, 1975.

[61] Iwan W. D, "On A Class of Models for The Yielding Behavior of Continuous and Composite Systems," Journal of Applied Mechanics, ASME, Vol. 34, pp. 612-617, 1967.

[62] Mroz Z., "On the Description of Anisotropic Work-Hardening," Journal of the Mechanics and Physics of Solids, Vol. 15, pp. 163-175, 1967.

[63] Bardet J.P. and Tobita T., "NERA: A Computer Program for Nonlinear Earthquake Site Response Analyses of Layered Soil Deposits," Department of Civil Engineering, University of Southern California, CA, Los Angeles, 2001.

[64] Lee M. K. and Finn W.D.L., "DESRA-1, Program for the dynamic effective stress response analysis of soil deposits including liquefaction evaluation," Soils Mechanics No 36, Department of Civil Engineering, University of British Columbia, Vancouver, B.C. Canada, 1975.

[65] Geomotions L., "D-MOD2000 A Nonlinear Computer Program for Seismic Response Analysis of Horizontally Layered Soil Deposits," Earth fill Dams, and Solid Waste Landfills, 2000.

[66] McKenna, F., Scott, M.H., and Fenves, G.L., "Nonlinear Finite Element Analysis Software Architecture Using Object Composition," Journal of Computing in Civil engineering, Vol. 24(1), pp. 95-107, January 2010.

[67] Finn W.D. Laim, Yogendrakumar M., Yoshida N., and Yoshida H., "TARA-3: A Program to Compute the Response of 2-D Embankments and Soil Structure Interaction Systems to Seismic Loadings," Department of Civil Engineering, University of British Columbia, Vancouver, Canada, 1986.

[68] Detournay, Christine (ed.); Hart, Roger (ed.): (FLAC) and numerical modeling in geomechanics. Proceedings of the international (FLAC) symposium held in Minneapolis, MN, USA, September 1999.

[69] Brinkgreve R.B.J., "PLAXIS-2D Version 8 user's manual," Balkema, Rotterdam, 2004.

[70] Irgens F., "Continuum Mechanics,", Springer-Verlag, Berlin, 649 pp., 1980.

[71] Reissner E, "Note on the formulation of the problem of the plate on an elastic foundation," Acta Mech, Vol. 4(1), pp. 88–91, 1967.

[72] Horvath J. and Colasanti R, "New Hybrid Subgrade Model for Soil-Structure Interaction Analysis: Foundation and Geosynthetics Applications.," in ASCE, Proceedings of the Geo-Frontiers 2011 Conference, 2011, 10 pp.

[73] Teodoru I.B, "Beams on Elastic Foundation the Simplified Continuum Approach," Bulletin of Polytechnic Institute of Jassy Constructions, Architecture Section, Vol. LV (LIX), No. 4, pp. 37-46, 2009.

[74] Shoaei D., Huat B. B. K., Jaafar M. S., and Elkarni A., "Soil- framed interaction analysis – A new interface element," Latin American Journal of Solids and Structures. Vol. 12, pp. 226-249, 2014.

[75] Wang, X. and Wang, L., "Continuous interface elements subject to large shear deformations," International Journal of Geomechanics, Vol. 6, No. 2, pp. 97-107, 2006.

[76] Kontoe S., Zdravkovic L., and Potts D.M., "The use of absorbing boundaries in dynamic analyses of soil-structure interaction problem," in Proc. 4th Int. Conf. on Earthquake Geotechnical Engineering, 2007.

[77] Mylonakis G., Nikolaou S., and Gazetas G., "Footings Under Seismic Loading: Analysis and Design Issues with Emphasis on Bridge Foundations," ELSEVIER Soil dynamics And Earthquake Engineering, Vol. 26, pp. 824-853, 2006.

[78] Pais A. and Kausel E., "Approximate Formulas for Dynamic Stiffnesses Of Rigid Foundations," ELSEVIER Soil Dynamics and Earthquake Engineering, Vol. 7, No. 4, pp. 213-227, 1988.

[79] Nevine A. Markous, Sameh S. F. Mehannyand, and Mourad M. Bakhoum., "Scaling of Earthquake Ground Motion Records for Seismic Analysis and Design of Bridges," Jl. Egyptian Society of Engineer, 2014.